ADDIS ABABA UNIVERSITY

SCHOOL OF GRADUATE STUDIES

DEPARTMENT OF CHEMISTRY

GRADUATE THESIS (CHEM 750)

SYNTHESIS AND CHARACTERIZATION OF SOME DONOR-ACCEPTOR TYPE LOW BAND GAP POLYMERS BASED ON THIOPHENE AND QUINOXALINE

A Graduate Thesis Submitted in Partial Fulfillment of the Requirements for the Degree of Master of Science in Chemistry.

By: Kumasser Kusse

Advisor: Professor Wendimagegn Mammo

October 2014

Addis Ababa, Ethiopia

ADDIS ABABA UNIVERSITY

SCHOOL OF GRADUATE STUDIES

SYNTHESIS AND CHARACTERIZATION OF SOME DONOR-ACCEPTOR TYPE LOW BAND GAP POLYMERS BASED ON THIOPHENE AND QUINOXALINE

By: Kumasser Kusse

Department of Chemistry

College of Natural Sciences

Approved by:

Prof. Wendimagegn Mammo _____

Advisor

Prof. Ermias Dagne _____

Examiner

Dr. Ashebir Fiseha _____

Examiner

DECLARATION

I, the undersigned, declare that this MSc. Thesis is my original work and has not been presented for any degree in any other university and that all sources of materials used for this project have been duly acknowledged.

Name: **Kumasser Kusse**

Signature: _____

This MSc. Thesis has been submitted for examination with my approval as a university advisor.

Name: **Wendimagegn Mammo (Professor)**

Signature: _____

Date and Place of Submission: Department of Chemistry

Addis Ababa University

October 2014

Acknowledgements

It is my pleasure to express my deepest sense of gratitude, sincere appreciation and profound regards to my supervisor **Professor Wendimagegn Mammo** for his scholastic guidance, constant encouragement throughout the course of my work.

My special appreciation goes to my colleagues working with me in the laboratory Dr. Zelalem Abdissa and Ms. Meseret Asrat for their valuable suggestions and encouragement. I would also like to thank Mr. Yadessa Melaku for running the NMR spectra of all the intermediate compounds, Dr. Desta Anteneh for forwarding me soft copy of some journal articles. I express my indebtedness to W/r Woynishet Gebeyehu for running FT-IR spectra of all of the compounds, Mr. Yisak Tsegazab for running UV-Vis spectra of most of the compounds and Mr. Zewdneh Genene for running UV-Vis spectra and CV of the polymers as well as for his valuable suggestions and encouragement during lab work. I would like to thank my family and friends for their encouragement and ongoing support during the work.

Finally, I would like to extend my gratitude to Haramaya University for sponsorship of the study and the Department of Chemistry, Addis Ababa University for giving the chance for study.

Table of Contents

LIST OF APPENDICES

List of Tables

List of Schemes

List of Figures

List of Abbreviations

D: Donor
A: Acceptor
HOMO: Highest Occupied Molecular Orbital
LUMO: Lowest Unoccupied Molecular Orbital
PA: Polyacetylene
DMF: N,N-Dimethylformamide
DMSO: Dimethyl sulfoxide
HAc: Acetic acid
NMR: Nuclear Magnetic Resonance
DEPT: Distortionless enhancement by polarization transfer
FT-IR: Fourier Transform-Infra red
OPV: Organic photovoltaics
UV-Vis: Ultraviolet Visible
ppm: parts per million
δ: Chemical shift
J: Coupling constant
Hz: Hertz
s: singlet
d: doublet
t: triplet
q: quintet
dd: doublets of doublet
m: multiplet
λ_{max}: maximum absorption wavelength
TLC : thin-layer chromatography
E_g: band gap
eV: Electron volt
CV: Cyclic voltammetry
SWV: Square wave voltammetry
Ag/AgCl: Silver/silver chloride electrode
$[Pd_2(dba)_3]$: tris(dibenzylideneacetone)dipalladium(0)
EDTA: Ethylenediaminetetraacetic acid disodium salt dihydrate
PSCs: polymer solar cells
^oC: degree Celsius
THF: Tetrahydrofuran
ODCB: *ortho*-dichlorobenzene
CB: Chlorobenzene
ICT: Intramolecular charge transfer
h: hour(s)
%: percentage
TQ: Thiophene-Quinoxaline-based polymer
LBG: Low band gap
PCE: power conversion efficiency
m: medium intensity
s: strong
str.: stretching
TBAB: tetra n-butyl ammonium bromide

SYNTHESIS AND CHARACTERIZATION OF SOME DONOR-ACCEPTOR TYPE LOW BAND GAP POLYMERS BASED ON THIOPHENE AND QUINOXALINE

By: Kumasser Kusse

Advisor: Prof. Wendimagegn Mammo

Abstract

*A series of four low band gap, conjugated copolymers containing thiophene and quinoxaline were synthesized via palladium(0)-catalyzed Stille coupling polymerization reaction, with different alkoxy side chains. The synthesis started first by the preparation of the required monomers for the copolymerization reaction. The monomers were characterized by NMR, UV-Vis and IR spectroscopic techniques. The resulting copolymers were a dark purple solid and showed very good solubility in common organic solvents like chlorobenzene, o-*dichlorobenzene*, chloroform, THF and toluene. The synthesized copolymers were characterized by ^{1}H-NMR, UV-Vis spectroscopy, Square wave voltammetry and cyclic voltammetry.*

UV-Vis spectra of the polymers in a solution and in thin films indicated that there are two prominent absorption maxima around 350 and 550 nm in solution and around 367 and 596 nm in film, which are attributable to π-π transition and intramolecular charge transfer at the backbone of copolymers, respectively. All the synthesized polymers have low band gaps around 1.74 eV, which were estimated from onset of UV-Vis spectra of thin films of the polymer. The electrochemical band gaps of the polymers were estimated from onset of square wave voltammograms and found to be around 2.0 eV.*

1. INTRODUCTION

A polymer is a substance composed of molecules with large molecular mass consisting of repeating units connected by covalent chemical bonds. The small molecules that combine with each other to form polymer molecules are called monomers.[1–3]

Polymers can be naturally occurring (biopolymers), manmade (synthetic polymers) or semi-synthetic polymers. Some of the natural polymers are cellulose (e.g., cotton, flax and papyrus), polypeptides (e.g. wool, silk, leather, horn), and polyisoprenes (e.g., natural rubbers).[4]

Among the semi-synthetic polymers, the most famous ones are Ebonite (prepared by vulcanizing natural rubber), Celluloid (the first thermoplastic, which was obtained from nitrocellulose and camphor in 1870) and Galalith (prepared from milk protein casein).

The oldest recorded fully-synthetic polymer was Bakelite, which was prepared and patented by Leo Hendrik Baekeland in 1907.[4]

Polymers are normally regarded as insulators, which are unable to conduct electricity or absorb sunlight. This was later changed when conjugated polymers were developed that showed conductivity upon doping. The first example of doping, rendering a polypyrrole polymer was reported by McNeill *et al.*[5] in 1963 as a modest conducting material. In 1977, Shirakawa *et al.* [6] reported polyacetylene doped with iodine, resulting in a conductive material.

Shirakawa, MacDiarmid and Heeger were awarded the Nobel Prize in 2000 for their contribution on the discovery and development of conjugated polymers.[4] Polymers with large π-conjugated systems have attracted much attention as new electronic and optoelectronic substances mainly used for active semiconducting layers in light-emitting diodes, photovoltaic cells and field-effect transistors. One of the most important advantages of conjugated polymers is a rather facile tuning of their optical, spectroscopic, and electronic properties by appropriate design of their chain structure. A

common characteristic between all the conjugated polymers is their extended π-conjugated system.

Conjugated polymers with various combinations of donors and acceptors have attracted great attention due to their optoelectronic applicability in several areas including organic photovoltaics, organic light-emitting diodes, organic field-effect transistors, chemical sensors and electrochromic devices.[7,8] Some examples of conjugated polymers are depicted in the Figure 1.

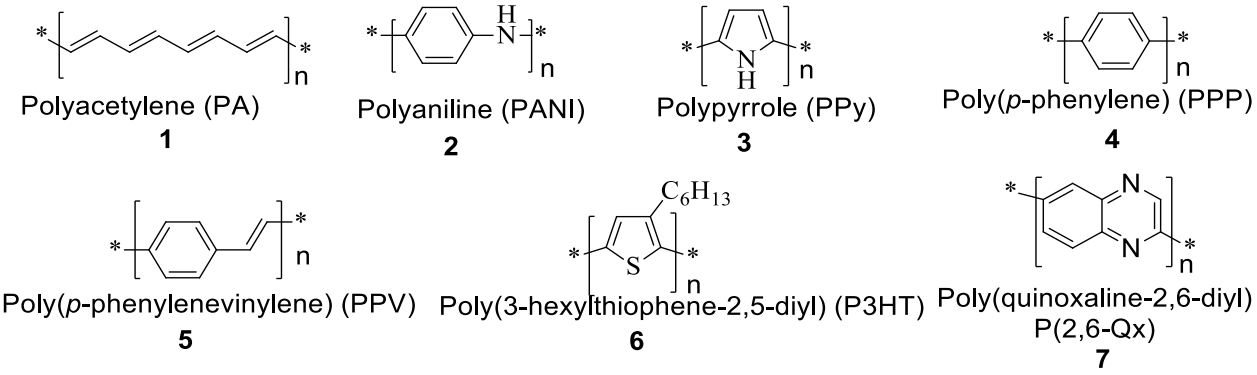

Figure 1: Structures of some conjugated polymers.

Due to their potential use in organic solar cells, conjugated copolymers having both electron rich (donor) and electron poor (acceptor) aromatic, and heteroaromatic units have gained much interest in the last few decades. For example, incorporating acceptor units in to polythiophenes is expected to shift the HOMO energy level towards lower energies resulting in a higher stability of the polymers against oxidation and photo oxidation, and to lower the HOMO–LUMO energy gap, which allows the absorption of an enlarged portion of the sunlight.[9]

The urge for developing renewable energy sources as well as the concern for global warming is increasing every year. On that account, the sun is a good alternative as energy source for converting light into electricity. In order to use the sun as an energy source, photovoltaic cells that convert sunlight into electricity are required. The commercial use of traditional silicon-based solar cells has been limited due to its high production costs. To overcome this problem, solar cells based on organic materials (like

conjugated polymeric materials) have been extensively studied as an alternative during the last few years.[10] Therefore, polymer solar cells (PSCs) are promising sustainable solar energy converters, because of their unique advantages over traditional silicon-based solar cells, such as low fabrication cost, lightweight and their potential for making flexible large area devices by roll-to-roll manufacturing.[11]

As electron donor materials in PSC devices, narrow band gap conjugated polymers are desired to harvest the sunlight, and different strategies of molecular design have been developed to prepare such materials. Building a donor−acceptor (D−A) alternating structure has been proved to be an effective way to reduce band gap of conjugated polymer materials. [12] To achieve high performance in optoelectronic devices, it is critical to tune physical properties such as solubility, band gap, molecular energy level, and carrier mobility by chemically modifying the polymer structure.

The band gap (E_g) of a polymer is defined as the energy difference between the HOMO and the LUMO, and is typically reported in electron volt (eV).[13] The band gap can be measured in different ways, where the two most important ones are the optical band gap, estimated from UV-Vis spectroscopy, and the electronic band gap, determined from Cyclic Voltammetry (CV).

Low band gap (LBG) polymers are loosely defined as polymers with a band gap below two eV, thus absorbing light with wavelengths longer than 620 nm. The band gap of a conjugated polymer is influenced by several factors, such as bond length alternation, aromaticity, conjugation length, substituents effect, intra-chain charge transfer and intermolecular interaction. Changing the bond length alternation will affect the size of the band gap. This has been demonstrated with polyisothianaphthene where the six-membered ring achieves aromaticity and stabilizes the quinoid structure resulting in a band gap of 1 eV compared to 2 eV for polythiophenes.[13,14]

Low band gap donor-acceptor (D-A) π-conjugated polymers which contain aromatic hetrocycles (Figure 2) have been synthesized using electron accepting units like quinoxaline (**8**), thienopyrazine (**9**), benzothiadazole (**10**), pyrazinoquinoxaline (**11**), and

electron donating units like carbazole (**12**), thiophene (**13**), phenylene (**14**) and fluorene (**15**).

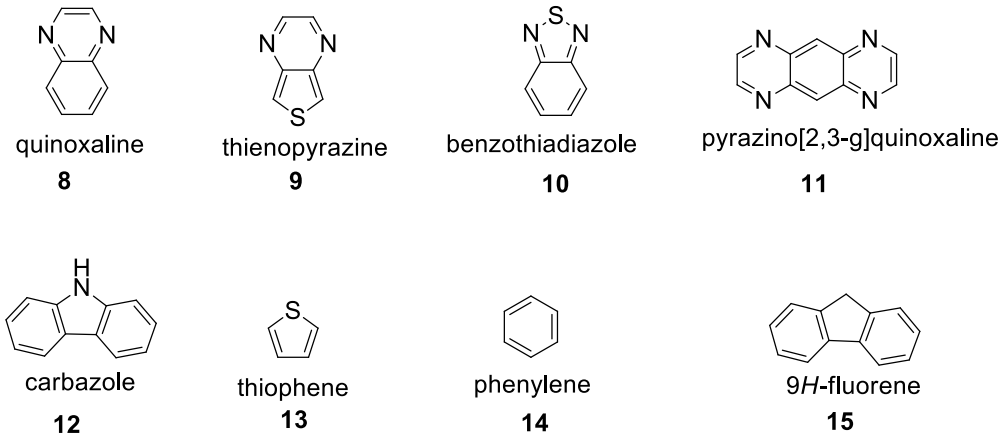

Figure 2: Chemical structures of some electron accepting and donating units used for synthesis of low band gap polymers.

2. LITERATURE REVIEW

Thiophene-containing polymers have emerged as an important class of semiconducting polymers. From applications to organic photovoltaics to light-emitting devices, this class of polymers has proven itself to be at the forefront of emerging organic materials technology, particularly in the field of energy related polymers. Polymers from these highly electron-rich thiophene monomers are easily synthesized using Stille coupling; thus, the method of Stille coupling conveys a key advantage in this area. The most important advantage of the Stille polycondensation over other methods is the wide tolerance of the method to a variety of functional groups.[15]

2.1. Synthesis of 1,2-diketones as intermediates toward the quinoxalines

A number of alternative methods for the synthesis of 1,2-diones are reported in the literature.

2.1.1. Diketones form alkenes and alkynes

One of the methods uses alkynes as starting materials rather than alkenes in order to synthesize the corresponding 1,2-diketones by oxidizing with potassium permanganate (Scheme 1).

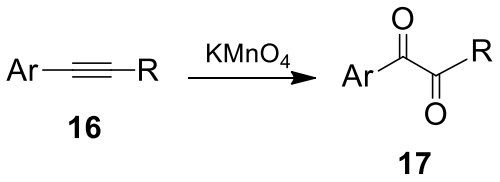

16 **17**

Scheme 1: Oxidation of alkynes to diketones using $KMnO_4$.

A convenient one-pot procedure via a Brønsted acid-promoted ″hydration″ and a DMSO-based oxidation sequence has also been achieved, which gives diketones in high yields Scheme 2.[16,17]

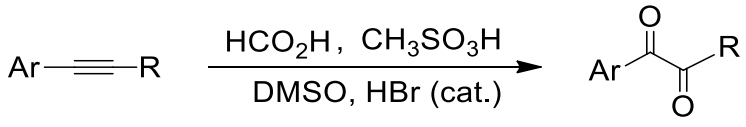

18 **19**

Scheme 2: Hydration and DMSO-based oxidation of alkynes to diketones.

Diketones were also constructed via a novel Ru-catalyzed alkene oxidation as shown in Scheme 3.[18,19]

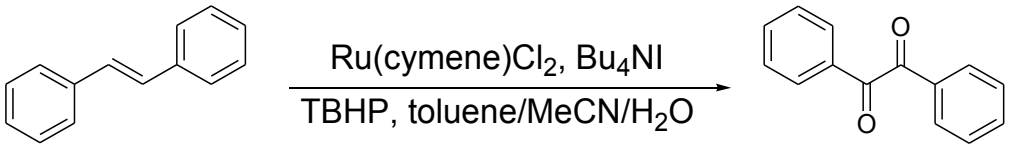

20 **21**

Scheme 3: Synthesis of benzil (**21**) from 1,2-diphenylethene (**20**)

2.1.2. The Grignard route towards diketones

The second alternative method uses Grignard reaction to prepare 1,2-diones. Thus, alkyl halides can be converted to the corresponding Grignard reagents and then reacted with oxalyl chloride to afford symmetrical diketones in a good yield (Scheme 4).[20–22]

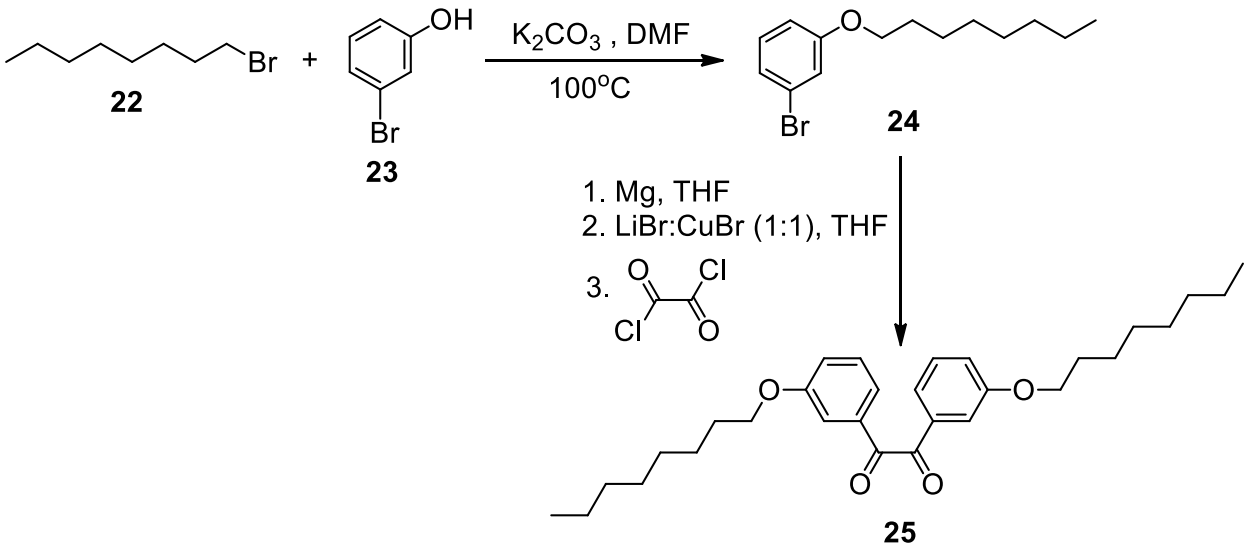

22 **23** **24** **25**

Scheme 4: Synthesis of diketone **25**

2.1.3. Diketones via the benzoin condensation

The third alternative method proceeds via benzoin condensation of aromatic aldehydes in the presence of alkali metal cyanide [23] in aqueous solution. Methods have also been developed using thiamine hydrogen chloride in basic medium, N,N-dimethylbenzimidazolium iodide in NaOH[24] and tetra-*n*-butylammonium bromide (TBAB) with KCN as a catalyst.[25] Alkylmethylimidazolium salts and 1,8-diazabicyclo[5.4.0]undec-7-ene (DBU) have also been used as catalysts for the benzoin condensation using solvent-free microwave activation conditions.[26]

The benzoin condensation catalyzed by cyanide ion was first described by Wöhler and Liebig in 1832 in which cyanide ion can serve four different roles such as high nucleophilic activity, facilitating the proton transfer, ability to stabilize the negative charge in active aldehyde intermediate and ability to depart finally.[27] In 1958 Breslow first recognized that the N-heterocyclic carbenes (NHCs) could also serve all these roles similar to that of cyanide ion in benzoin condensation and have better nucleophilic properties and leaving group abilities than cyanide as reported by Mavis *et al.*[28]

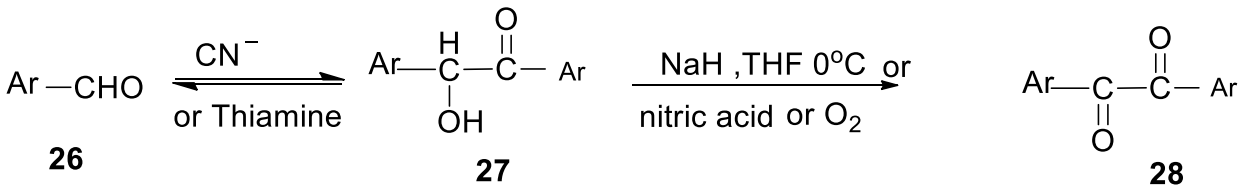

26 **27** **28**

Scheme 5: Benzoin condensation of benzaldehyde and its oxidation to 1,2-diketones.

The oxidative transformations of α-hydroxyketones to the corresponding α-diketones have been accomplished by the use of a wide variety of oxidizing reagents or catalysts and different reaction procedures. Among these are nitric acid, thallium(III) and Y(III) nitrate, bismuth(III) nitrate, copper(II) acetate, copper sulfate, ammonium nitrate, iron(II) thiolate and oxone, trichlorooxyvanadium and vanadium oxide, titanium(IV) chloride and triethylamine or molecular oxygen [29] and sodium hydride (Scheme 5).[30]

While all these methods can generate the desired products efficiently, many of the above oxidants are toxic and hazardous compounds, generating waste disposal problems. Therefore, the HBr-DMSO oxidation of benzoin to benzil was preferable and environmentally friendly to afford diketones in high yield.[31–33]

2.2. Synthetic approaches towards quinoxaline core-monomeric unit

Quinoxaline, or 1,4-benzodiazine, which is also known as benzopyrazine, is a heterocyclic compound containing a benzene ring and a pyrazine ring.[34] The syntheses of a large number of quinoxalines have been reported in the literature because of their importance in pharmaceuticals, in dyes, in organic semiconductors, etc... Such compounds usually display high electron affinities, good thermal stabilities, and good processability.[35] Quinoxaline derivatives have been widely used as the electron acceptors in donor–acceptor-type low-band-gap polymers for OPVs because of their good electron-accepting ability owing to the strong electronegativity of the two nitrogen atoms.

A number of synthetic strategies have been developed for preparation of substituted quinoxalines. Among these are condensation of aromatic diamines and dicarbonyl compounds, intramolecular cyclization of N-substituted aromatic *o*-diamines, oxidative ring transformation of benzodiazapines (Scheme 6), etc.[36–38] The most common method relies on the condensation of an aryl 1,2-diamines with 1,2-dicarbonyl compounds in refluxing ethanol or acetic acid for 2-12 h and this typically gives yields up to 70- 80%.[39]

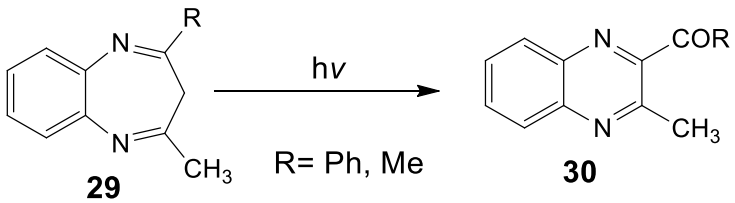

29 **30**

Scheme 6: Synthesis of quinoxaline from 1,5-benzodiazepine.

In 2005 Ji and Lee[40] demonstrated the synthesis of quinoxalines (Scheme 7) by the condensation between 1,2-phenylenediamines and 1,2-diketo compounds, which are prepared by the cross-coupling reactions of oxalyl chloride with mixed copper-magnesium reagents with yields as high as 96%.

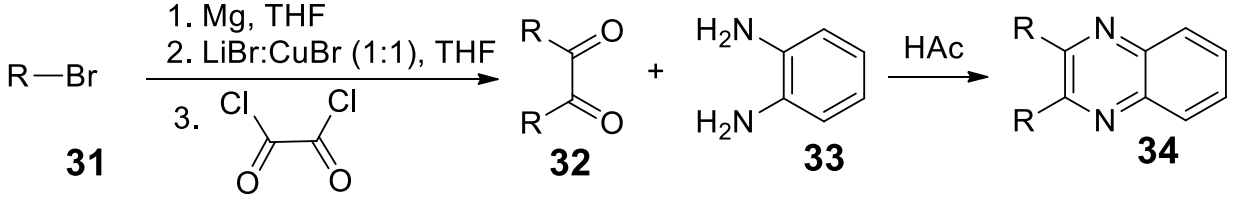

Scheme 7: Synthesis of quinoxalines starting from halides.

Quinoxalines have also been synthesized widely starting from benzo[*c*][1,2,5]thiadiazole (**10**) as shown in Scheme 8.

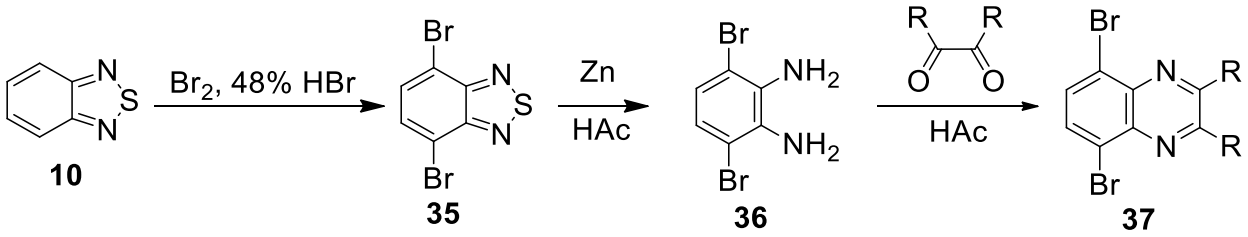

Scheme 8: Quinoxalines starting from benzo[*c*][1,2,5]thiadiazole.

Many conjugated polymers with D−A backbones have been prepared by using quinoxaline or its derivatives as electron-withdrawing building blocks in their backbones. These quinoxaline-based polymers generally exhibited interesting photovoltaic behaviors, and power conversion efficiencies (PCEs) up to 7% have been reported with polymers based on thiophene and quinoxaline (TQ).[41,42]

2.3. Synthesis of low band gap polymers

In recent years, low-band gap polymers based on the internal donor–acceptor (D–A) interaction have attracted great interest because their electronic properties can be easily tuned by proper combination of D and A units and their absorption ranges can be extended to longer wavelengths.[43] Such low band gap materials are promising for the development of photovoltaic cells (PVCs) because of the improved absorption of the solar photon flux. Besides improving processability by incorporating alkyl side chains on the polymer backbone, band-gap control can be achieved by incorporating alternating D and A moieties in the polymer main-chain. This causes a partial charge separation along the polymer backbone, which gives the polymer a lower band-gap.[44]

Currently two different approaches are usually employed in developing new narrow band gap polymers for bulk heterojunction (BHJ) solar cells.[34,45] The most common approach for low band gap polymer design was the donor-acceptor, also known as the push-pull approach to covalently link an electron-donating moiety and an electron-accepting moiety as the repeating units of the D-A copolymer.[46] Accordingly, its energy levels will be given by the lowest ionization potential and the highest electronic affinity of the monomers that compose the polymers. The band gap of such a polymer is tightened through the formation of a quinoid resonance structure via intramolecular charge transfer (ICT) (Scheme 9). The unique feature of this approach is that the HOMO levels of these D-A copolymers are predominantly determined by the donor moiety, and the LUMO almost exclusively resides on the acceptor moiety. This allows a largely independent control of the HOMO energy level (affecting open circuit voltage (V_{oc})) and the band gap (deciding the short circuit current (J_{sc})).[45]

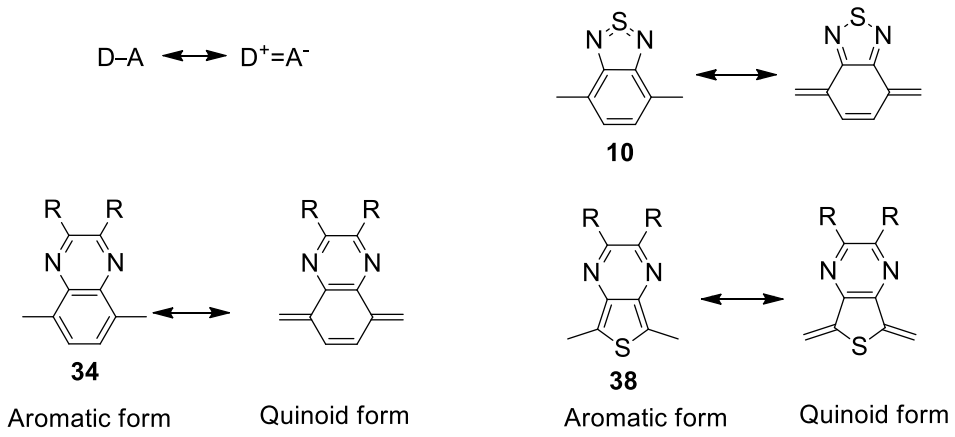

Scheme 9: Aromatic and quinoid forms of quinoxaline (**34**),benzo[*c*][1,2,5]thiadiazole (**10**) and thienopyrazine (**38**) units

Recently, the quinoxaline moiety has been shown to be a good acceptor that can be combined with appropriate donors in order to synthesis D-A type low band gap polymers because it can easily form ICT complexes with other donor components. PSCs fabricated from polymers containing quinoxaline units exhibited PCEs up to 7.08% as reported lately by Kim *et. al*.[47, 42] Some examples of D-A type low band gap polymers based on quinoxaline are depicted in Figure 3.

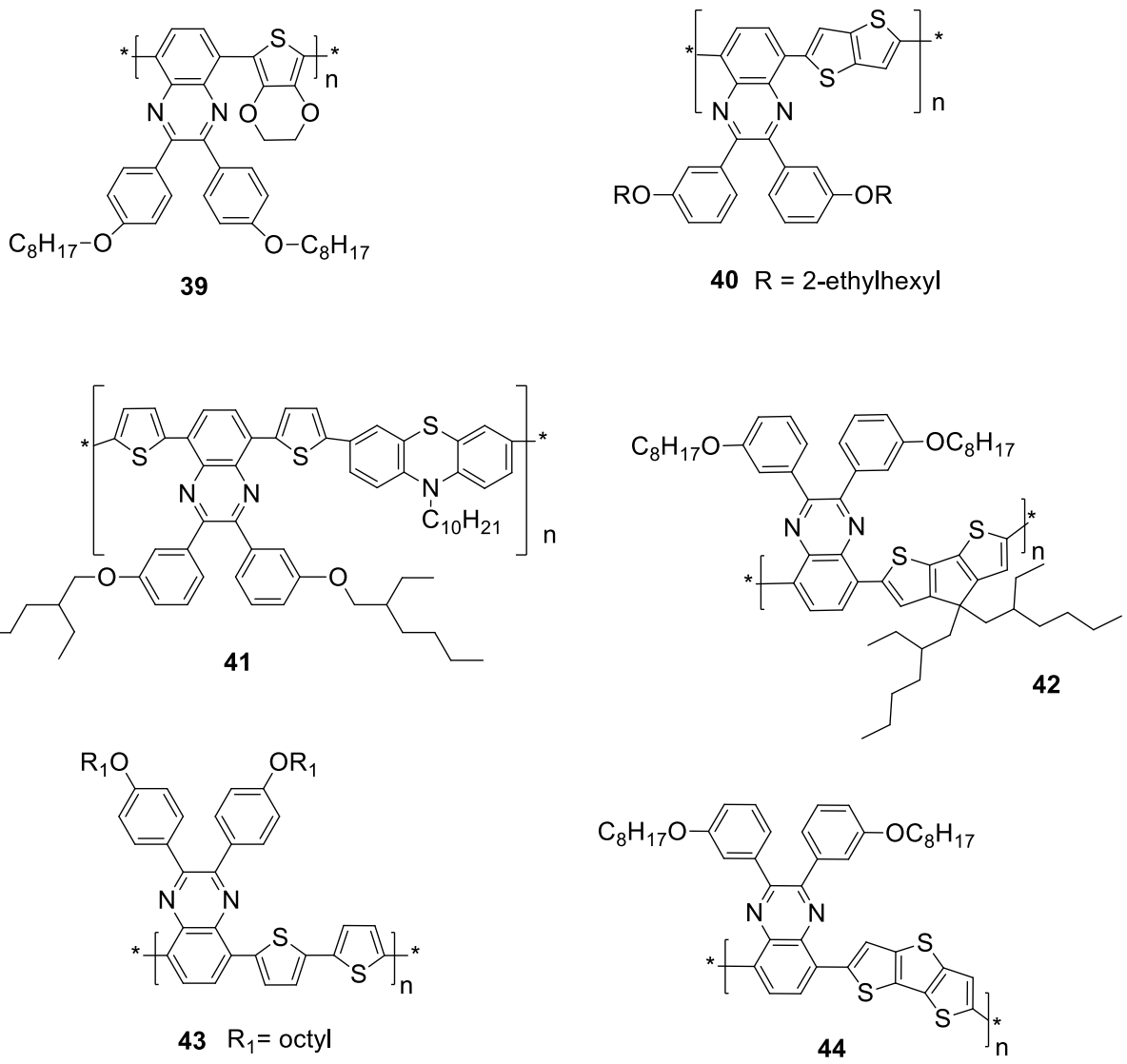

Figure 3: Examples of some quinoxaline-containing low band gap polymers

The second approach for low band gap polymer design was quinoid resonance structure stabilization, since the quinoid resonance form is lower in energy than the aromatic form. Therefore, stabilizing the quinoid form will effectively reduce the band gaps of the conjugated polymers.[48] The complete elimination of charged species in the resonance structure of the conjugated backbone and continuous π orbitals, both of which could potentially improve the hole mobility due to fewer instances of charge trapping, are the advantages of the approach. Its drawback is difficulty to control the HOMO/LUMO energy levels independently. This is due to lack of a designated electron donor and acceptor.[48]

The HOMO-LUMO band gap decreases linearly as a function of the increasing quinoid character of a conjugated polymer.[49] As a result, the acceptor that induces more quinoid population in the polymer backbone will have stronger band gap lowering ability. For acceptors **38**, **10** and **34** (Scheme 9), the increasing degree of the quinoid character was shown to be **38** > **10** > **34**. The thienopyrazine unit in the conjugated main chain tend to favorably adopt the quinoid form through π-electron delocalization in order to selectively preserve the pyrazine's aromaticity.[50]

2.4. Synthesis of polymers based on quinoxaline and thiophene

Thiophene and quinoxaline are typical electron-donating and electron-accepting units, respectively, used for the synthesis of conjugated low band gap polymers for solar cells. In 1996 Yamamoto *et al.*[51,52] prepared π-conjugated copolymers with thiophene as electron donating material and substituted quinoxalines as strong electron withdrawing material in high yield (Scheme 10).

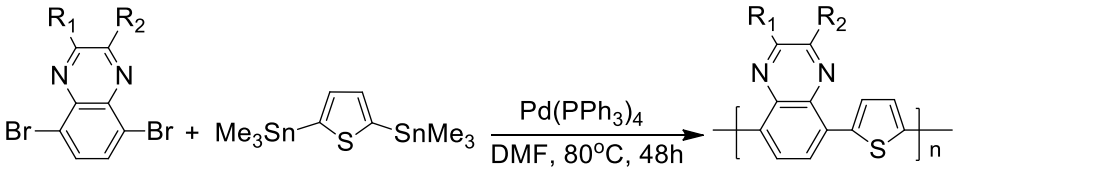

Scheme 10: Synthesis of alternating thiophene-quinoxaline copolymers by Stille cross-coupling reaction.

In 2002, Jonforsen *et al.*[53–55] prepared a poly(quinoxaline vinylene) (**50**) with dialkoxyphenyl side groups using Stille cross-coupling reaction (Scheme 11). Polymer **50** was found to be a better candidate as n-type material and was therefore expected to be more stable as well as soluble in common organic solvents.

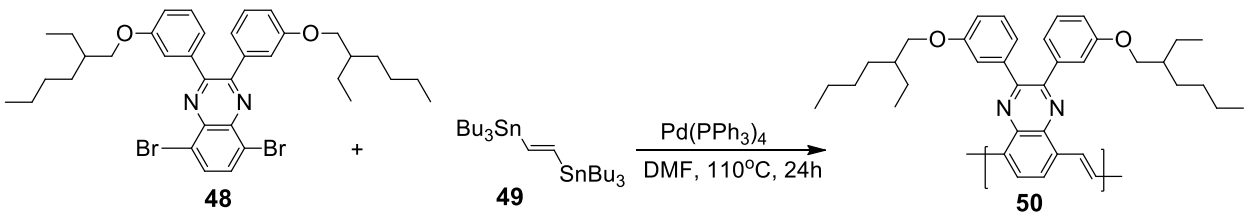

Scheme 11: Synthesis of a poly(quinoxaline vinylene) via the Stille cross-coupling reaction.

A simple conjugated copolymer based on thiophene and quinoxaline (**TQ1**) was synthesized and reported by Yamamoto *et al.* [56] in 2003 as depicted in Scheme 12. To obtain good solubility of the polymer, they introduced two *m*-octyloxyphenyl groups on to the pyrazine ring and the resulting polymer was soluble in common organic solvents and showed a broad absorption spectrum with absorption out to 700 nm.

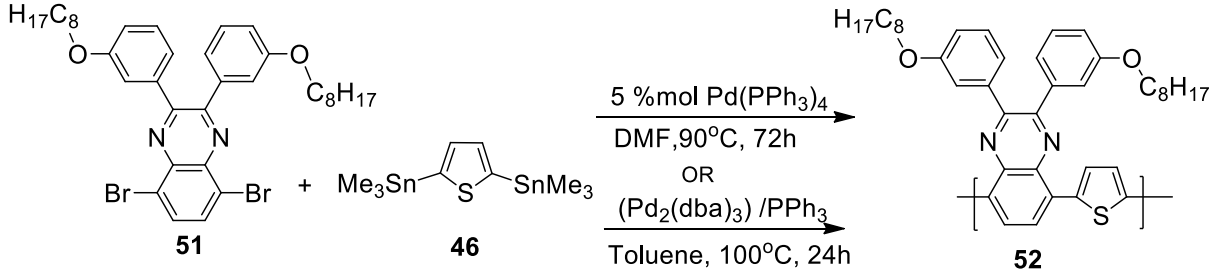

Scheme 12: Synthesis of TQ1 (**52**)

In 2010 Wang *et al*. [41] synthesized and used **52** in PSCs and achieved devices with efficiencies up to 6.0% in combination with $PC_{70}BM$ and 4.9% with $PC_{60}BM$. In addition to the high PCEs, the fabricated devices showed high V_{oc} values up to 0.9 V.

In 2013 Kim *et al.*[42] reported a maximum PCE higher than 7% for PSCs fabricated from **52** in combination with $PC_{71}BM$. Upon adding 5% (v/v) 1-chloronaphthalene to the BHJ active layer, a PCE as high as 7.08% with a J_{SC} of 12 mA cm^{-2} and V_{oc} of 0.91 V was achieved which was realized by the means of nanoscale morphology control induced by practical processing additives.

In order to further lower the HOMO energy level of **TQ1**, Dutta *et al.* [57] inserted fluorine atoms onto the quinoxaline moieties within the polymer backbone and synthesized two fluorinated analogues of **TQ**1 atoms as showed in Scheme 13. The effects of addition of F atoms on the optical properties, nature of charge transport, and molecular organization were investigated. **TQ-F** (**59**) and **TQ-FF** (**60**) showed a decrease in both the HOMO and the LUMO energy levels relative to the original **TQ1**. Moreover, the HOMO energy levels were lowered more than the LUMO energy levels, slightly widening the energy band gaps as the number of F atoms increased. Thus, use of these polymers in BHJ solar cells led to large V_{OC} values. The PCEs of the optimized PSCs based on **TQ-F** in combination with $PC_{71}BM$ without any additive reached 4.41%.[58]

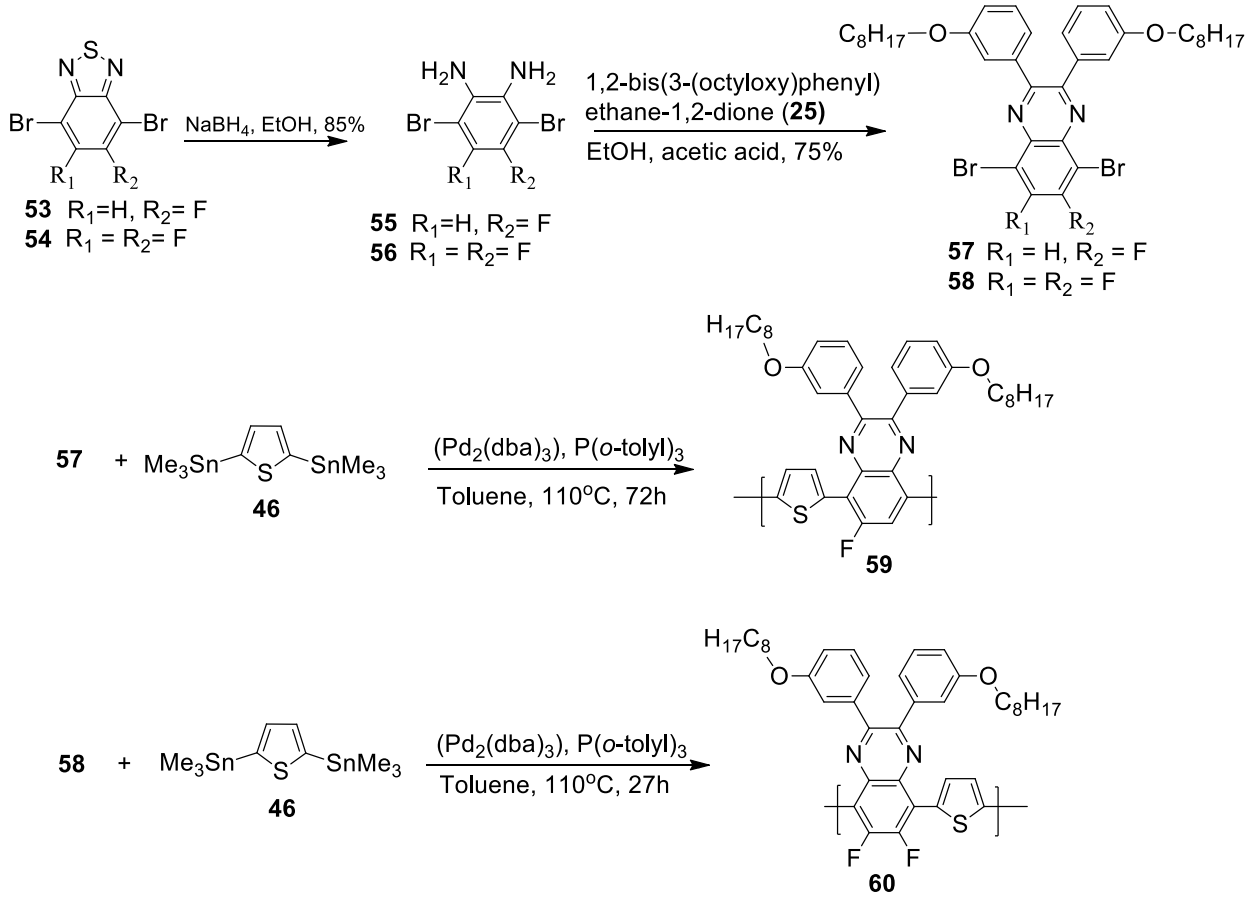

Scheme 13: Synthetic routes to TQ-F (**59**) and TQ-FF (**60**)

3. OBJECTIVE OF THE WORK

General objective

The aim of this graduate thesis is to synthesize some conjugated, low band gap alternating thiophene-quinoxaline (TQ)-based copolymers.

Specific objectives

- Syntheses and characterization of intermediate compounds and monomers starting from commercially available compounds.
- Synthesis of polymers by palladium(0)-catalyzed Stille cross coupling polymerization reaction.
- Characterization of the polymers by spectroscopic (UV, NMR) and electrochemical techniques (cyclic voltammetry, square wave voltammetry).
- Determination of optical and electrochemical band gaps of the polymers.

4. RESULTS AND DISCUSSION

In the course of this work, four conjugated alternating copolymers based on quinoxaline derivatives and thiophene units were synthesized using palladium(0)-catalyzed Stille coupling polymerization reactions.

The polymers were, poly[2,3-bis-(3-hexyloxyphenyl)quinoxaline-5,8-diyl-*alt*-thiophene-2,5-diyl] (**81**), poly[2,3-bis-(3-octyloxyphenyl)quinoxaline-5,8-diyl-*alt*-thiophene-2,5-diyl] (**52**), poly[2,3-bis-(3-decyloxyphenyl)quinoxaline-5,8-diyl-*alt*-thiophene-2,5-diyl] (**82**), and poly[2,3-bis-(3-dodecyloxyphenyl)quinoxaline-5,8-diyl-*alt*-thiophene-2,5-diyl] (**83**). The preparation and characterization of these polymers are discussed in the following sections.

4.1. Synthesis of quinoxaline derivatives

The synthesis of the quinoxaline derivatives began with the bromonation of benzo[*c*][1,2,5]thiadiazole (**10)** as shown in Scheme 14.

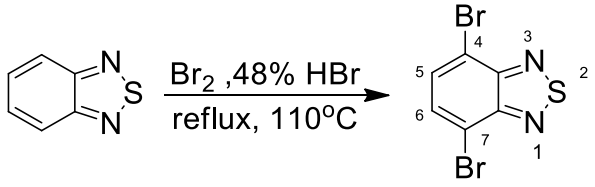

10 **35**

Scheme 14: Synthesis of 4,7-dibromobenzo[*c*][1,2,5]thiadiazole (**35**)

4,7-Dibromobenzo[*c*][1,2,5]thiadiazole (**35**) was prepared by dissolving benzo[*c*][1,2,5]thiadiazole (**10**) in 48% HBr followed by dropwise addition of molecular bromine (Br_2) in order to limit bromination to positions 4 and 7 as depicted in Scheme 14. The resulting product was purified by recrystallization from isopropanol to afford pure product **35** in 73.3% yield as a light yellow solid which melted at 164.1-165.5^oC (Lit.[59], mp = 187-188^oC). The ^{1}H-NMR spectrum of **35** showed only a singlet at δ 7.75 in agreement with the two chemically equivalent aromatic protons H-5 and H-6 in the molecule. The ^{13}C-NMR spectrum of **35** (Appendix 2) displayed only three carbon

resonances among which two are due to quaternary carbon atoms. The carbon resonance at δ 153.0 is due to the quaternary carbon atoms connected to the thiadiazole moiety at C-8 and C-9. The carbon signal at δ 113.9 is attributable to C-4 and C-7 to which the bromine atoms are attached. The only methine carbon signal at δ 132.4 is due to C-5 and C-6. The FT-IR spectrum of **35** showed aromatic C-H stretching at 3042 cm^{-1} and aromatic mode at 1641(C=N), 1310, 1185 and C-Br stretching band at 586 cm^{-1}. The UV-Vis spectrum of the **35** in chloroform solution showed λ_{max} around 306 and 356 nm, which correspond to π-π^* and n-π transitions, respectively.

4.2. Syntheses of 1,2-diketones

Scheme 15 shows the general strategy adopted to prepare 1,2-diketones. The syntheses began by alkylating 3-hydroxybenzaldehyde (**61**) with a variety of alkylating agents as described below.

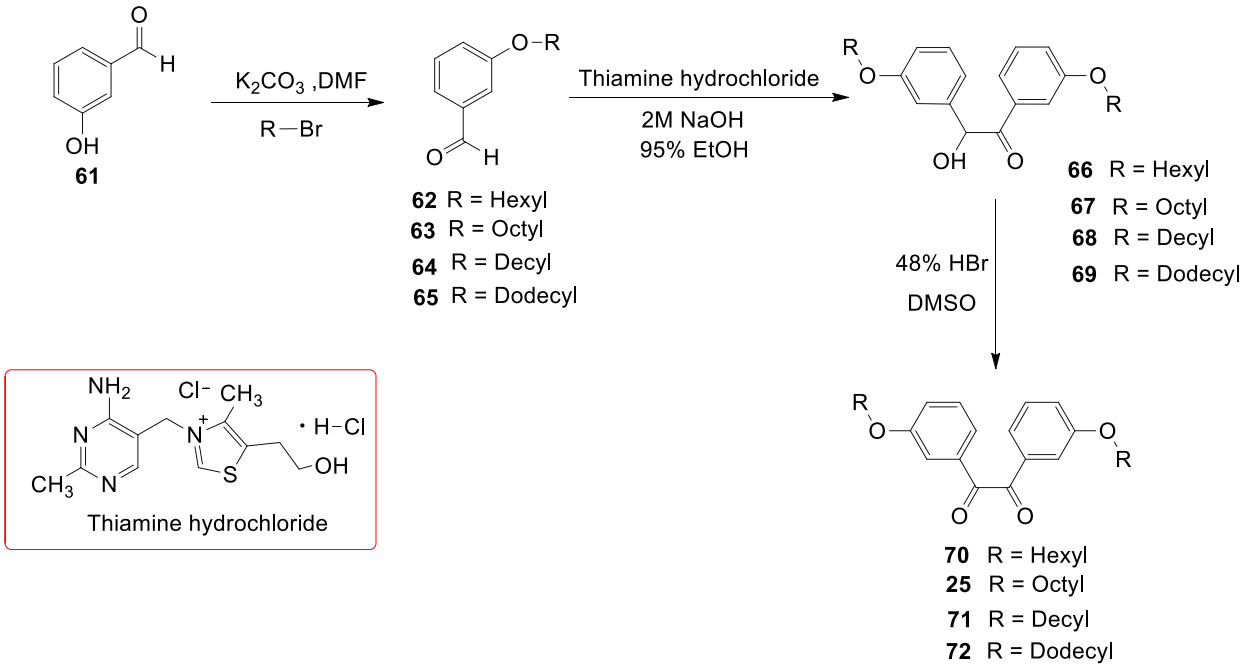

Scheme 15: Syntheses of 1,2-diketones.

4.2.1. Synthesis of 3-(decyloxy)benzaldehyde (64)

3-(Decyloxy)benzaldehyde (**64**) was synthesized by the alkylation of 3-hydroxybenzaldehyde (**61**) with 1-bromodecane in the presence of K_2CO_3 in DMF at 100^oC as outlined in Scheme 15. Purification of the crude product was achieved by passing it through a short column of silica gel using petroleum ether as eluent. Compound **64** was obtained as a yellow oily liquid in 97.1% yield. The ^{1}H-NMR spectrum of **64** (Appendix 4, Table 1) showed a singlet at δ 9.97 due to the aldehyde proton. The two-proton multiplet at δ 7.45- 7.42 is due to H-6 and H-2. The doublet at δ 7.38 (*J* = 2.0 Hz) is due to aromatic proton that attribute to H-5. The multiplet centered at δ 7.17 is due to aromatic proton, which is attributed to H-4. The triplet at δ 4.01 integrating for two protons is assigned to the H-1′, which is on the carbon atom attached to oxygen, and the quintets centered at δ 1.81 and δ 1.47, integrating for two protons each, are due to the methylene protons at C-2′ and C-9′, respectively. The multiplet between δ 1.33-1.29, integrating for twelve protons, is attributed to the six-methylene groups and the triplet at δ 0.89, integrating for three protons, is attributed to the terminal methyl group (Figure 4).

The ^{13}C-NMR spectrum of **64** displayed a total of fourteen carbon resonances of which seven appeared in the aromatic region and seven in the aliphatic region. The DEPT-135 spectrum revealed that there are one methyl, nine methylene, five methine and two quaternary carbon atoms. The carbon signals at δ 159.7 and 137.8 are quaternary carbons, which correspond to C-3 and C-1, respectively. The methine carbon signal at δ 192.2 is due to the aldehyde carbon. The remaining methine carbon signals in the aromatic region, which appeared at δ 130.0, 123.3, 121.9 and 112.7, are attributable to C-5, C-6, C-4 and C-2, respectively. The nine methylene carbon resonances appeared in the region between at δ 68.3 and 22.7 and the signal due to the terminal methyl group appeared at δ 14.1 (Table 2). The FT-IR spectrum of **64** showed an intense absorption band at 2962 cm^{-1} due to the C-H stretching of the alkylated benzaldhyde. The weak bands at 3069 and 2724 cm^{-1} are due to aromatic C-H and aldehyde H-C=O stretching, respectively. The intense sharp band at 1702 cm^{-1} is due to the carbonyl C=O stretching and the sharp band at 1263 cm^{-1} is due to C-O stretching. The weak

bands between 1599 and 1453 cm^{-1} are due to the aromatic C=C stretching and C-H bending. The UV-Vis spectrum of compound **64** in $CHCl_3$ solution showed absorption maxima (λ_{max}) at 256 and 316 nm which correspond to electronic transitions due to the conjugated aromatic system (π-π^*) and lone pair of oxygen (n-π^*), respectively.

4.2.2. Synthesis of 3-(octyloxy)benzaldehyde (63)

3-(Octyloxy)benzaldehyde (**63**) was synthesized following similar procedure like compound **64** in which 1-bromooctane was used as the alkylating agent. Compound **63** was obtained as a yellowish oily liquid.

The ^{1}H-NMR spectrum (Table 1) resembled that of **64** except for the number of methylene protons. The ^{13}C-NMR (Table 2) and DEPT-135 spectra of **63** displayed only seven methylene carbon resonances in the aliphatic region in agreement with the structure of compound **63**. The FT-IR spectrum of **63** revealed similar signals as that of **64** except for some small shifts. The UV-Vis spectrum of **63** was identical to that of **64**.

4.2.3. Synthesis of 3-(hexyloxy)benzaldehyde (62)

The synthesis of compound **62** followed a similar synthetic procedure as that described above for compound **64** except that 1-bromohexane was used as the alkylating agent to afford **62** as an oily material. The ^{1}H-NMR spectrum (Table 1) revealed signals due to thirteen aliphatic protons, four aromatic protons and one aldehydic proton. The ^{13}C-NMR (Table 2) and DEPT-135 spectra of **62** displayed six aliphatic carbon resonances in the aliphatic region of which five are due to methylene carbon resonances in agreement with the structure of **62**. The FT-IR spectrum of **62** was similar to those of **64** and **63**. The UV-Vis spectrum of **62** in chloroform solution displayed λ_{max} at 255 and 312 nm which correspond to the (π-π*) and (n-π*) electronic transition, respectively.

4.2.4. Synthesis of 3-(dodecyloxy)benzaldehyde (65)

3-(Dodecyloxy)benzaldehyde (**65**) was prepared by alkylation of 3-hydroxybenzaldehyde (**61**) using 1-bromododecane as the alkylating agent in the

presence of K_2CO_3 in DMF following a similar synthetic procedure as that used for the preparation of **64** to afford the tittle compound as an oily material.

The ^{1}H-NMR spectrum (Table 1) of **65** showed an intense broad signal centered at δ 1.27 integrating for sixteen protons. The remaining proton resonances had similar chemical shifts as those observed for **64.** The ^{13}C-NMR (Table 2) and DEPT-135 spectra revealed the presence of eleven methylene carbon resonances in agreement with the structure of **65**. The UV-Vis spectrum of **65** in chloroform solution displayed λ_{max} at 254 and 311 nm which are attributable to the (π-π^*) and (n-π^*) electronic transition, respectively.

Table 1: ^{1}H-NMR (400.13 MHz, $CDCl_3$) data (δ_{ppm}) of 3-alkoxybenzaldehydes **62**, **63**, **64** and **65**.

62	**63**	**64**	**65**
9.97	9.98	9.97	9.95
(1H, s, CHO)	(1H, *s*, CHO)	(1H, *s*, CHO)	(1H, *s*, CHO)
7.44-7.41	7.46-7.44	7.44-7.42	7.43-7.41
(2H, *m*, H-6, H-2)	(2H, *m*, H-6, H-2)	(2H, *m*, H-2, H-6)	(2H, *m*, H-6, H-4)
7.38	7.40	7.38	7.37
(1H, *d*, *J*=2.1Hz, H-5)	(1H, *d*, *J*=2.3Hz, H-5)	(1H,*d*, *J*=2.0Hz, H-5)	(1H, *s*, H-2)
7.18	7.20-7.17	7.17	7.16
(1H, *m*, H-4)	(1H, *m*, H-4)	(1H, *m*, Ar-H, H-4)	(1H, *m*, H-5)
4.01	4.01	4.01	3.99
(2H, *t*, H-1′)	(2H, *t*, H-1′)	(2H, *t*, H-1′)	(2H, *m*, H-1′)
1.81	1.81	1.81	1.79
(2H, *q*, H-2′)	(2H, *q*, H-2′)	(2H, *q*, H-2′)	(2H, *q*, H-2′)
1.47	1.49	1.47	1.46
(2H, *m*, H-5′)	(2H, *m*, H-7′)	(2H, *m*, H-9′)	(2H, *m*, H-11′)
1.38-1.31	1.37-1.32	1.33-1.29	1.27
(4H, *m*, 2xCH_2)	(8H, br, 4xCH_2)	(12H, *br*, 6xCH_2)	(16H, *br*, 8xCH_2)
0.91	0.90	0.89	0.88
(3H, *t*, H-6′)	(3H, *t*, H-8′)	(3H, *t*, H-10′)	(3H, *t*, H-12′)

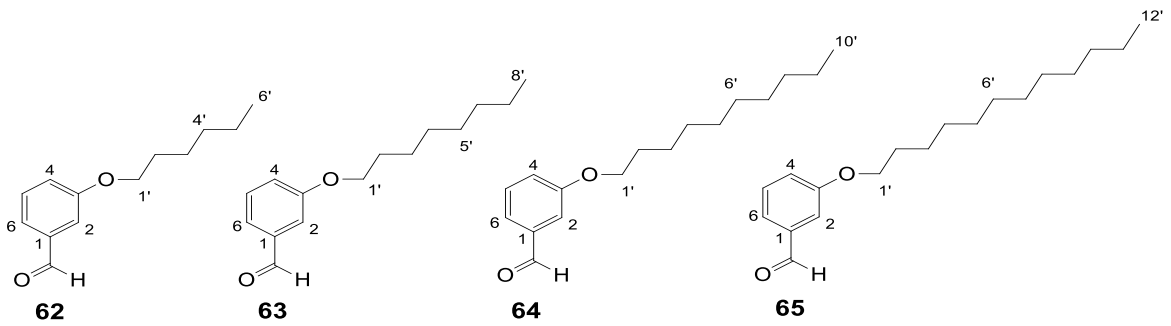

Figure 4: Structures of alkylated benzaldehydes.

Table 2: ^{13}C-NMR (100.6 MHz, $CDCl_3$) data (δ_{ppm}) of 3-alkoxybenzaldehydes **62**, **63**, **64** and **65**.

Carbon	62	63	64	65
C=O	192.2	192.2	192.2	192.2
1	137.8	137.8	137.8	137.8
2	112.4	112.8	112.7	112.8
3	159.7	159.7	159.7	159.7
4	121.9	121.9	121.9	121.9
5	130.0	130.0	130.0	129.9
6	123.3	123.3	123.3	123.2
1′	68.3	68.3	68.3	68.3
2′	29.1	29.4	29.6	29.7
3′	25.7	26.0	26.0	26.0
4′	31.5	29.3	29.6	29.5
5′	22.6	29.2	29.4	29.4
6′	14.0	31.8	29.3	29.6
7′	-	22.7	29.1	29.6
8′	-	14.1	31.9	29.7
9′	-	-	22.7	29.1
10′	-	-	14.1	31.9
11′	-	-	-	22.7
12′	-	-	-	14.1

4.2.5. Benzoin condensation of the aldehydes

The benzoin condensation reactions of the 3-alkoxybenzaldehydes discussed above were conducted with thiamine hydrochloride as the catalyst in the presence of NaOH as shown in Scheme 15. The resulting oily crude products were then purified by silica gel column chromatography using hexane: ethyl acetate (12:1) as eluent to afford the corresponding α-hydroxylketones in an overall yield of 9.0**%** - 16.3%.

The first step in the reaction mechanism (Scheme 16) is to convert thiamine to its thiazolium ion by deprotonation with NaOH. Since the thiazolium ion is a good nucleophile, it will attack the benzaldehyde carbonyl to form an alkylated thiazole derivative. Intramolecular proton transfer followed by attack of a second benzaldehyde molecule by the resulting carbanion will give rise to an oxyanion, which will fragment to give an α-hydroxylketone and the thiazolium ion catalyst.[60,61]

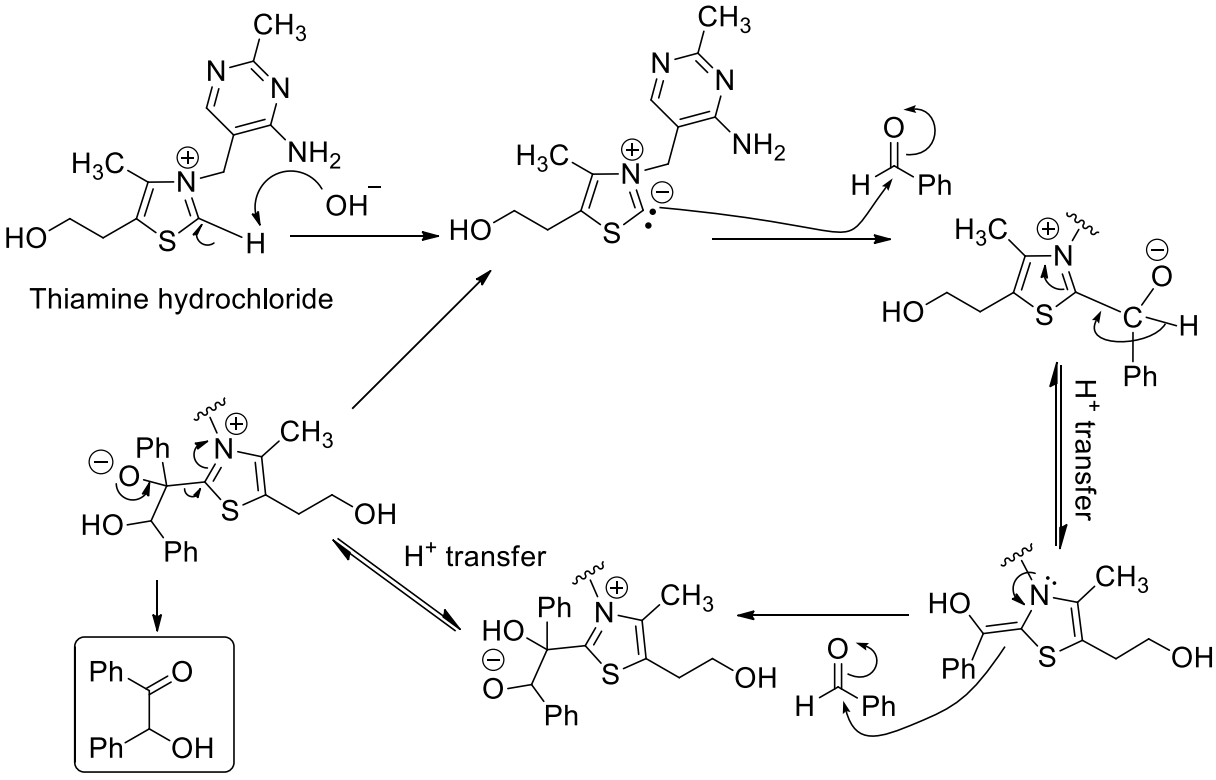

Scheme 16: The mechanism of the thiamine-catalyzed benzoin condensation.

4.2.5.1 Synthesis of 2-hydroxy-1,2-bis(3-decyloxyphenyl) ethanone (68)

The thiamine-catalyzed benzoin condensation reaction of 3-decyloxybenzaldehyde (**64**) afforded compound **68** as a pale yellow solid that melts at 42.2-43.5^{o}C in an overall yield of 14.1%.

The ^{1}H-NMR spectrum of compound **68** (Table 3, Appendix 7) showed six signals in the aromatic and six signals in the aliphatic region. The multiplet at δ 7.49-7.46 is due to two aromatic protons, and is attributable to H-2 and H-6. The two-proton multiplet at δ 7.31-7.22 is due to H-5 and H-5′. The one-proton doublet of doublet at δ 7.07 (*J* = 2.0, 8.2 Hz) is due to H-4′. The doublet at δ 6.92 (*J* = 7.7 Hz) is assigned to H-4. The one-proton doublet at δ 6.86 (*J* = 2.0 Hz) is attributed to H-6′. The doublet of doublet between δ 6.83 and 6.80 (*J* = 2.0, 8.0 Hz) corresponds to H-2′. The signal due to the aliphatic proton alpha to the carbonyl appeared as a singlet at δ 5.90. The overlapping multiplets at δ 3.97-3.90 integrated for four protons are due to the H-1″ and H-1‴ methylene protons attached to oxygen atoms. The multiplet at δ 1.81-1.72 and 1.45-1.42 integrated for four protons each are attributed to methylene protons H-2″, H-2‴ and H-9″, H-9‴, respectively. The intense broad signals at δ 1.32-1.29 integrated to twenty-four protons are due to aliphatic proton of methylene, which attributes to H-3″– H-8″ and H-3‴– H-8‴. The signals due to the six terminal methyl protons were displayed at δ 0.91 as a triplet.

The ^{13}C-NMR spectrum of compound **68** (Table 4 and Appendix 8) displayed total of twenty-five carbon resonances of which thirteen appeared in the aromatic region and twelve in the aliphatic region. The DEPT-135 spectrum revealed that there are two methyl, nine methylene, nine methine and five quaternary carbon atoms. The carbon signals at δ 198.7, 159.7, 159.3, 140.4 and 134.7 are quaternary carbons which correspond to C-b, C-3′, C-3, C-1, and C-1′, respectively, in agreement with the structure of **68**. The methine carbon signal at 76.2 is attributable to C-a. There are two methylene carbon signals at δ 68.3 and 68.0, which are assignable to the oxygenated carbon atoms C-1″ and C-1‴, respectively. The remaining eight-methylene carbon resonances appeared between δ 22.7 and 31.9, and correspond to a total of 16 carbon

atoms. The methyl carbon signal at δ 14.4 is due to terminal methyl groups(C-10″ and 10‴).

The FT-IR (KBr, cm^{-1}) spectrum of compound **68** (Appendix 41) shows a broad band at 3446 cm^{-1} due to the O-H stretching which confirms the formation of the α-hydroxyketone. Intense sharp bands at 2922 and 2852 cm^{-1} are due to aliphatic C-H stretching of the α-hydroxyketone derivative. Medium intensity bands at 1676 cm^{-1} and 1585 cm^{-1} are due to the carbonyl C=O and aromatic symmetric C=C stretching vibrations, respectively. The weak band at 1447 cm^{-1} is due to the aromatic C=C stretching with in the ring and C-H bending. The sharp band at 1269 cm^{-1} is due to C-O stretching. A weak band around 1030 cm^{-1} is due to aromatic C-H in plane and out of plane deformation. A weak band around 780 cm^{-1} is due to methylene ($-CH_2$) rocking. The UV-Vis of compound **68** in $CHCl_3$ solution showed λ_{max} at 259 and 319 nm which correspond to electronic transition due to conjugated aromatic system (π-π^*) and lone pair of oxygen (n-π^*), respectively.

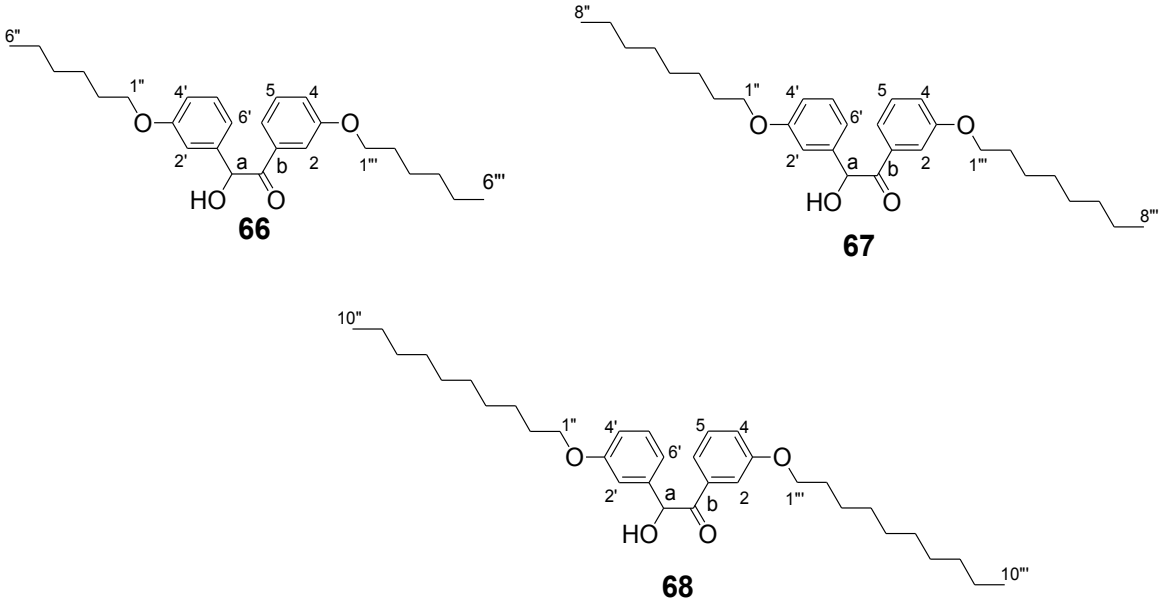

Figure 5: Structures of the α-hydroxyketones **66**, **67** and **68.**

4.2.5.2. Synthesis of 2-hydroxy-1,2-bis(3-octylyloxyphenyl)ethanone (67)

Compound **67** was synthesized following the same procedure discussed above for **68** in which **63** was used as a starting material instead of **64** (Scheme 15) to afford the tittle compound as an oily product in an overall yield of 9.1**%**.

The ^{1}H-NMR spectrum (Table 3) of **67** revealed the presence of two 1,3-disubstituted aromatic rings and gave characteristic signals for the alipahatic protons. The ^{13}C-NMR spectrum of **67** showed signals at δ 198.7 and 76.2 confirming the presence of the α-hydroxyketone moiety which was further confirmed by the FT-IR spectrum, which showed bands at 1681, and 3451 cm^{-1} due to carbonyl and hydroxyl groups, respectively. The DEPT-135 spectrum revealed five quaternary and eight methine carbon signals above δ 100 ppm and one methine, seven methylene and one methyl carbon signals in the aliphatic region in agreement with structure **67.** The UV-Vis spectrum (in $CHCl_3$ solution) showed absorption maxima at 259 and 316 nm which correspond to electronic transitions due to conjugated aromatic system (π-π^*) and lone pair of electron on oxygen (n-π^*), respectively.

4.2.5.3. Synthesis of 2-hydroxy-1,2-bis(3-dodecyloxyphenyl)ethanone (69)

Compound **69** was synthesized following the same synthetic procedure as described above for **68** to afford the α-hydroxyketone as a light yellow oily material. The ^{1}H-NMR spectrum of compound **69** confirms the isolated product as the mixture of the desired product and its oxidation product, which was used for the next reaction without further purification.

4.2.5.4. Synthesis of 2-hydroxy-1,2-bis(3-hexyloxyphenyl)ethanone (66)

Compound **66** was prepared following the same synthetic procedure described above for **68.** It was obtained in 16.3% overall yield as a pale yellow solid which melted at 47.6- 49.2^{o}C.

The ^{1}H (Table 3) and ^{13}C-NMR spectrum of **66** had similar patterns as the corresponding spectra of compound **68** except for the differences arising because of the numbers of proton and carbon atoms. The FT-IR and UV-Vis spectra of the two compounds revealed similar behaviors.

Table 3: ^{1}H-NMR ($CDCl_3$, 400.13 MHz) data (δ_{ppm}) of benzoin derivatives.

66	**67**	**68**
7.49-7.47	7.49-7.47	7.49-7.46
(2H, *s*, H-2, H-6)	(2H, *m*, H-2, H-6)	(2H, *m*, H-6, H-2)
7.32-7.22	7.29-7.20	7.32-7.22
(2H, *m*, H-5, H-5′)	(2H, *m*, H-5, H-5′)	(2H, *m*, H-5, H-5′)
7.09-7.06	7.07-7.04	7.08-7.05
(1H, *dd*, *J*=2.4, 8.2Hz, H-4′)	(1H, *dd*, *J*=1.9, 8.6 Hz, H-4′)	(1H, *dd*, *J*= 2.0, 8.2 Hz, H-4′)
6.94	6.93-6.91	6.92
(1H, *d*, *J*= 7.7Hz , H-4)	(1H, *d*, *J*=7.7Hz , H-4)	(1H, *d*, J = 7.7 Hz, H-4)
6.86	6.88	6.86
(1H, *s,* H-2′)	(1H, *s,* H-2′)	(1H, *d, J*= 2.1 Hz, H-6′)
6.83-6.80	6.82-6.79	6.83-6.80
(1H, *dd*, *J*=2.3, 8.2Hz, H-6′)	(1H, *dd*, *J*=1.8, 8.2Hz, H-6′)	(1H, *dd*, *J*=2.1, 8.0Hz, H-2′)
5.90	5.90	5.90
(1H, *s*, H-b)	(1H, *s*, H-b)	(1H, *s*, H-b)
3.96-3.90	3.96-3.88	3.97-3.90
(4H, *m*, H-1″, H-1‴)	(4H, *m*, H-1″, H-1‴)	(4H, *m*, H-1″, H-1‴)
1.80-1.74	1.79-1.71	1.81-1.72
(4H, *m*, H-2″, H-2‴)	(4H, *m*, H-2″, H-2‴)	(4H, *m*, H-2″, H-2‴)
1.46-1.43	1.45-1.42	1.45-1.42
(4H, *m*, H-5″, H-5‴)	(4H, *m*, H-7″, H-7‴)	(4H, *m*, H-9″, H-9‴)
1.37-1.34	1.35-1.31	1.32-1.29
(8H, *br*, 4x -CH_2)	(16H, *br*, 8 x -CH_2)	(24H, *br*, 12 x -CH_2)
0.93	0.92	0.91
(6H, *t*, H-6″, H-6‴)	(6H, *t,* H-8″, H-8‴)	(6H, *t,* H-10″,H-10‴)

Table 4: ^{13}C-NMR (100.6 MHz, $CDCl_3$) data (δ_{ppm}) of benzoin derivatives **66**, **67** and **68**.

Carbon	66	67	68
b	189.7	198.7	198.7
a	76.2	76.2	76.2
1	140.4	140.4	140.4
2	113.7	113.7	113.7
3	159.3	159.3	159.3
4	119.9	119.9	119.9
5	129.6	129.6	129.6
6	121.0	121.0	121.6
1′	134.7	134.7	134.7
2′	113.8	114.7	114.7
3′	159.7	159.7	159.7
4′	114.7	113.9	112.8
5′	130.1	130.1	130.1
6′	121.6	121.6	121.1
1″, 1‴	68.2, 68.0	68.2, 68.0	68.3, 68.0
2″, 2‴	29.2, 29.1	29.4	29.4
3″, 3‴	25.7	26.0	26.0
4″, 4‴	31.6, 31.5	29.3	29.4
5″, 5‴	22.6	29.1	29.3
6″, 6‴	14.0	31.8, 32.8	29.2
7″, 7‴	-	22.7	29.1
8″, 8‴	-	14.1	31.9
9″, 9‴	-	-	22.7
10″, 10‴	-	-	14.1

4.2.6. Conversion of α-hydroxyketones to 1,2-diketones

The 1,2-diketones **25**, **70**, **71** and **72** (Figure 6) were synthesized by the oxidation of the respective α-hydroxyketones with 48% hydrobromic acid in dimethyl sulfoxide at 90^{o}C (Scheme 15). The products were first obtained as yellow suspension, which were poured in to cold water, filtered, and then washed with cold water and ethanol to afford the 1,2-diketones in high yield.

4.2.6.1. 1,2-Bis(3-(decyloxy)phenyl)ethane-1,2-dione (71)

Compound **71** was prepared by the oxidation of **68** and was obtained as a yellow solid in 93.3% yield, which melted at 57.6- 58.4^{o}C. The ^{1}H-NMR spectrum of **71** (Table 5, Appendix 16) showed four signals in the aromatic and five signals in the aliphatic region. The multiplet at δ 7.53 (*J* = 2.4 Hz) and doublet δ 7.47 (*J* = 7.6 Hz) integrating for one proton each are due to H-6 and H-5, respectively. The triplet at δ 7.40 is due to H-2′ and the doublet of doublet at δ 7.21 (*J* = 8.1, 2.6 Hz) corresponds to H-4′. The triplet at δ 4.03 integrating for two protons is due to methylene protons at C-1′, which are on the carbon atoms attached to oxygen. The quintets at δ 1.81 and 1.48, integrating for two protons each, are due to the methylene proton at C-2′ and C-9′, respectively. The intense broad signal between δ 1.36 and 1.30, integrating for twelve protons, is due to the methylene protons H-3′ – H-8′. The triplet at δ 0.91 is due to the terminal methyl protons at C-10′.

The ^{13}C-NMR spectrum of **71** (Table 6, Appendix 17) displayed seventeen carbon resonances of which one is due to a carbonyl carbon, six are due to aromatic carbons, and ten are due to aliphatic carbons. The DEPT-135 spectrum revealed that there are one methyl, nine methylene, four methine and three quaternary carbon resonances. The carbon signals at δ 194.5, 159.6 and 134.2 are quaternary carbons which correspond to C-a, C-3 and C-1, respectively. The four methine carbon signals at δ 130.0, 122.9, 122.2 and 113.7 are assignable to C-5, C-6, C-4 and C-2, respectively. The methylene carbon resonance at δ 68.4 is due to C-1′ and the remaining eight methylene carbon resonances between δ 22.7 and 31.9 are attributable C-2′-C-9′. The carbon signal at δ 14.1 is due to the terminal methyl group (C-10′). The FT-IR (KBr, cm^{-1}) spectrum of **71** showed intense sharp bands around 2953 and 2925 cm^{-1} due to aliphatic C-H stretching. The weak band around 3076 cm^{-1} is due to the aromatic C-H stretching. The absence of a broad band at 3446 cm^{-1} confirms complete conversion of the α-hydroxyketone to the corresponding 1,2-diketone. The sharp band at 1678 cm^{-1} is due to conjugated carbonyl (C=O) stretching and the band around 1438 cm^{-1} is due to -C=C- stretching with in the aromatic systems. The sharp intense bands at 1155 and 1262 cm $^{-1}$ are due to C–O stretching. The UV-Vis spectrum of **71** in $CHCl_3$ solution showed

absorption maxima at 265 and 325 nm which correspond to electronic transition due to conjugated aromatic system (π-π^*) and lone pair of oxygen (n-π^*), respectively. These are similar to that of the starting material **68** except for small shift to higher wavelengths due to conjugation of C=O with the aromatic system.

4.2.6.2. 1,2-Bis (3-(octyloxy)phenyl)ethane-1,2-dione (25)

Compound **25** was prepared by oxidation of **67** as shown in Scheme 15 following the same procedure discussed above for **71**. It was obtained as a yellow solid in 82.7% yield, which melted in the range of 50.7-51.6^{o}C.

The ^{1}H- (Table 5) and ^{13}C-NMR spectra of **25** (Table 6) had similar patterns as the corresponding spectra of compound **71** except for the differences arising because of the numbers of proton and carbon atoms in the aliphatic region. The FT-IR (KBr, cm^{-1}) spectrum of **25** revealed similar bands as **71**. The weak band at 3074cm^{-1} is attributed to aromatic C-H stretching. Intense bands at 2953, 2927 and 2856 cm-1 were due to aliphatic C-H stretching of the corresponding alkylated 1,2-diketones. The absence of broad band at 3451 cm^{-1} also confirms complete conversion of the α-hydroxyketone to the corresponding 1,2-diketone . A sharp intense band at 1679cm^{-1} is due to conjugated carbonyl (C=O) stretching. The band at 1597-1438 cm^{-1} is due to (-C=C) stretching with in the aromatic systems. The UV-Vis spectrum (in $CHCl_3$ solution) showed absorption maxima at 265 and 324 nm which correspond to electronic transitions due to conjugated aromatic system (π-π^*) and lone pair of electrons on oxygen (n-π^*), respectively.

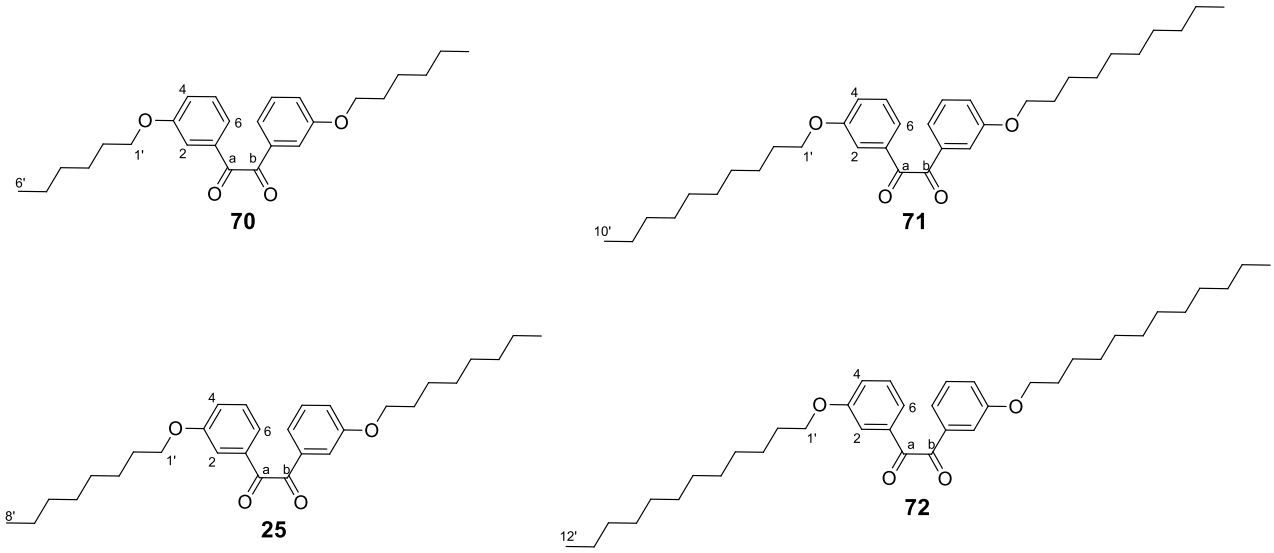

Figure 6: Structures of 1, 2-bis(3-(alkyloxy)phenyl)ethane-1,2-diones.

4.2.6.3. 1,2-Bis(3-(dodecyloxy)phenyl)ethane-1,2-dione (72)

Compound **72** was prepared by oxidation of **69** as shown in Scheme 15 following the same synthetic procedure discussed above for **71**. It was obtained as a yellow suspension and was further purified by recrystallization from ethanol to afford pure **72** as a yellow solid in 50.1**%** yield which melted in the range between 61.3-62.0^{o}C.

The ^{1}H- and ^{13}C-NMR spectra of **72** (Table 5 and 6) revealed similar signals as those of compound **71**. The only exception was the number of protons and carbons in the aliphatic region. The DEPT-135 spectrum revealed the presence of three quaternary and four methine carbon signals in the aromatic region, and eleven methylene carbon resonances in the aliphatic region. The signal due to the terminal methyl groups was displayed at δ 14.2. The FT-IR (KBr, cm^{-1}) spectrum of **72** revealed the absence of a broad band around 3437 cm^{-1} confirming the complete conversion of **69** to 1,2-diketones. The UV-Vis spectrum of the compound showed two absorption maxima at 266 and 327 nm which are attributable to the conjugated π-π^{*} and n-π electronic transitions, respectively.

4.2.6.4. 1,2-Bis(3-(hexyloxy)phenyl)ethane-1,2-dione (70)

The preparation of **70** from **66** followed a similar synthetic procedure as discussed above for **71** to afford the 1,2-diketone as a pale yellow solid in 96.4**%** yield that melted in between 50.5^{o}C and 51.8^{o}C.

Table 5: ^{1}H-NMR ($CDCl_3$, 400.13 MHz) data (δ_{ppm}) of 1,2-diketones **25**, **70**, **71** and **72**.

70	**25**	**71**	**72**
7.53	7.53	7.54	7.53
(2H, *m*, H-6)	(2H, *s*, H-6)	(2H, *m*, H-6)	(2H, *s*, H-2)
7.48	7.47	7.46	7.48
(2H, *d*, *J*=7.6 Hz, H-5)	(2H, *d*, *J*=7.5 Hz, H-5)	(2H, *d*, *J*=7.6 Hz, H-5)	(2H, *d*, *J*=7.2 Hz, H-6)
7.39	7.40	7.40	7.42
(2H, *t*, *J*=7.6 Hz, H-2)	(2H, *t*, *J*=7.8 Hz, H-2)	(2H, *t*, *J*=7.9 Hz, H-2)	(2H, *t*, *J*=7.6 Hz, H-5)
7.22-7.19	7.21	7.22- 7.20	7.22
(2H, *d*, *J*=8.1, Hz, H-4)	(2H, *d*, *J*=7.9 Hz, H-4)	(2H, *d*, *J*=8.1 Hz, H-4)	(2H, *d*, *J*=7.6 Hz, H-4)
4.02	4.02	4.03	4.02
(4H, *t*, *J*= 6.5 Hz, H-1′)	(4H, *t*, *J*= 6.3 Hz, H-1′)	(4H, *t*, *J*= 6.5 Hz, H-1′)	(4H, *t*, *J*= 5.7 Hz, H-1′)
1.81	1.81	1.81	1.81
(4H, *q*, H-2′)	(4H, *q,* H-2′)	(4H, *q,* H-2′)	(4H, *m*, H-5′)
1.48	1.48	1.48	1.47
(4H, *q*, H-5′)	(4H, *br*, H-7′)	(4H, *br*, H-9′)	(4H, *br*, H-11′)
1.37-1.35	1.36-1.30	1.36-1.30	1.29
(8H, *br*, H-3′, H-4′)	(16H, *br*, 8xCH_2)	(24H, *br*, 12xCH_2)	(32H, *br*, 16xCH_2)
0.93	0.91	0.91	0.90
(6H, *t*, *J*=7.0 Hz, H-6′)	(6H, *t*, *J*=6.3 Hz, H-8′)	(6H, *t*, *J*=6.8 Hz, H-10′)	(6H, *t*, *J*=6.3 Hz, H-12′)

The ^{1}H- and ^{13}C-NMR spectra of **70** (Table 5 and 6) revealed similar signals as those of compound **71** except the number of methylene proton and carbon resonances in the aliphatic region. The DEPT-135 revealed the presence of three quaternary, four methine, five methylene and one methyl carbon resonances in agreement with the structure **70**. The FT-IR (KBr, cm^{-1}) spectrum of **70** revealed similar characteristic bands like the other synthesized 1,2-dikertones. The UV-Vis spectrum of the compound

similarly showed two absorption maxima at 265 and 327 nm which are attributable to the π-π^* and n-π electronic transitions, respectively.

Table 6: ^{13}C-NMR (100.6 MHz, $CDCl_3$) data (δ_{ppm}) of 1,2-diketones **25**, **70**, **71** and **72**.

Carbon	70	25	71	72
a, b	194.6	194.6	194.5	194.6
1	134.2	134.2	134.2	134.2
2	113.6	113.6	113.7	113.6
3	159.6	159.6	159.6	159.6
4	122.2	122.2	122.2	122.3
5	130.0	130.0	130.0	130.0
6	122.9	123.0	122.9	122.9
1′	68.4	68.4	68.4	68.4
2′	29.1	29.3	29.6	29.7
3′	25.7	26.0	26.0	26.0
4′	31.5	29.3	29.4	29.6
5′	22.6	29.1	29.4	29.6
6′	14.0	31.8	29.3	29.4
7′	-	22.7	29.1	29.7
8′	-	14.1	31.9	29.6
9′	-	-	22.7	29.1
10′	-	-	14.1	31.9
11′	-	-	-	22.7
12′	-	-	-	14.2

4.2.7. Conversion of 1,2-diketones to quinoxalines

Quinoxaline has been a frequently used building block in donor-acceptor polymers for PSCs. Scheme 17 shows the syntheses of 5,8-dibromo-2,3-bis(3-(alkyloxy)phenyl)quinoxalines (**51**, **73**, **74**, and **75**) following modified literature procedures.[18,41] Thus, the reduction of 4,7-dibromo-2,1,3-benzothiadiazole (**35**) using zinc in acetic acid gave the intermediate 1,4-dibromo-2,3-diaminobenzene (**36**) which was condensed with the corresponding 1,2-dicarbonyl compounds to afford the respective qunoxalines as solid materials. The quinoxalines were isolated via vacuum

filtration followed by washing with cold methanol and ethanol successively to give pure products in high yield.

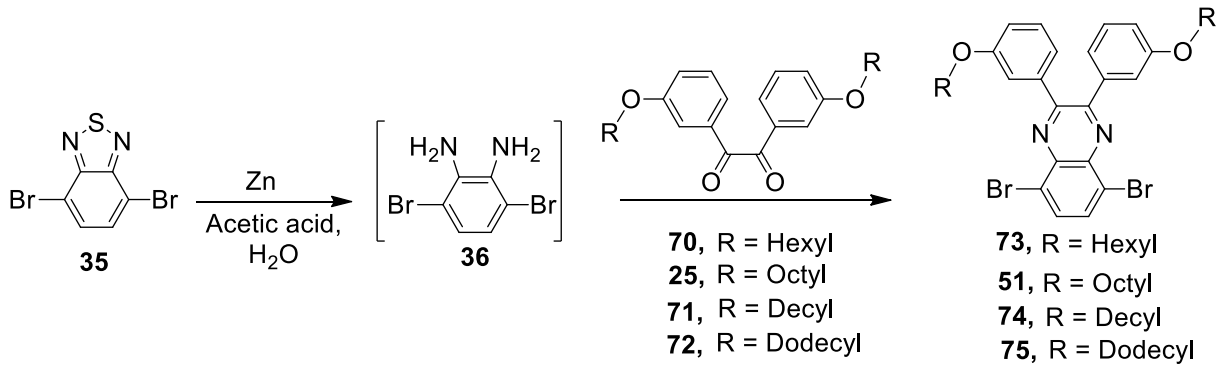

Scheme 17: The syntheses of quinoxaline derivatives starting from 4,7-dibromobenzo[*c*][1,2,5]thiadiazole (**35**).

4.2.7.1. 5,8-Dibromo-2,3-bis(3-decyloxyphenyl) quinoxaline (74)

Compound **74** was synthesized following synthetic procedure outlined in Scheme 17 to afford the desired compound as a pale yellow solid in 63.8% yield, which melted at 85.1- 86.1^{o}C.

The ^{1}H-NMR spectrum of **74** (Table 7 and Appendix 22) showed a singlet at δ 7.94 due to the two equivalent quinoxaline protons H-6 and H-7. The multiplets between δ 7.28 and 7.24 integrating for four protons are due to H-5′ and H-6′, respectively. The doublet at δ 7.20 (*J*= 7.8 Hz) and the doublet of doublet at δ 6.94 (*J* = 8.2, 2.2 Hz) are attributed to H-2′ and H-4′, respectively. The triplet at δ 3.88 (*J* = 6.6 Hz) is due to methylene protons H-1″ attached to oxygen atoms. The quintet at δ 1.75 integrating for four protons is due to equivalent methylene protons H-2″. The intense broad signal between δ 1.46 and 1.31 integrating for twenty-eight protons is due to methylene protons H-3″ to H-9″. The triplet at δ 0.91 is due to the terminal methyl protons.

The ^{13}C-NMR spectrum of **74** (Table 7 and Appendix 23) displayed a total of twenty carbon resonances of which ten appeared in the aromatic region and the remaining ten in the aliphatic region. The DEPT-135 spectrum revealed that there are nine methylene,

five methine, one methyl and five quaternary carbon signals. The carbon signals at δ 159.1, 154.1, 139.3, 139.1 and 123.7 are quaternary carbons, which are attributed to C-3′, C-2, C-9, C-1′ and C-5, respectively. The methine carbon resonances at δ 133.1, 129.3, 122.5, 116.5 and 115.7 are assignable to C-6, C-5′, C-6′, C-4′ and C-2′, respectively. The methylene carbon signals appeared between δ 68.1 and 22.7 and are assignable to C-1′ - C-7′ of the side chains as shown in Table 7. The carbon signal at δ 14.1 is due to the terminal methyl group at C-10′.

The FT-IR (KBr, cm^{-1}) spectrum of **74** showed intense bands at 2920 and 2850 cm^{-1}, and a weak band at 3070 cm^{-1} due to the aliphatic and aromatic C–H stretching of the of quinoxaline derivatives, respectively. Disappearance of an intense band at 1678 cm^{-1} confirms absence of (C=O) stretching of the starting material. The band at 1604 cm^{-1} is due to C=N stretching and confirms quinoxaline ring formation. The bands between 1573 and 1444 cm^{-1} are due to C=C stretching with in the aromatic systems and C-H bending. The sharp intense band at 1335 cm^{-1} is due to C–C stretching and the intense band at 1241 cm^{-1} is due to C–O stretching. The band at 587 cm^{-1} can be attributed to C–Br stretching. The UV-Vis spectrum of **74** (Figure 8, Table 9) in acetonitrile solution exhibited absorption maxima at 255, 272 and 353 nm. The maxima at 255 and 272 nm can be ascribed to conjugated aromatic π–π^* transitions while the maxima at 353 nm may be attributed to n-π^* transitions over oxygen and bromine.

4.2.7.2. 5,8-Dibromo-2,3-bis(3-hexyloxyphenyl) quinoxaline (73)

Compound **73** was synthesized following the same synthetic procedure discussed above for the preparation of **74** to afford the title compound as pale pink solid in 65.2% yield, which melted in the range between 88.5 and 90.5^{o}C.

The UV-Vis spectrum of **73 (**Figure 8 and Table 9**)** in acetonitrile solution showed absorption maxima at 254, 272 and 354 nm. The ^{1}H-NMR spectrum of **73** (Table 7 and Appendix 28) showed a singlet at δ 7.93 due to the equivalent protons H-6 and H-7. The multiplets between δ 7.28 and 7.25 are attributable to H-5′ and H-6′. The doublets at δ 7.21 (*J* = 7.2 Hz) and δ 6.95 (*J* = 7.9 Hz) integrating for two protons each are attributed to H-2′ and H-4′, respectively. The triplet at δ 3.89 (*J* = 6.4 Hz) is due to the four

methylene protons at C-1″ attached to oxygen atoms. The quintet at δ 1.76 integrating for four protons is due to H-2″. The intense broad signal at δ 1.48 to 1.36 integrating for twelve protons is due to methylene protons H-3″, H-4″ and H-5″. The triplet at δ 0.94 (*J* = 6.4 Hz) is due to terminal methyl protons at C-6″.The ^{13}C-NMR spectrum of **73** (Table 8 and Appendix 29) displayed a total of sixteen carbon resonances of which ten appeared in the aromatic region and six in the aliphatic region. The DEPT-135 spectrum revealed that there are five methylene, five methine, five quaternary and one methyl groups. The carbon signals at δ 159.1, 154.0, 139.3, 139.1, and 123.7 are quaternary carbons, which correspond to C-3′, C-2, C-9, C-1′ and C-5, respectively. The five methine carbons displayed signals at δ 133.1, 129.3, 122.6, 116.5 and 115.7 and are assignable to C-6, C-5′, C-6′, C-4′ and C-2′, respectively. The aliphatic carbon resonances appeared between δ 68.1 and 14.1 and are assigned to the carbon atoms on the side chains as shown in Table 8. The FT-IR (KBr, cm^{-1}) spectrum of **73** showed intense bands at 2931 and 2869 cm^{-1} due to the aliphatic C–H stretching. A weak band at 3070 cm^{-1} is due to aromatic C–H stretching. The band at 1603 cm^{-1} is due to C=N stretching of the quinoxaline ring. The bands at 1584-1442 cm^{-1} are due to C=C stretching with in the aromatic systems and C–H bending. The sharp intense band at 1334 cm^{-1} is due to C–C stretching. The intense band around 1205 cm^{-1} is due to C–O stretching. The band at 556 cm^{-1} is assignable to C–Br stretching.

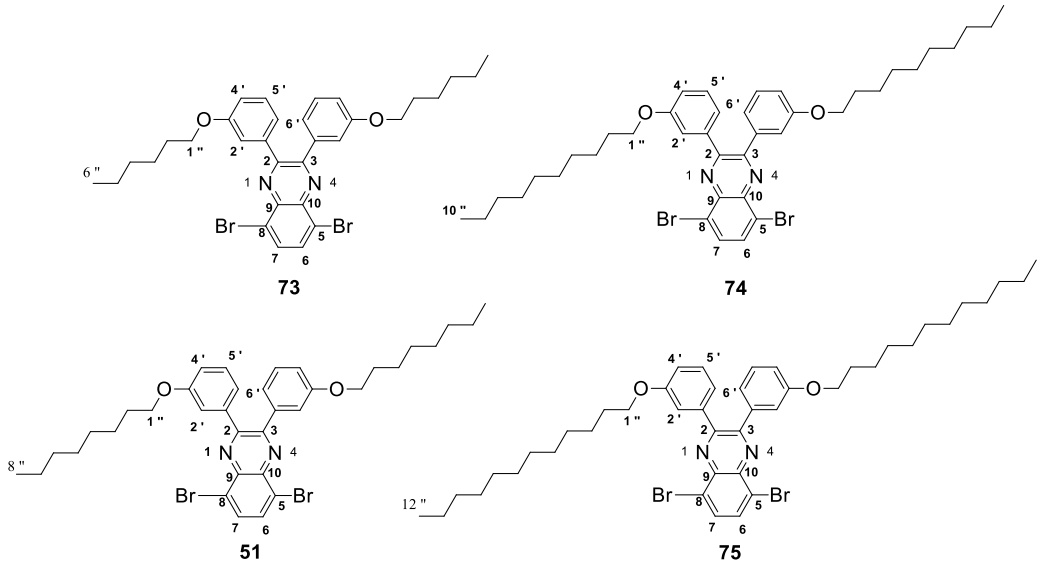

Figure 7: Structures of the four quinoxaline derivatives.

4.2.7.3. 5,8-Dibromo-2,3-bis(3-octyloxyphenyl) quinoxaline (51)

Compound **51** was synthesized following the same synthetic procedure discussed above for **74** to afford the title compound as pale yellow solid in 64.8% yield, which melted at 77.9-79.0^{o}C.

The UV-Vis spectrum of **51 (**Figure 8 and Table 9) in acetonitrile solution showed absorption maxima at 254, 272 and 354 nm. The FT-IR (KBr, cm^{-1}) spectrum of **51** revealed bands at 2920 and 2869 cm^{-1} due to the aromatic and aliphatic C–H stretching vibrations, respectively. The band at 1603 cm^{-1} is due to C=N stretching of the quinoxaline ring and the band at 1445 cm^{-1} is due to C=C stretching with in the aromatic systems and C-H bending. The sharp intense bands at 1340 cm^{-1} is due to C–C stretching while the intense band at 1241 cm $^{-1}$ is due to C–O stretching. The band at 587 cm^{-1} is assignable to C–Br stretching.

The ^{1}H-NMR spectrum of **51** (Table **7** and Appendix 25) showed five aromatic proton signals in the region between δ 6.96 and 7.94. The singlet at δ 7.94 is due to the two equivalent quinoxaline protons H-6 and H-7. The overlapping signals between δ 7.28 and 7.24 integrating for four protons are due to H-5′ and H-6′. The other aromatic proton signals appeared as doublets at δ 7.20 (*J* = 7.6 Hz) and 6.96 (*J* = 8.0 Hz) and are attributed to H-2′ and H-4′, respectively. The triplet at δ 3.88 (*J* = 6.6 Hz) is due to the methylene protons at C-1″ attached to oxygen atoms. The quintet at δ 1.75 integrating for four protons is due to H-2″. The intense broad signal at δ 1.48 to 1.32 integrating for twenty protons is due to the remaining ten methylene groups and the triplet at δ 0.92 (*J* = 7.0 Hz) is due to the terminal CH_3 groups.

The ^{13}C-NMR spectrum of **51** (Table 8 and Appendix 26) displayed a total of eighteen carbon resonances of which ten appeared in the aromatic region and eight in the aliphatic region. The DEPT-135 spectrum revealed that there are one methyl, seven methylene, five methine and five quaternary carbon atoms in agreement with structure **51**.

4.2.7.4. 5,8-Dibromo-2,3-bis(3-dodecyloxyphenyl) quinoxaline (75)

Compound **75** was prepared from dibromide **35** and diketone **72** following similar procedure discussed above for the synthesis of quinoxaline **74**. It was isolated as pale pink solid in 82.5% yield, which melted at 79.3-80.1^{o}C.

The UV-Vis spectrum of **75 (**Figure 8 and Table 9) in acetonitrile solution showed absorption maxima at 252, 273 and 345 nm. The FT-IR (KBr, cm^{-1}) spectrum of **75** showed intense bands at 2919 and 2850 cm^{-1} due to the aromatic and aliphatic C–H stretching vibrations. The presence of C=N and C=C groups was confirmed by the appearance of bands at 1603 and 1445 cm^{-1}, respectively. The intense band at 1241 cm^{-1} is due to C–O stretching of the alkoxy groups. The band at 691 cm^{-1} is assignable to C–Br stretching.

The ^{1}H-NMR spectrum of **75** (Table 7, Appendix 31) showed a singlet at δ 7.93 integrating for two protons due to H-6 and H-7. The multiplet at δ 7.26- 7.21 integrating for six protons are due to H-2′, H-5′ and H-6′. The doublet at δ 6.96 (*J* = 7.13 Hz) integrating for two protons is attributed to H-4′. The triplet at δ 3.88 (*J* = 5.5 Hz) is due to methylene protons H-1″. The quintet at δ 1.74 integrating for four protons is assigned to H-2″. The intense signal between δ 1.44 to 1.29 integrating for thirty-six protons is due to eighteen equivalent methylene groups. The triplet at δ 0.91 (*J* = 5.8 Hz) is due to the terminal methyl protons H-12″.

The ^{13}C-NMR spectrum of **75** (Table 8 and Appendix 32) displayed a total of nineteen carbon resonances of which ten appeared in the aromatic region and the remaining nine in the aliphatic region. The DEPT-135 spectrum revealed the presence of one methyl, eight methylene, five methine and five quaternary carbon atoms. The carbon signals at δ 159.0, 154.0, 139.3, 139.1, 133.1, and 123.7 are quaternary carbons, which are attributed to C-3′, C-2, C-9, C-1′ and C-5, respectively. The methine carbon signals appeared at δ 133.1, 129.3, 122.5, 116.5 and 115.7 and are assignable to C-6, C-5′, C-6′, C-4′ and C-2′, respectively. The signals at δ 68.1, 32.0, 29.1, 26.0 and 22.7 are methylene carbon resonances assignable to C-1′, C-10′, C-9′, C-3′ and C-11′. The

signals due to C-2′, C-4′, C-5′, C-6′, C-7′ and C-8′ overlap and appear together as an intense peak between 29.7 and 29.4. The carbon signal at 14.2 is due to the terminal methyl groups.

Table 7: ^{1}H-NMR ($CDCl_3$, 400.13 MHz) data (δ_{ppm}) of compounds **73**, **51**, **74** and **75.**

73	**51**	**74**	**75**
7.93 (2H, *s*, H-6, H-7)	7.94 (2H, *s*, H-6, H-7)	7.94 (2H, *s*, H-6, H-7)	7.93 (2H, *s*, H-6, H-7)
7.28- 7.25 (4H, *m*, H-5′, H-6′)	7.28- 7.24 (4H, *m*, H-5′, H-6′)	7.28- 7.24 (4H, *m*, H-5′, H-6′)	7.26- 7.21 (6H, *m*, H-2′, H-5′, H-6′)
7.21 (2H, *d*, J = 7.2Hz, H-2′)	7.20 (2H, *d*, J = 7.6, H-2′)	7.20 (2H, *d*, *J*=7.7Hz, H-2′)	-
6.96 (2H, *d*, *J*=7.9Hz, H-4′)	6.96 (2H, *d*, J = 8.0Hz, H-4′)	6.95 (2H, *dd*, J = 8.1, 1.5 Hz, H-4′)	6.96 (2H, *d*, *J*=7.1Hz, H-4′)
3.89 (4H, *t*, *J*=6.4Hz, H-1″)	3.88 (4H, *t*, *J*=6.6, H-1″)	3.88 (4H, t, *J* = 6.3 Hz, H-1″)	3.88 (4H, *t*, J=6.7Hz, H-1″)
1.78- 1.73 (4H, *q*, H-2″)	1.77-1.73 (4H, *q*, H-2″)	1.78-1.73 (4H, *q*, H-2″)	1.76- 1.73 (4H, *m*, H-2″)
1.48- 1.43 (4H, *m*, H-5″)	-	-	-
1.36 (8H, *br*, 4×CH_2)	1.44 -1.32 (20H, *m*, 10×CH_2)	1.43-1.30 (28H, *m*, 7× CH_2, H-3″– H-9″)	1.43 -1.29 (36H, *br*, H-3″– H-11″)
0.94 (6H, *t*, *J*=6.4Hz, H-6″)	0.92 (6H, t, *J*=6.9Hz, H-8″)	0.91 (6H, t, *J*=6.7 Hz, H-10″	0.91 (6H, t, *J*= 5.8Hz, H-12″)

Table 8: ^{13}C-NMR (100.6 MHz, $CDCl_3$) data (δ_{ppm}) of compounds **73**, **51**, **74** and **75.**

Carbon	73	51	74	75
2, 3	154.0	154.0	154.1	154.0
5, 8	123.7	123.7	123.7	123.7
6,7	133.1	133.1	133.1	133.1
9. 10	139.3	139.3	139.3	139.3
1′	139.1	139.1	139.1	139.1
2′	115.7	115.7	115.7	115.7
3′	159.1	159.0	159.1	159.0
4′	116.5	116.5	116.6	116.5
5′	129.3	129.3	129.3	129.3
6′	122.6	122.5	122.5	122.5
1″	68.1	68.1	68.1	68.1
2″	29.1	29.1	29.6	29.7
3″	25.7	26.0	26.0	26.0
4″	31.6	29.3	29.6	29.7
5″	22.6	29.4	29.4	29.7
6″	14.1	31.9	29.4	29.7
7″		22.7	29.1	29.4
8″	-	14.1	31.9	29.4
9″	-	-	22.7	29.1
10″	-	-	14.1	32.0
11″	-	-	-	22.7
12″	-	-	-	14.2

Table 9: Optical and melting point data of **73**, **51**, **74** and **75**.

monomers	CH_3CN solution λ_{max} (nm)			Melting point (^{o}C)
73	254	272	354	88.5-90.5
51	254	272	354	77.9-79.0
74	255	272	353	85.1-86.1
75	252	273	345	79.3-80.1

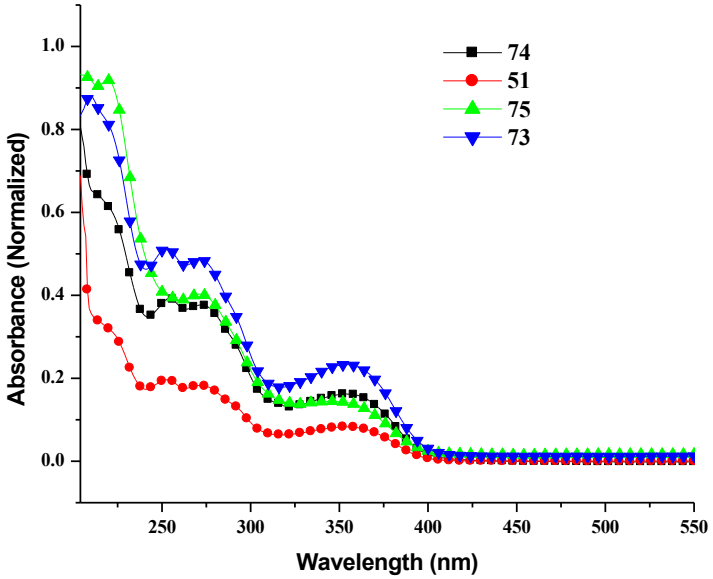

Figure 8: UV-Vis spectra of **73**, **51**, **74** and **75**.

4.3. Synthesis of 2,5-bis(tri-*n*-butylstannyl)thiophene (78)

2,5-Bis-(tri-*n*-butylstannyl)thiophene (**78**) was one of the monomers used in the preparation of polymers in this thesis work. It was prepared starting from 2,5-dibromothiophene (**76**) following a modified literature procedure[62] as shown in Scheme 18. Thus, the reaction of the Grignard reagent derived from **76** with tri-n-butyltinchloride (**77**) in a Sonochemical Barbier-like reaction led to the corresponding distannlated product **78** as a colorless oily liquid, which was purified by vacuum distillation.

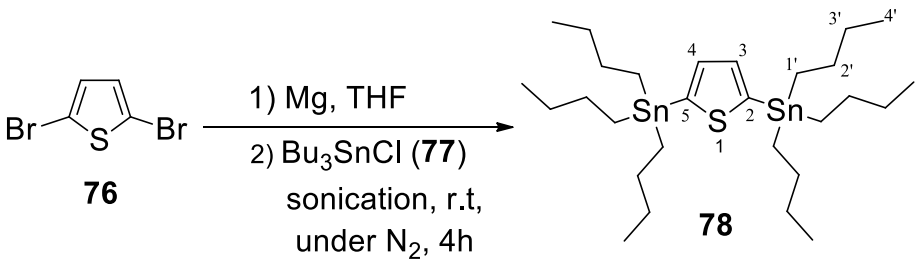

Scheme 18: Synthesis of 2,5-bis-(tri-*n*-butylstannyl)thiophene (**78**)

The FT-IR (KBr, cm^{-1}) spectrum of **78** showed intense bands at 2957, 2926, 2852 cm^{-1} and a weak band at 3054 cm^{-1} due to the aliphatic and aromatic C-H stretching vibrations.

The ^{1}H-NMR spectrum of **78** (Appendix 34, Table 10) showed five different proton environments. The singlet at δ 7.49 integrated for two protons and is due to the chemically equivalent thiophene ring protons H-3 and H-4. The quintet centered at δ 1.68 is attributed to H-3′ and the sextet centered at δ 1.45 is due to H-2′. The triplets at δ 1.22 and 0.99 are due to H-1′ and H-4′, respectively.

The ^{13}C-NMR spectrum of **78** (Table 11, Appendix 35) showed six carbon resonances, out of which two are in the aromatic region and four are in the aliphatic region. The most down field signal at δ 141.8 is due to quaternary carbon atoms C-2 and C-5 on the thiopnene ring. This is further confirmed by the absence of signals in the DEPT-135 spectrum (Appendix 36). The next most down field signal at δ 135.8 is due to C-2 and C-4 of the thiophene ring. The aliphatic carbon signals at δ 29.1, 27.4 and 13.7 are due to methylene groups and correspond to C-2′, C-3′ and C-1′, respectively. The carbon resonance at δ 10.9 is due to the terminal methyl groups (C-4′).

Table 10: ^{1}H-NMR ($CDCl_3$, 400.13 MHz) data (δ_{ppm}) of compound **78**.

δ_{ppm}
7.49 (2H, *s,* H-3, H-4)
1.68 (12H, *q*, H-3′)
1.45 (12H, *sextet,* H-2′)
1.22 (12H, *t,* H-1′)
0.99 (18H, *t,* H-4′)

Table 11: ^{13}C-NMR (100.6, $CDCl_3$) data (δ_{ppm}) of compound **78**.

Carbon	δ_{ppm}
C-2, C-5	141.8
C-3, C-4	135.8
C-2′	29.1
C-3′	27.4
C-4′	13.7
C-1′	10.9

4.4. Syntheses of the polymers

The Stille coupling is one of the most versatile and efficient methods for making aryl-aryl bonds, which is important for making high molecular weight conjugated and narrowly dispersed polymers under mild condition. The polymerization reaction also tolerates a varity of functional groups and typically gives excellent yields.[15]

In the course of this work, four thiophene-quinoxaline (TQ)-based polymers were prepared using the Stille polycondensation reaction as shown in Scheme 20. The reactions were conducted in toluene as a solvent at 110^{o}C using tetrakis[triphenylphosphine]palladium(0) ($Pd(PPh_3)_4$) as a catalyst to afford the TQ-based polymers in a good yield. Initial attempts to synthesize the polymers using tris(dibenzylideneacetone)dipalladium(0) ($Pd_2(dba)_3$ and bis(triphenylphosphine)palladium(II) dichloride ($Pd(PPh_3)_2Cl_2$) as catalysts did not result in polymerization presumably due to deactivation or purity of the catalysts. These simple facts, however, are often ignored because usually these catalysts are purchased from reputable vendors and regarded as 'pure'. But, Zalesskiy and Ananikov recently advised that commercially available $Pd_2(dba)_3$ could contain up to 40% Pd nanoparticles, which would not participate in the catalytic cycle.[63] For D-A copolymerization, such a high level of impurity in the catalyst could lead to unexpectedly low molecular weight and even worse, more metal residue in the finished polymers. $Pd(PPh_3)_2Cl_2$ is even more prone to oxygen attack. Furthermore, the Pd(II) in $Pd(PPh_3)_2Cl_2$ needs to be reduced to Pd(0) by the distannyl compound before entering the catalytic cycle. Therefore, excess distannyl monomers need to be added to maintain the desired stoichiometric balance of monomers in order to achieve high molecular weight.

In order to check whether the $Pd(PPh_3)_2Cl_2$ in our laboratory was still active, an attempt was made to synthesize compound **80** (Scheme 19) from compounds **79** and **74**. Compound **80** was obtained in 51.9% as a yellow solid after prolonged reaction time and heavy catalyst loading. This suggested that the catalyst was not very active and hence the failure to do Stille polymerization reactions with $Pd(PPh_3)_2Cl_2$ as catalyst.

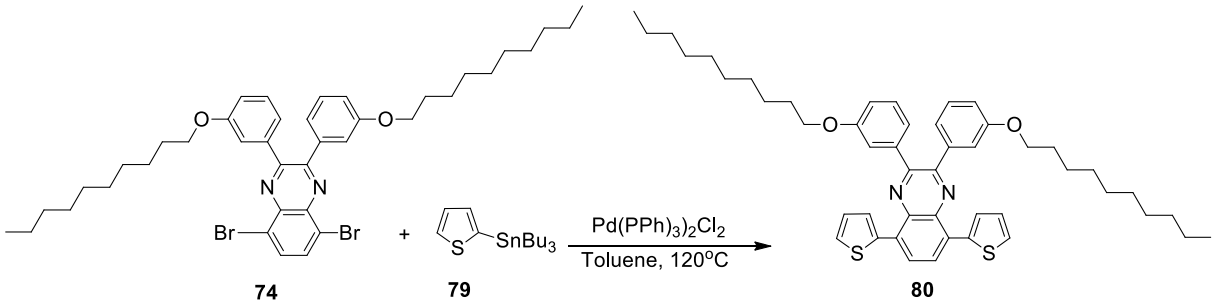

Scheme 19: Synthesis of 2,3-bis-(3-decyloxyphenyl)-5,8-dithiophene-2-yl-quinoxaline (**80**)

Having failed to achieve any polymerization using the commercial catalysts, fresh $Pd(PPh_3)_4$ was synthesized [64] as shown in Equation 1 to afford the catalyst in high yield. This catalyst was used in subsequent polymerization reactions.

$$2PdCl_2 + 8PPh_3 + 5NH_2NH_2.H_2O \xrightarrow{DMSO} 2Pd(PPh_3)_4 + 4NH_2NH_2.HCl + N_2 + 5H_2O$$

Equation 1: Synthesis of ($Pd(PPh_3)_4$

The syntheses of the quinoxaline-based polymers are outlined in Scheme 20. A typical polymerization reaction was performed using 1:1 molar mixture of the two monomers and 14 mol% of the freshly prepared catalyst in toluene as a solvent. The mixture was then heated at 110^oC for about 44 hours to afford crude polymeric materials as deep blue product. The polymer was precipitated by slow addition of the product mixture into methanol while stirring vigorously. The crude polymer was collected by filtration, dissolved in chloroform, stirred overnight with EDTA and then washed with deionized water, concentrated and reprecipitated from methanol. Further purification of the polymer was achieved by Soxhlet extraction of the product with methanol, acetone and chloroform successively. The chloroform extract was further precipitated from methanol to afford the polymer as dark purple solids in high yield. All of the polymers had good solubility in common organic solvents such as $CHCl_3$, THF, CB, ODCB and toluene. The good solubilities arise from the introduction of long alkoxy side chains. The polymers were characterized by ^1H, UV-Vis spectroscopy and square wave voltammetry (SWV) as discussed below. The ^1H-NMR of the polymers are assigned by comparing separately its ^1H-NMR of the monomers and all consistent with the proposed structures.

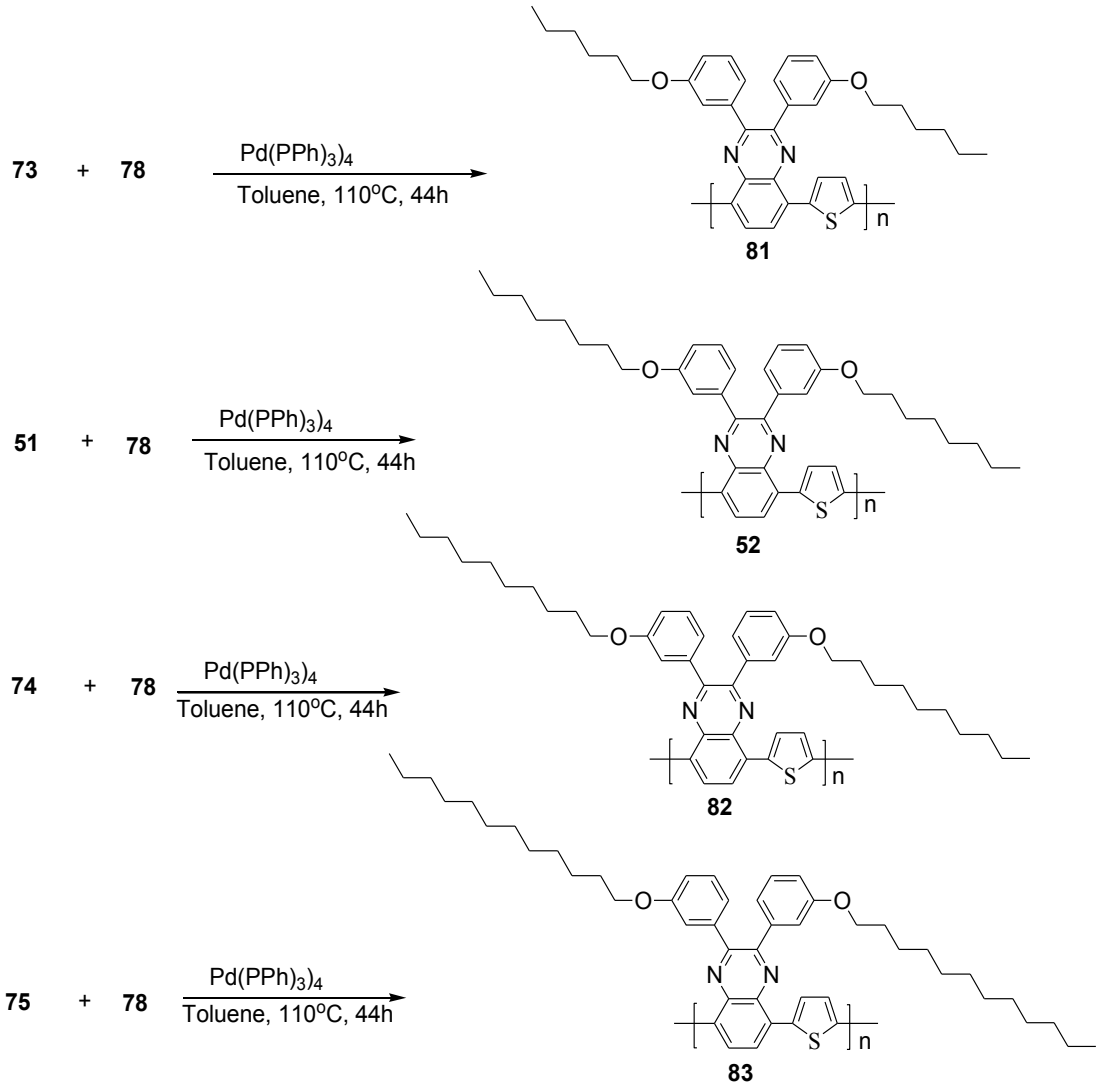

Scheme 20: Stille coupling reactions for the syntheses of polymers **81**, **82**, **52** and **83**.

4.5. Characterization of the polymers

4.5.1. Optical properties

Optical absorption measurements are of significant importance, not only to compare the absorption spectrum of the conjugated polymer relative to the solar irradiance spectrum, but also to obtain a value of the optical band gap. The band gap determines which wavelength of light is absorbed and emitted by the material. Among the factors that

influence the band gap of a polymer are conjugation length, solid state ordering and the presence of electron withdrawing or donating moieties.

The value of the optical band gap is often determined by the onset of absorption. The most widely accepted procedure to obtain an onset value is to draw a baseline in the spectrum and retrieve the point of intersection with the line of the maximum slope of the absorption peak.[65]

The normalized UV-Vis absorption spectra of copolymers **81**, **52**, **82** and **83** in dilute chloroform solutions and as thin films of the polymers spin-coated on glass are shown in Figure 9 and 10, respectively. The main optical properties of the polymers are summarized in Table 12. All the four synthesized polymers showed two absorption bands in chloroform solutions and as thin films. The short wavelength absorption bands between 300 and 400 nm are attributable to the π-π^* transition of the conjugated backbone while the long wavelength absorption bands (> 550 nm) correspond to the intramolecular charge transfer (CT) from donor to acceptor.

Thus, for all the synthesized polymers, the absorption maxima (λ_{max}) were detected around 350 and 570 nm in solution and around 366 and 596 nm as thin film. As shown in Figure 9 and Table 12, the absorption maxima at shorter wavelength are almost the same for all four polymers because of the similarity of the donor in the polymer backbone. However, the longer wavelength absorption maxima showed no significant difference between each polymers in chloroform solution, indicating the selected alkoxy side chain length have no significant effect on optical properties of the polymers.[66]

The introduction of an alkoxy side chain on the phenyl group of the quinoxaline unit affects the electronic structure of the resulting copolymer in two ways, i.e., by withdrawing or donating electrons thereby lowering or raising the HOMO level. The alkoxy group exerts both an inductive electron-withdrawing effect on a conjugated system, due to the stronger electronegativity of oxygen than carbon, and a resonance electron-donating effect, due to the lone pair electrons of oxygen. Since the resonance electron-donating effect is dominant over the inductive electron-withdrawing effect, the

alkoxy group can be seen as a typical electron-donating group. However, the alkoxy group's contribution to the *ortho*- and *para*- positions of the phenyl group by the resonance electron-donating effect is stronger than that to the *meta*-position. It is known that electron donor groups elevate both the HOMO and LUMO levels.[67]

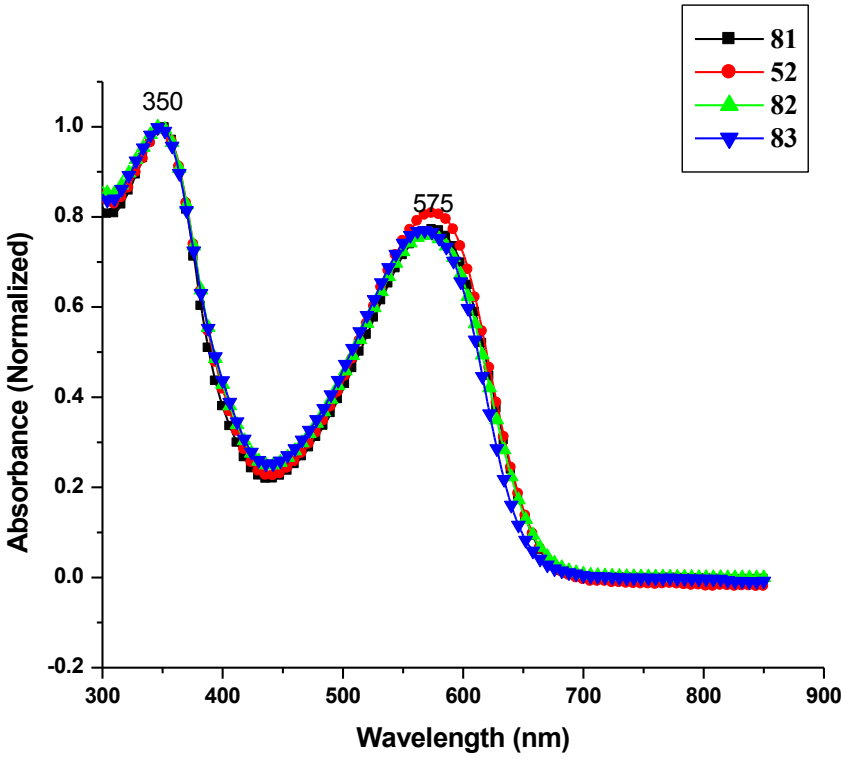

Figure 9: UV-Vis spectra of **81**, **52**, **82** and **83** in chloroform solutions.

Table 12: Optical properties of the polymers in solution and as thin films.

polymer	λ_{max} (nm)		λ_{onset} (nm)		E_g^{opt} (eV)	
	$CHCl_3$	Film	$CHCl_3$	Film	$CHCl_3$	Film
81	350, 575	367, 594	658	714	1.88	1.74
52	350, 576	366, 599	665	711	1.86	1.75
82	347, 570	367, 593	665	703	1.86	1.77
83	350, 566	367, 596	650	713	1.91	1.74

The optical band gap can be estimated from the onset of absorption of the polymer thin film. Additionally, the shift between the absorption maximum for the solution spectrum and the thin-film spectrum can be used to estimate the degree of inter-chain interaction.

Stronger stacking and aggregation of polymer in film is usually accompanied by a larger red shift of the absorption maximum from the solution to the film.

The short- and long-wavelength absorption maxima of all the polymer thin films exhibited red shifts of approximately 17 and 23 nm, respectively, compared to the absorption maxima in solution. This can be attributed to the extended conjugation length and enhanced planarity of the copolymer chains due to the interchain π-π stacking effect in the solid state. This indicates that the molecules could be well arranged and aggregated in the solid state owing to the strong interchain interactions, which may facilitate charge transport.[68,69] It is also known that the absorption spectra of conjugated polymers are closely related to their effective conjugated length, which is susceptible to the steric hindrance caused by side chains. Since the absorption maxima in the thin film spectra of all polymers are red-shifted to almost the same extent, the alkoxy groups in the *meta*-positions of the aromatic rings did not seem to have caused much difference in steric hindrance.

The onsets of optical absorptions of **81**, **52**, **82** and **83** were deduced from the solution spectra to be 658, 665, 665 and 650 with optical band gaps of 1.88, 1.86, 1.86 and 1.91 eV, respectively. Similarly, the onsets of optical absorptions deduced from the thin film spectra of **81**, **52**, **82**, and **83** were 714, 711, 703 and 713 nm with optical band gaps of 1.74, 1.75, 1.77 and 1.74 eV, respectively. The result of optical band gap indicates that the increase in side chain length by two methylene groups lead to an increase in optical band gaps of approximately 0.01ev and then turned back as side chain further increased. Therefore, further increase in side chain length does not result up on a significant change on optical band gaps of the polymers.

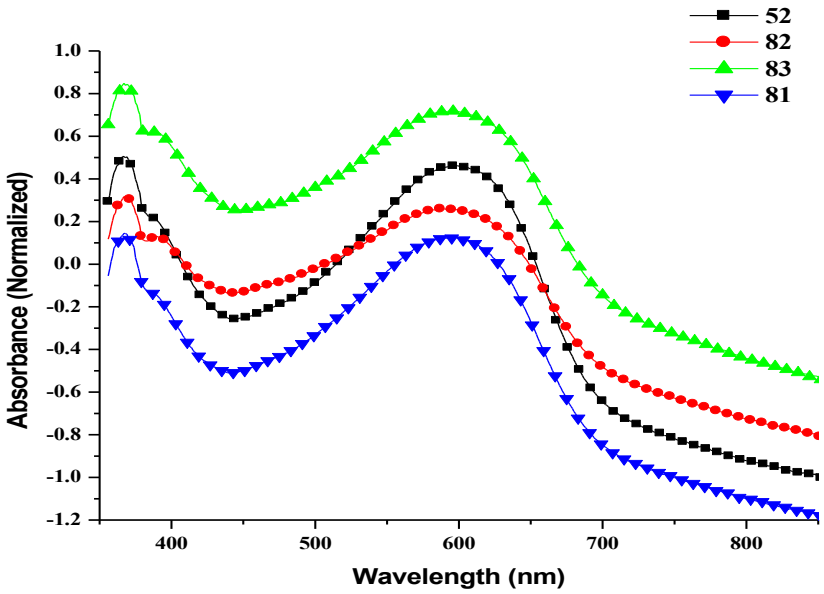

Figure 10: UV-Vis spectra of **81**, **52**, **82** and **83** as thin films.

4.5.2. Electrochemical properties

Cyclic voltammetry (CV) is a widely used method to investigate oxidation and reduction processes as well as to determine the respective oxidation and reduction potentials of conjugated polymers. These values can be used to estimate the ionization potential (I_p), the electron affinity (E_a), and the band gap which is the gap between the highest occupied molecular orbital (HOMO) and lowest unoccupied molecular orbital (LUMO).[59,70,71]

CV is usually performed in a three-electrode electrochemical cell containing a working electrode, a counter electrode, and a reference electrode. The working electrode is coated with a thin film of the polymer. When the potential of the working electrode is increased the conjugated polymer will eventually be oxidized, which means that electrons are extracted from the material as indicated by a current flow between the working electrode and counter electrode.[70]

The HOMO and LUMO levels, which correspond to ionization potential (I_p) and electron affinity (E_a), can be estimated from the oxidation and reduction potentials revealed in cyclic or square wave voltammograms, respectively. The oxidation process corresponds to the removal of charge from the HOMO band, whereas the reduction cycle corresponds to the filling of the LUMO band by electrons. Therefore, the onsets of oxidation and reduction potentials are closely related to the energies of the HOMO and LUMO levels of an organic molecule and thus can provide important information regarding the magnitude of the energy gap. The onset potentials are determined from the intersection of the two tangents drawn at the rising current and baseline charging current of the CV or square wave voltammetry (SWV) traces.

The polymer films were coated on platinum working electrode, supported in 0.10 M *tetra-n*-butylammonium perchlorate (Bu_4NClO_4) in anhydrous acetonitrile and were measured at a scanning rate of 100 mV/s. The electrochemical data obtained from all copolymers are shown in Figure 11 and Table and were estimated according to the following empirical relationships proposed by Bredas *et al.* who found a linear correlation between ionization potential (I_p) and oxidation potential (E_{ox}) and also between electron affinity (E_a) and reduction potentials (E_{red}). [70,72,73]

$$E_a\ (E_{LUMO}) = -\ (E'_{red} + 4.39)\ eV$$

$$I_p\ (E_{HOMO}) = -\ (E'_{ox} + 4.39)\ eV$$

where E'_{red} and E'_{ox} are onset of reduction and oxidation potential *versus* the Ag/AgCl as a reference electrode

The square wave voltammograms of **52**, **81**, **82** and **83** are shown in Figure 11. The electrochemical band gaps (E_g^{ec}) of copolymers **52**, **81**, **82** and **83** were estimated from the HOMO and LUMO energy levels to be 2.0, 2.2, 2.2, and 2.1 eV, respectively. These values are in the same range as the values reported for polymers having thiophene and quinoxaline. Zuhang *et al.*[74] reported the optical band gaps (E_g^{opt}) of TQ-based polymers to be between 1.70 and 1.75 eV while the electrochemical band gaps, estimated from SWV studies, were between 2.08 and 2.37 eV.

Table 13: Electrochemical properties of polymers **81**, **52**, **82** and **83**.

polymer	E_{ox}^{onset} (V)	E_{red}^{onset}(V)	E_{HOMO} (eV)	E_{Lumo} (eV)	E_g (eV)
81	1.02	-1.12	- 5.42	-3.28	2.1
52	0.98	-1.01	- 5.40	-3.40	2.0
82	0.92	-1.27	-5.32	-3.13	2.2
83	0.96	-1.25	- 5.36	-3.15	2.2

The electrochemical behaviors of polymers **52** and **82** were further investigated by cyclic voltammetry (CV). Figure 12 shows the cyclic votammograms. The HOMO energy levels of **52** and **82** were estimated to be 5.44 and 5.32 eV whereas the LUMO energy levels were estimated to be 3.34 and 3.32 eV, respectively. These values are similar to those obtained from SWV studies. The electrochemical band gaps were calculated to be 2.10 and 2.0 eV for **52** and **82**, respectively. In general, results indicate that the optical and electrochemical properties of the polymers do not exhibit noticeable dependence on the length of the alkoxy side chains. It was expected that the alkoxy side chain length may have a significant effect on thermal stability, molecular packing, mobility, molecular weight as well as device performance.[75–77]

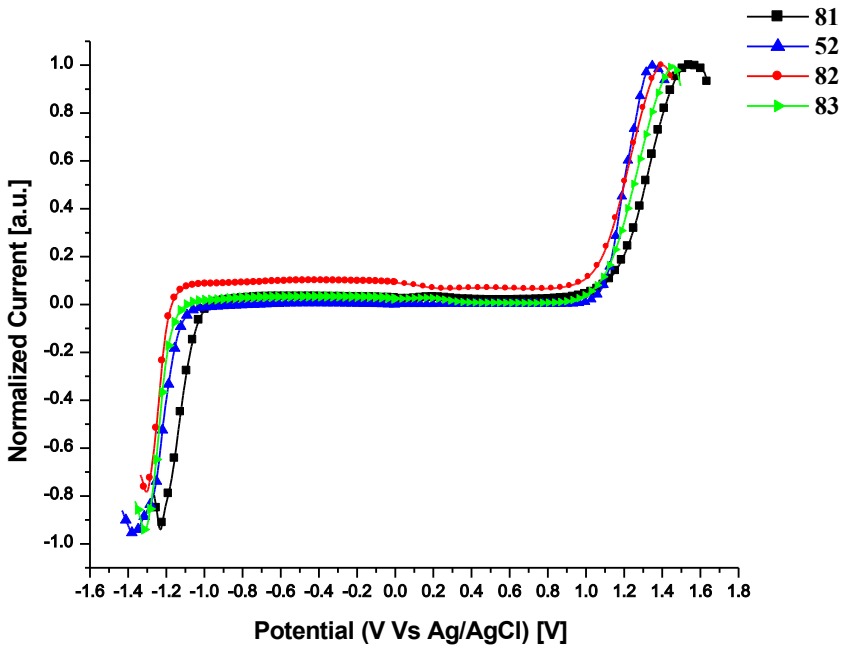

Figure 11: Square wave voltammograms of polymers **81**, **52**, **82** and **83**.

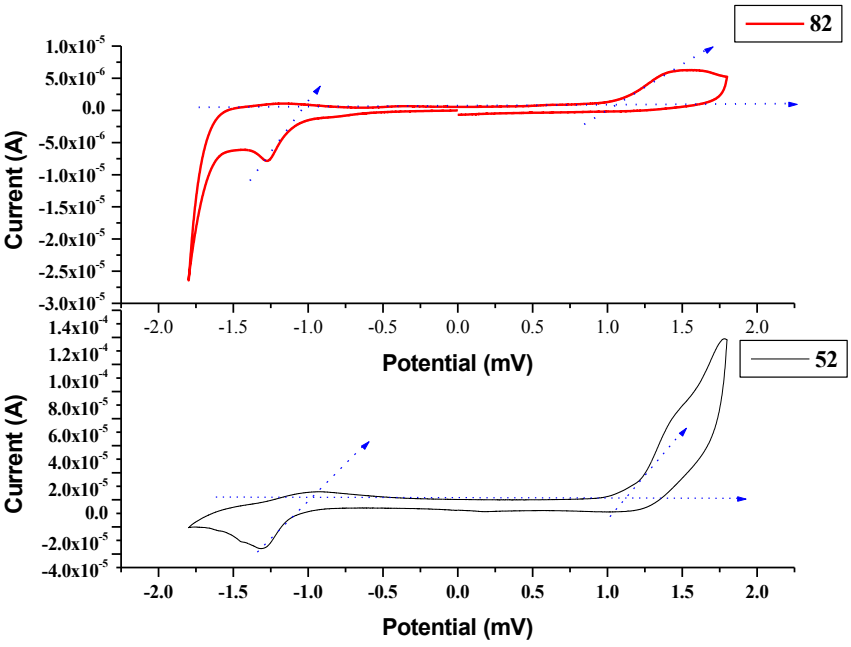

Figure 12: Cyclic voltammograms of polymers **52** and **82**.

5. CONCLUSION

Four polymers (**81**, **52**, **82** and **83**) containing thiophene and quinoxaline units were successfully synthesized through palladium-catalyzed Stille coupling reactions. The polymers were a dark purple solid and had good solubility in common organic solvents like $CHCl_3$, THF, CB, ODCB and toluene. The good solubility of the polymer arises from the introduction of the longer alkoxy side chain having six, eight, ten and twelve carbons. Therefore, the fabrication of the material using the product can be easily performed without solubility interference since solubility is one of the challenges for device preparation from organic polymers. The $CHCl_3$ solutions of all polymers had red purple color. Thus, the optical band gaps were determined from onset of the UV-Vis spectra of all polymers in $CHCl_3$ solution as well as form the thin films of the polymers on glass. The optical band gaps obtained from onsets of absorption of thin films of the polymers were 1.74, 1.75, 1.77 and 1.74 eV for polymer **81**, **52**, **82** and **83**, respectively indicating slight increases as number of carbon increase then turned back. An increase in side chain length result up on an increase in around 0.01eV that is insignificant value.

Similarly, the electrochemical band gaps were estimated from square wave valtomograms of the polymers. Thus, the electrochemical band gaps of the polymers were estimated from onset of SWV and found around 2.0 eV. The result indicates that they had relatively small optical and electrochemical band gaps. Further studies on physical properties such as molecular weight determination, thermal properties, etc., should be made in order to fully characterize the polymers and fabrication of the devices using the material should be made in order to show potential power conversion efficiency of the polymers.

6. EXPERIMENTAL

6.1. Materials and Methods

Melting points were measured using Mettler-Toledo FP82HT hot stage with FP90 central processor and LEICA GALEN^{TM} III microscope apparatus and are uncorrected. The ^{1}H-NMR and ^{13}C-NMR spectra were recorded on a Bruker Avance 400 spectrometer at 400.13 and 100.6 MHz, respectively in $CDCl_3$ and reported in δ units. IR spectra were recorded on a Perkin-Elmer Spectrum 65 IR spectrometer. FT-IR spectra of the crystalline solid compounds were obtained as KBr pellets, whereas for an oily liquid compounds it was obtained as a thin films. The UV-Vis spectra of all the intermediate compounds were recorded in chloroform solution except quinoxaline derivatives, which were recorded in acetonitrile solution using Perkin Elmer Lambda 950 UV/Vis/NIR spectrophotometer at room temperature. Cyclic voltammetric studies were performed on a BASi Epsilon Electrochemical Workstation using platinum electrodes at a scan rate of 100 mV s^{-1} and a Ag/Ag+ (0.10 M of $AgNO_3$ in acetonitrile) reference electrode in a solution of 0.1 M of *tetra-n*-butylammonium perchlorate (Bu_4NClO_4) in acetonitrile.

6.2. Reagents

All reactions were carried out under nitrogen atmosphere. The progresses of reactions were monitored by analytical thin-layer chromatography using 0.25 mm pre-coated silica gel plates. Column chromatography was conducted on 70-230 mesh silica gel. All reagents were purchased from commercial suppliers. Chemicals used: benzo[*c*][1,2,5]thiadiazole (Aldrich), HBr, bromine (BDH), sodium bisulfite ($NaHSO_3$), sodium thiosulfate ($Na_2S_2O_3$), 2-propanol, acetone, 3-hydroxybenzaldehyde, thiamine hydrochloride, ethanol, sodium hydroxide, triethylamine, toluene (Reidel-de Haën), potassium carbonate (Riedel-de Haën), diethyl ether, dimethyl sulfoxide (Aldrich), 1-bromohexane (Aldrich), 1-bromooctane, 1-bromodecane, 1-bromododecane, sodium chloride (Aldrich), glacial acetic acid (Merck), N,N-dimethylformamide, anhydrous sodium sulfate (Riedel-de Haën), conc. HCl, petroleum ether, hexane, chloroform

(BDH), ethyl acetate, 2,5-dibromothiophene, magnesium turnings, dichloromethane (Aldrich), tri-n-butyltin chloride , iodine, triphenylphosphine, ammonium chloride, methanol, zinc, acetonitrile, EDTA (Aldrich), hydrazine hydrate ($NH_2NH_2.H_2O$), palladium dichloride ($PdCl_2$), tris(dibenzylideneacetone)dipalladium(0) ($Pd_2(dab)_3$) (Aldrich), bis(triphenylphosphine)palladium(II) dichloride ($Pd(PPh_3)_2Cl_2$ (Aldrich), tris(dibenzylideneacetone)dipalladium(0) ($Pd_2(dab)_3$) (Aldrich), *tetra-n*-butylammonium perchlorate (Bu_4NClO_4) (Fluka), KCl, $K_3Fe(CN)_6$ (BDH). THF was freshly dried over sodium and benzophenone, prior to use.

6.3. Procedures

6.3.1. Synthesis of 4,7-dibromobenzo[*c*][1,2,5]thiadiazole (35)

In 1000 mL flask, a mixture of benzo[*c*][1,2,5]thiadiazole (**10**) (19.0 g, 0.14 mol) and 48% HBr (76 mL) were heated at 110^{o}C with continuous stirring. Bromine (21 mL) was added to the mixture from a pressure equalizing dropping funnel. During refluxing, a white solid deposited on the walls of the flask. Additional HBr (66 mL) was added and the mixture was refluxed for 3 hours. The mixture was then allowed to cool to room temperature and sufficient saturated solution of $NaHSO_3$ was added to consume completely any excess Br_2. It was then filtered by suction, washed with 5% $Na_2S_2O_3$ and water. The product was recrystallized from isopropyl alcohol and then dried in a vacuum oven to afford compound **35** (30.1 g, 73.3%) yield.

^{1}H-NMR (400.13 MHz, $CDCl_3$) δ_{ppm}: 7.64 (2H, *s*, H-5, H-6); ^{13}C-NMR (100.6 MHz, $CDCl_3$) δ_{ppm}: 153 (C-8, C-9), 132.4 (C-5, C-6), 113.9 (C-4, C-7); Dept-135, $CDCl_3$) δ_{ppm}: 132.4 (C-5, C-6); IR: (KBr, cm^{-1}), 3042 (ArC-H), 1651(w), 1587, 1447, 1310, 1185, 937(m), 875, 787, 587; UV-Vis ($CHCl_3$): λ_{max} (nm) 306, 356; Melting point: 164.1-165.5^{o}C. [Lit.[59] 188-190^{o}C].

6.3.2. Synthesis of 3-(decyloxy)benzaldehyde (64)

In a 250 mL 3-necked round bottomed flask equipped with a reflux condenser, pressure equalizing dropping funnel and nitrogen inlet, 3-hydroxybenzaldehyde (**61**) (10.0 g,

81.96 mmol) was dissolved in dimethylformamide (DMF,100.0 mL). Potassium carbonate (56.7 g, 410.87 mmol) was suspended in to the solution and the mixture was heated to 100^{o}C under nitrogen atmosphere. To the heated mixture 1-bromodecane (36.8 g, 166.6 mmol) was added dropwise over 1.5 h and stirred at 100^{o}C under nitrogen overnight. The reaction mixture was cooled to room temperature and the solid material was filtered off. Water (200 mL) was added to the filtrate solution, which was extracted three times with diethyl ether (3x75 mL). The combined ether extract was washed with 2M HCl (50 mL), 1M NaOH (50 mL) and water (100 mL) before drying over anhydrous Na_2SO_4. Rotary evaporation of the solvent gave crude compound **64** (24.8 g) as a yellowish oil. An attempt was made to purify the crude product by passing through short column of silica gel using petroleum ether followed by ethyl acetate as eluent in order to remove excess alkyl bromide. Finally, the solvent was removed and compound **64** (20.9 g) with small amount of alkyl bromide was isolated as yellow oily material that was used for the next reaction without further purification.

^{1}H NMR (400.13 MHz, $CDCl_3$) δ_{ppm}: 9.97 (1H, *s*, CHO), 7.44-7.42 (2H, *m*, H-2, H-6), 7.38 (1H, *d*, *J* = 1.98 Hz, H-5), 7.17 (1H, *m*, Ar-H, H-4), 4.01 (2H, *t*, H-1′), 1.81 (2H, *q*, H-2′), 1.47 (2H, *m*, H-9′), 1.33-1.29 (12H, *br*, 6xCH_2), 0.89 (3H, *t*, H-10′).
^{13}C-NMR (100.6 MHz, $CDCl_3$) δ_{ppm}: 192.2 (C=O), 159.7 (C-3), 137.8 (C-1), 130.0 (C-5), 123.3 (C-6), 121.9 (C-4),112.7 (C-2), 68.3 (C-1′), 31.9 (C-8′), 29.6 (C-5′), 29.6 (C-4′), 29.4(C-6′), 29.3 (C-2′), 29.1 (C-7′), 26.0 (C-3′), 22.7 (C-9′), 14.1 (C-10′). IR (KBr, cm^{-1}): 3069 (w, ArC-H str.) 2962, 2855 (s, C-H str.), 2722 (w, H-C=O str.), 1702 (s, (C=O) str.), 1599, 1453, 1386 (m, (Ar-C=C str. or C-H bending), 1263 (s, C-O str.), 1148, 1041, 870, 787, 683. UV-Vis: λ_{max} ($CHCl_3$, nm): 256 and 316.

6.3.3. Synthesis of 3-(octyloxy)benzaldehyde (63)

Compound **63** was synthesized following similar procedure like that of compound **64** by using 1-bromooctane (31.7 g, 164.24 mmol) and maintaining all the other reaction condition similar to afford crude product **63** (23.0 g) as yellow oily material which was used for the next reaction without further purification.

^{1}H-NMR (400.13 MHz, $CDCl_3$) δ_{ppm}: 9.98 (1H, *s*, CHO), 7.46-7.44 (2H, *m*, H-6, H-2), 7.40 (1H, *d*, *J* = 2.3 Hz, H-5), 7.20- 7.17 (1H, *m*, H-2), 4.01 (2H, *t*, H-1′),1.81 (2H, *q*, H-2′), 1.49 (2H, *q*, H-7′), 1.37- 1.32 (8H, br, 4xCH_2), 0.90 (3H, *t*, H-8′). ^{13}C-NMR (100.6 MHz, $CDCl_3$) δ_{ppm}: 192.2 (C=O), 159.7 (C-3), 137.8 (C-1), 130.0 (C-5), 123.3 (C-6), 121.9 (C-4),112.8 (C-2), 68.3 (C-1′), 31.8 (C-6′), 29.4 (C-2′), 29.3 (C-4′), 29.1 (C-5′), 26.0 (C-3′), 22.7 (C-7′), 14.1 (C-8′). IR (KBr, cm^{-1}): 3069 (w, ArC-H str.), 2925, 2857 (C-H str.), 2725 (w, H-C=O str.), 1703 (C=O) str.), 1598, 1452 (Ar-C=C str. or C-H bending), 1263 (C-O str.), 1148, 1039, 870, 787, 683. UV-Vis: λ_{max} ($CHCl_3$, nm): 256 and 316.

6.3.4. Synthesis of 3-(hexyloxy)benzaldehyde (62)

Compound **62** was synthesized following similar procedure like that of compound **64** by using 1-bromohexane (27.2 g, 164.85 mmol) and maintaining all the other reaction condition similar to afford crude product **62** (18.4 g) as yellow oily material which was used for the next reaction without further purification.

^{1}H NMR (400 MHz, $CDCl_3$) δ_{ppm}: 9.97 (1H, s, CHO), 7.44-7.41 (2H, *m*, H-6, H-2), 7.38 (1H, *d*, *J* = 2.1 Hz, H-5), 7.18 (1H, *m*, H-4), 4.01 (2H, *t*, H-1′), 1.81 (2H, *q*, H-2′), 1.47 (2H, *m*, H-5′), 1.38-1.31 (4H, *m*, 2xCH_2), 0.91 (3H, *t*, H-6′). ^{13}C-NMR (100.6 MHz, $CDCl_3$) δ_{ppm}: 192.2 (C=O), 159.7 (C-3), 137.8 (C-1), 130.0 (C-5), 123.3 (C-6), 121.9 (C-4),112.4 (C-2), 68.3 (C-1′), 31.5 (C-4′), 29.1 (C-2′), 25.7 (C-3′), 22.6 (C-5′), 14.0 (C-6′). IR (KBr, cm^{-1}): 3070 (w, ArC-H str.), 2932, 2859 (C-H str.), 2726 (w, H-C=O str.), 1699 (s, C=O) str.), 1586, 1452, 1387 (Ar-C=C stretching or C-H bending), 1264 (C-O str.), 1148, 1030, 786, 683. UV-Vis: λ_{max} ($CHCl_3$, nm): 255 and 312.

6.3.5. Synthesis of 3-(dodecyloxy)benzaldehyde (65)

Compound **65** was synthesized following similar procedure like that of compound **64** by using 1-bromododecane (41.2 g, 165.46 mmol) as the alkylating agent to afford crude product **65** (22.3 g) as a yellow oily material, which was used for the next reaction without further purification.

^{1}H NMR (400.13 MHz, $CDCl_3$) δ_{ppm}: 9.95 (1H, *s*, CHO), 7.43-7.41 (2H, *m*, H-6, H-4), 7.37 (1H, *s*, H-2), 7.16 (*m*, 1H, H-5), 3.99 (2H, *m*, H-1′), 1.79 (2H, *q*, H-2′), 1.46 (2H, *m*, H-11′), 1.27 (16H, *br*, 8xCH_2), 0.88 (3H, *t*, H-12′). ^{13}C-NMR (100.6 MHz, $CDCl_3$) δ_{ppm}: 192.2 (C=O), 159.8 (C-3), 137.8 (C-1), 129.9 (C-5), 123.2 (C-6), 121.9 (C-4),112.8 (C-2), 68.3 (C-1′), 31.9 (C-10′), 29.7 (C-2′, C-8′), 29.6(C-6′, C-7′), 29.5 (C-4′), 29.4(C-5′), 29.1 (C-9′), 26.0 (C-3′), 22.7 (C-11′), 14.1 (C-12′). IR (KBr, cm^{-1}): 3018 (w, ArC-H str.), 2926, 2855 (C-H str.), 2730 (w, H-C=O str.), 1698 (C=O) str.), 1599, 1455, 1386, (Ar-C=C str. or C-H bending), 1263 (C-O str.), 1148, 1034, 760, 682. UV-Vis: λ_{max} ($CHCl_3$, nm): 254 and 311.

6.3.6. Synthesis of 2-hydroxy-1,2-bis(3-decyloxyphenyl)ethanone (68)

In a 250 mL 2-necked round bottomed flask, thiamine hydrochloride (2.0 g, 5.93 mmol) was dissolved in distilled water (4 mL). To this colorless solution, 95% ethanol (15.6 mL) was added and cooled in an ice bath while swirling the flask to maintain temperature less than 20^{o}C. Using Pasteur pipette, 2M NaOH (5.9 mL) was added dropwise and the solution turned light yellow. After the addition of the base was completed, the mixture was stirred and crude 3-decyloxybenzaldehyde (**64**) (23.3 g) was added. A reflux condenser was attached to the flask and the mixture was heated gently at 60^{o}C for 2h while stirring the solution. After two hours of stirring TLC of the reaction mixture using petroleum ether:ethyl acetate (5:1) as eluent showed two spots which corresponded to the starting material and the α-hydroxyketone product. The reaction mixture was cooled to room temperature and then in an ice bath. The organic layer was separated and the aqueous layer was extracted with chloroform twice. The chloroform extract was combined with the organic layer, washed with water twice, and then dried over anhydrous Na_2SO_4. The solvent was removed under reduced pressure to afford the crude product (22.8 g) which was adsorbed on silica gel and purified by silica gel column chromatography using petroleum ether:ethyl acetate (12:1) as eluent to afford compound **68** (6.2 g, 14.4%) as pale yellow solid.

Mp = 42.2-43.5^{o}C, ^{1}H-NMR (400.13 MHz, $CDCl_3$), δ_{ppm}: 7.49-7.46 (2H, *m*, H-6, H-2), 7.32-7.22 (2H, *m*, H-5, H-5′), 7.08-7.05 (1H, *dd*, *J* = 2.0, 8.2 Hz, H-4′), 6.92 (1H, *d*, J =

7.66 Hz, H-4), 6.86 (1H, *d, J* = 2.1 Hz, H-6′), 6.83- 6.80 (1H, *dd*, *J* = 2.1, 8.0 Hz, H-2′), 5.90 (*s*, 1H, H-b), 3.97- 3.90 (4H, *m*, H-1″, H-1‴), 1.81- 1.72 (4H, *m*, H-2″, H-2‴), 1.45-1.42 (4H, *m*, H-9″, H-9‴), 1.32- 1.29 (24H, *br*, 12 x -CH_2), 0.91(6H, *t,* H-10″,H-10‴); ^{13}C-NMR (100.6 MHz, $CDCl_3$) δ_{ppm}: 198.7 (C-a), 159.7 (C-3′), 159.3 (C-3), 140.4 (C-1), 134.7 (C-1′), 130.1 (C-5′), 129.6 (C-5), 121.1 (C-6′), 121.6 (C-6), 119.9 (C-4), 114.7 (C-2′), 113.7 (C-2), 112.8 (C-4′), 76.2 (C-b), 68.3 (C-1″), 68.0 (C-1‴), 31.9 (C-8″, C-8‴), 29.4 (C-2″, C-2‴), 29.4 (C-4″, C-4‴), 29.3 (C-5″, C-5‴), 29.2 (C-6″, C-6‴), 29.1 (C-7″, C-7‴), 26.0 (C-3″, C-3‴), 22.7 (C-9″, C-9‴), 14.1 (C-10″, C-10‴); IR (KBr, cm^{-1}): 3446 (br, O-H str.), 2922, 2852 (s, C-H str.), 1676(s, C=O str.), 1585, 1452 (m, Ar C=C and C-H bending), 1269 (m, C-O str.), 1148, 1038m, 787, 683; UV-Vis: λ_{max} ($CHCl_3$, nm): 259 and 319.

6.3.7. Synthesis of 2-hydroxy-1,2-bis(3-octyloxyphenyl)ethanone (67)

The synthesis of compound **67** followed the same synthetic procedure as that of compound **68.** Thus, **63** (22.9 g) was used as the starting material and all the other reaction conditions were maintained the same to afford a crude product (23.0 g) which was purified by silica gel column chromatography using hexane: ethyl acetate (12:1) as eluent to yield **67** (3.5 g, 9.1%) as an oily material.

^{1}H-NMR (400.13 MHz, $CDCl_3$), δ_{ppm}: 7.49-7.47 (2H, *m*, H-2, H-6), 7.29-7.20 (2H, *m*, H-5, H-5′), 7.07-7.04 (1H, *dd*, *J* = 1.9, 8.6 Hz, H-4′), 6.93- 6.91 (1H, *d*, *J* = 7.7 Hz, H-4), 6.88 (1H, *s,* H-2′), 6.82- 6.79 (1H, *dd*, *J* = 1.8, 8.2 Hz, H-6′), 5.90 (1H, *s*, H-b), 3.96-3.88 (4H, *m*, H-1″, H-1‴), 1.79-1.71(4H, *m*, H-2″, H-2‴), 1.45-1.42 (4H, *m*, H-7″, H-7‴), 1.35-1.31(16H, *br*, 8 x -CH_2), 0.92 (6H, *t,* H-8″, H-8‴); ^{13}C-NMR (100.6 MHz, $CDCl_3$,) δ_{ppm}: 198.7 (C-a), 76.2 (C-b), 140.4 (C-1), 113.7 (C-2), 159.3 (C-3), 119.9 (C-4), 129.6 (C-5), 121.0 (C-6), 134.7 (C-1′), 114.7 (C-2′), 159.7 (C-3′), 113.9 (C-4′), 130.1 (C-5′), 121.6 (C-6′), 68.2 (C-1″), 68.0 (C-1‴), 29.4 (C-2″), 26.0 (C-3″, C-3‴), 29.3 (C-4″, C-4‴), 29.1 (C-5″, C-5‴), 31.8 (C-6″, C-6‴), 22.7 (C-7″, C-7‴), 14.1(C-8″, C-8‴); IR (KBr, cm^{-1}): 3451(O-H str.), 2926, 2856 (s, C-H str.), 1681 (C=O) str.), 1598, 1443 (Ar-C=C or str.C-H bending), 1266 (C-O str.), 1034, 874, 780, 708; UV-Vis λ_{max} ($CHCl_3$, nm): 259 and 316.

6.3.8. Synthesis of 2-hydroxy-1,2-bis(3-dodecyloxyphenyl)ethanone (69)

The synthesis of compound **69** followed the same procedure as that of compound **68.** Thus, crude compound **65** (21.7 g) was used as the starting material and all reaction conditions were maintained the same to afford crude **69** (21.3 g). Attempt to purify the crude material by silica gel column chromatography using hexane:ethyl acetate (12:1) as eluent could not afford pure **69**. ^{1}H- and ^{13}C-NMR spectra of this material confirmed that it was a mixture of **69** and its oxidation product. Thus, the isolated yellow oily product was converted to the diketone without further purification.

6.3.9. Synthesis of 2-hydroxy-1,2-bis(3-hexyloxyphenyl)ethanone (66)

The synthesis of compound **66** followed the same method like that of compound **68**. Accordingly, crude compound **63** (18.3 g), thiamine hydrochloride (2.3 g, 6.82 mmol), distilled water (4.5 mL), ethanol (95%, 18.1 mL) and NaOH (2M, 6.8 mL) were used by maintaining all the other reaction conditions the same to afford the crude product (18.3 g) which was purified by silica gel column chromatography using hexane: ethyl acetate (12:1) as eluent to afford pure **66** (5.5 g, 16.3%).

Mp = 47.6-49.2. ^{1}H-NMR (400.13 MHz, $CDCl_3$) δ_{ppm}: 7.49-7.47 (2H, *s*, H-2, H-6), 7.32-7.22 (2H, *m*, H-5, H-5′), 7.09-7.06 (1H, *dd*, *J* = 2.3, 8.2 Hz, H-4′), 6.94 (1H, *d*, *J* = 7.7 Hz , H-4), 6.86 (1H, *s,* H-2′), 6.83-6.80 (1H, *dd*, *J* = 2.3, 8.2 Hz, H-6′), 5.90 (1H, *s*, H-b), 3.96-3.90 (4H, *m*, H-1″, H-1‴), 1.80-1.74 (4H, *m*, H-2″, H-2‴), 1.46-1.43 (4H, *m*, H-5″, H-5‴), 1.37-1.34 (8H, *br*, 4x -CH_2), 0.93 (6H, *t*, H-6″, H-6‴); ^{13}C-NMR (100.6 MHz, $CDCl_3$) δ_{ppm}: 198.7 (C-a), 159.7 (C-3′), 159.3 (C-3), 140.4 (C-1), 134.7 (C-1′), 130.1 (C-5′), 129.6 (C-5), 121.6 (C-6′), 121.0 (C-6), 119.9 (C-4), 114.7 (C-4′), 113.8 (C-2′), 113.7 (C-2), 76.2 (C-b), 68.2 (C-1″), 68.0 (C-1‴), 31.6 (C-4‴), 31.5 (C-4″), 29.2 (C-2″, C-2‴), 25.7 (C-3″, C-3‴), 22.6 (C-5″, C-5‴), 14.0 (C-6″, C-6‴); IR (KBr, cm^{-1}): 3447 (O-H str.), 2941, 2867 (C-H str.), 1679 (C=O) str.), 1582,1475, 1444, 1394 (C-H bending or Ar-C=C str.), 1269 (C-O str.), 1185, 1033, 783, 724; UV-Vis λ_{max} ($CHCl_3$, nm): 259 and 317.

6.3.10. Synthesis of 1,2-bis (3-(decyloxy)phenyl)ethane-1,2-dione (71)

In a 250 mL, three-necked, round bottomed flask equipped with a magnetic stirrer, a reflux condenser, a nitrogen inlet, and pressure equalizing addition funnel compound **68** (4.2 g, 8.02 mmol) was dissolved in DMSO (9.3 mL) with continuous stirring at room temperature. Hydrobromic acid (48%, 4.5 mL) was then added dropwise over a period of 1h from addition funnel while string the reaction mixture at room temperature. After the addition of HBr completed, the reaction mixture was heated to 50^{o}C and stirred for 4 h. The reaction mixture was then slowly heated to 90^{o}C and maintained at that temperature overnight. TLC of the reaction mixture using hexane:ethyl acetate (5:1) as eluent showed complete conversion of starting material. The reaction mixture was allowed to cool to room temperature and was then poured into ice-cold water (100 mL). The yellow precipitate that formed was collected by filtration, washed with cold water followed by cold ethanol and dried in a vacuum oven to afford pure **71** (3.9 g, 93.3%) as a yellow solid.

Mp = 57.6-58.4^{o}C. ^{1}H-NMR (400.13 MHz, $CDCl_3$) δ_{ppm}: 7.54 (2H, *m*, H-6), 7.46 (2H, *d*, *J* = 7.6 Hz, H-5), 7.40 (2H, *t*, *J* = 7.9 Hz, H-2), 7.22-7.20 (2H, *d*, *J* = 8.1 Hz, H-4), 4.03 (4H, *t*, *J* = 6.5 Hz, H-1′), 1.81 (4H, *q,* H-2′), 1.48 (4H, *br*, H-9′), 1.36-1.30 (24H, *br*, 12xCH_2), 0.91 (6H, *t*, *J* = 6.8 Hz, H-10′); ^{13}C-NMR (100.6 MHz, $CDCl_3$,) δ_{ppm}: 194.5 (C=O), 159.6 (C-3), 134.2 (C-1), 130.0 (C-5), 113.7 (C-2), 122.9 (C-6),122.2 (C-4), 68.4 (C-1′), 31.9 (C-8′), 29.6 (C-2′), 29.4 (C-4′), 29.4 (C-5′), 29.3 (C-6′), 29.1 (C-7′), 26.0 (C-3′), 22.7 (C-9′), 14.1 (C-10′); FT-IR (KBr, cm^{-1}): 3069 (w, ArC-H str.), 2953, 2925, 2853 (C-H str.), 1678 (C=O) str.), 1594, 1471, 1438 (Ar-C=C str. or C-H bending), 1336, 1262 (C-O str.), 1155, 1031, 972, 827, 789, 735, 640; UV-Vis λ_{max} ($CHCl_3$, nm): 265 and 325.

6.3.11. Synthesis of 1,2-bis(3-(octyloxy)phenyl)ethane-1,2-dione (25)

Compound **25** was synthesized following the same synthetic procedure as that of compound **71**. Thus, compound **67** (3.4 g, 7.25 mmol) was dissolved in DMSO (8.4 mL) followed by dropwise addition of 48%HBr (4.1 mL) within 60 minutes while stirring the reaction mixture at room temperature under nitrogen atmosphere. The temperature was

raised to 50°C and maintained at this temperature for 4h and then raised to 90°C and heated overnight. The resulting yellow suspension was poured in to cold water, filtered and washed with cold water and cold ethanol to afford **25** (2.8g, 82.7%) as a yellow solid.

Mp = 50.7-51.6°C. ^{1}H-NMR (400.13 MHz, $CDCl_3$) δ_{ppm}: 7.53 (2H, *s*, H-6), 7.47 (2H, *d*, *J* = 7.5 Hz, H-5), 7.40(2H, *t*, *J* = 7.8 Hz, H-2), 7.21 (2H, *d*, *J* = 7.9 Hz, H-4), 4.02 (4H, *t*, *J* = 6.3 Hz, H-1′), 1.81(4H, *q,* H-2′), 1.48 (4H, *br*, H-7′), 1.36-1.30 (16H, *br*, 8xCH_2), 0.91 (6H, *t*, *J* = 6.3 Hz, H-8′); ^{13}C-NMR (100.6 MHz, $CDCl_3$) δ_{ppm}: 194.6 (C=O), 159.6 (C-3), 134.2 (C-1), 130.0 (C-5), 123.0 (C-6), 122.2 (C-4), 113.6 (C-2), 68.4 (C-1′), 31.8 (C-6′), 29.3 (C-2′), 29.3 (C-4′), 29.1 (C-5′), 26.0 (C-3′), 22.7 (C-7′), 14.1 (C-8′). IR (KBr, cm^{-1}): 3074 (w, ArC-H), 2953, 2927, 2856 (C-H str.), 1660 (C=O) str.), 1597, 1485, 1438 (Ar-C=C str. or C-H bending), 1265(s, C-O str.), 1154, 1032, 790, 732, 646. UV-Vis λ_{max} ($CHCl_3$, nm): 265 and 324.

6.3.12. Synthesis of 1,2-bis(3-(hexyloxy)phenyl)ethane-1,2-dione (70)

The synthesis of compound **70** followed the same procedure as that of compound **71.** Thus, compound **66** (3.9 g, 9.44 mmol), DMSO (17.8 mL) and 48% HBr (11.3 mL) were used to afford compound **70** (3.8g, 96.4%) as a yellow solid.

Mp = 50.5-51.8°C. ^{1}H-NMR (400.13 MHz, $CDCl_3$), δ_{ppm}: 7.53 (2H, *m*, H-6), 7.48 (2H, *d*, *J* = 7.6 Hz, H-5), 7.39 (2H, *t*, *J* = 7.6 Hz, H-2), 7.22-7.19 (2H, *d*, *J* = 8.1 Hz, H-4), 4.02 (4H, *t*, *J* = 6.5 Hz, H-1′), 1.81 (4H, *q*, H-2′), 1.48 (4H, *q*, H-5′), 1.37-1.35 (8H, *br*, H-3′, H-4′), 0.93 (6H, *t*, *J*=7.0Hz, H-6′); ^{13}C-NMR (100.6 MHz, $CDCl_3$) δ_{ppm}: 194.6 (C=O), 159.6 (C-3), 134.2 (C-1), 130.0 (C-5), 122.9 (C-6), 122.2 (C-4), 113.6 (C-2), 68.4 (C-1′), 31.5 (C-4′), 29.1 (C-2′), 25.7 (C-3), 22.6 (C-5′), 14.0 (C-6′). IR (KBr, cm^{-1}): 3076 (ArC-H), 2924, 2853 (C-H str.), 1679 (C=O) str.), 1595, 1473, 1438 (Ar-C=C str. or C-H bending), 1336, 1264(s, C-O str.), 1155, 1028, 734, 646. UV-Vis λ_{max} ($CHCl_3$, nm): 265 and 327.

6.3.13. Synthesis of 1,2-bis(3-(dodecyloxy)phenyl)ethane-1,2-dione (72)

Compound **72** was synthesized following the same procedure used for the synthesis of compound **71.** Thus, compound **69** (3.8 g, 6.55 mmol), DMSO (12.3 mL) and 48% HBr (8.0 mL) were used to afford **72** (1.9 g, 50.1%) as yellow solid.

Mp = 61.3-62.0^{o}C. ^{1}H-NMR (400.13 MHz, $CDCl_3$) δ_{ppm}: 7.53 (2H, *s*, H-2), 7.48 (2H, *d*, *J* = 7.2 Hz, H-6), 7.42 (2H, *t*, *J* = 7.6 Hz, H-5), 7.22 (2H, *d*, *J* = 7.6 Hz, H-4), 4.02 (4H, *t*, *J* = 5.7 Hz, H-1′), 1.81 (4H, *m*, H-5′), 1.47 (4H, *br*, H-11′), 1.29 (32H, *br*, 16xCH_2), 0.90 (6H, *t*, *J* = 6.3 Hz, H-12′). ^{13}C-NMR (100.6 MHz, $CDCl_3$) δ_{ppm}: 194.6 (C=O), 159.6 (C-3), 134.2 (C-1), 130.0 (C-5), 122.9 (C-6), 122.3 (C-4), 113.6 (C-2), 68.4 (C-1′), 31.9 (C-10′), 29.7 (C-2′, C-7′), 29.6 (C-4′,C-5′, C-8′), 29.4 (C-6′), 29.3 (C-2′), 29.1 (C-9′), 26.0 (C-3′), 22.7 (C-11′), 14.2 (C-12′). IR (KBr, cm^{-1}): 3082 (w, ArC-H str.), 2933, 2871 (C-H str.), 1672 (C=O str.), 1599, 1444 (Ar-C=C str. or C-H bending), 1266 (s, C-O str.), 1155, 1030, 736, 642. UV-Vis λ_{max} ($CHCl_3$, nm): 266 and 327.

6.3.14. Synthesis of 5,8-dibromo-2,3-bis(3-(decyloxy)phenyl)quinoxaline (74)

In a 100 mL two necked round bottomed flask, zinc dust (6.1 g, 93.85 mmol), 4,7-dibromobenzo[*c*][1,2,5]thiadiazole (**35**) (2.2 g, 7.48 mmol), acetic acid (72.6 mL) and few drops of water were added. The mixture was stirred at 60^{o}C for 6 h. The solid residue was removed by filtration and then 1,2-bis(3-(decyloxy)phenyl)ethane-1,2-dione, **71** (1.0 g, 1.92 mmol) was added to the filtrate. The resulting solution was stirred at 60^{o}C overnight following the progress of the reaction by TLC using hexane:dichloromethane (1:1) as eluent. The reaction mixture was cooled to room temperature and the resulting solid material was filtered and washed with cold methanol followed by cold ethanol. The solid material was dried in a vacuum oven to afford the **74** (0.9 g, 63.8%) as a pale yellow solid.

Mp = 85.1-86.1^{o}C. ^{1}H-NMR (400.13 MHz, $CDCl_3$) δ_{ppm}: 7.94 (2H, *s*, H-6, H-7), 7.28-7.24 (4H, *m*, H-5′, H-6′), 7.20 (2H, *d*, *J* = 7.7 Hz, H-2′), 6.95 (2H, *dd*, *J* = 8.1, 1.5 Hz, H-4′), 3.88 (4H, t, *J* = 6.3 Hz, H-1″), 1.78-1.73 (4H, *q*, H-2″), 1.43-1.30 (28H, *m*, 7× CH_2, H-3″–H-9″), 0.91 (6H, *t*, *J* = 6.7 Hz, H-10″). ^{13}C-NMR (100.6 MHz, $CDCl_3$) δ_{ppm}: 159.1 (C-3′),

154.1 (C-2, C-3), 139.3 (C-9, C-10), 139.1(C-1′), 133.1(C-6, C-7), 129.3 (C-5′), 123.7 (C-5, C-8), 122.5 (C-6′), 116.6 (C-4′), 115.7 (C-2′), 68.1 (C-1″), 31.9 (C-8″), 29.6 (C-2″), 29.6 (C-4″), 29.4 (C-6″), 29.4(C-5″)29.1 (C-7″), 26.0 (C-3″), 22.7 (C-9″), 14.1 (C-10″); FT-IR (KBr, cm^{-1}): 3070 (w, ArC-H str.), 2920, 2850 (C-H str.), 1604 (C=N str.), 1577-1444 (Ar-C=C str. and C-H bending), 1335, 1241 (C-O str.), 1204, 1032, 939, 819, 715, 587 (C-Br str.); UV-Vis λ_{max} (CH_3CN, nm): 255, 272, and 353.

6.3.15. Synthesis of 5,8-dibromo-2,3-bis(3-(octyloxy)phenyl)quinoxaline (51)

Compound **51** was synthesized by following a similar procedure used for synthesis of compound **74**. Thus, zinc dust (6.1 g, 93.85 mmol), 4,7-dibromobenzo[*c*][1,2,5]thiadiazole (**35**) (2.2 g, 7.48 mmol), acetic acid (72.6 mL) and few drops of water and 1,2-bis(3-(octyloxy)phenyl)ethane-1,2-dione (**25)** (1.2 g, 2.57 mmol) were used. Compound **51** (1.2 g, 64.8%) was obtained as a pale yellow solid.

Mp = 77.9-79.0°C. ^{1}H-NMR (400.13 MHz, $CDCl_3$) δ_{ppm}: 7.94 (2H, *s*, H-6, H-7), 7.28- 7.24 (4H, *m*, H-5′, H-6′), 7.20 (2H, *d*, J = 7.6, H-2′), 6.96 (2H, *d*, *J* = 8.0 Hz, H-4′), 3.88 (4H, *t*, *J* = 6.6 Hz, 4H, H-1″), 1.77-1.73 (4H, *q*, H-2″), 1.44-1.32 (20H, *m*, 10×CH_2), 0.92 (6H, *t*, *J* = 6.9 Hz, H-8″). ^{13}C-NMR (100.6 MHz, $CDCl_3$) δ_{ppm}: 159.0 (C-3′), 154.0 (C-2, C-3), 139.3 (C-9, C-10), 139.1 (C-1′), 133.1 (C-6, C-7), 129.3 (C-5′), 123.7 (C-5, C-8), 122.5 (C-6′), 116.5 (C-4′), 115.7 (C-2′), 68.1 (C-1″), 31.9 (C-6″), 29.4 (C-5″), 29.3 (C-4″), 29.1 (C-2″), 26.0 (C-3″), 22.7 (C-7″), 14.1 (C-8″). FT-IR (KBr, cm^{-1}): 2920, 2852 (C-H str.), 1603 (C=N str.), 1578, 1546, 1445 (Ar-C=C str. and C-H bending), 1384, 1335 (C-C str.), 1241(C-O str.), 1203, 1030, 938, 715, 587(C-Br str.), 491. UV-Vis λ_{max} (CH_3CN, nm): 254, 272 and 354.

6.3.16. Synthesis of 5,8-dibromo-2,3-bis(3-(dodecyloxy)phenyl)quinoxaline (75)

In a 100 mL two necked round bottomed flask zinc dust (4.3 g, 66.17 mmol) and 4,7-dibromobenzo[*c*][1,2,5]thiadiazole (**35**) (1.6 g, 5.44 mmol), acetic acid (51 mL) and few drops of water were added. The mixture was stirred at 60°C for 6h. The solid residue was removed by filtration and then compound **72** (0.8 g, 1.35 mmol) was added to the filtrate. The resulting solution was stirred at 60°C overnight following the progress of

reaction by TLC using hexane:dichloromethane (1:1). The reaction mixture was cooled to room temperature and the resulting solid material was filtered and washed with cold methanol followed by cold ethanol in order to remove unreacted starting material and impurities from side reactions. The solid material was dried in a vacuum oven to afford **75** (0.9 g, 82.5%) as a pale violet solid.

Mp = 79.3-80.1^{o}C. ^{1}H-NMR (400.13 MHz, $CDCl_3$) δ_{ppm}: 7.93 (2H, *s*, H-6, H-7), 7.26- 7.21 (6H, *m*, H-2′, H-5′, H-6′), 6.96 (2H, *d*, *J* = 7.13 Hz, H-4′), 3.88 (4H, *t*, J=6.7Hz, H-1″), 1.76- 1.73 (4H, *m*, H-2″), 1.43- 1.29 (36H, *br*, H-3″– H-11″), 0.91 (4H, *t*, *J* = 5.8Hz, H-12″). ^{13}C-NMR (100.6 MHz, $CDCl_3$) δ_{ppm}: 159.0 (C-3′), 154.0 (C-2, C-3), 139.3 (C-9, C-10), 139.1 (C-1′), 133.1 (C-6, C-7), 129.3 (C-5′), 123.7 (C-5, C8), 122.5 (C-6′), 116.5 (C-4′), 115.7 (C-2′), 68.1 (C-1″), 32.0 (C-10″), 29.7 (C-2″, C-4″), 29.7 (C-5″, C-6″), 29.4 (C-7″, C-8″), 29.1 (C-9″), 26.0 (C-3″), 22.7 (C-11″), 14.2 (C-12″). FT-IR (KBr, cm^{-1}): 2919, 2841 (C-H str.), 1603 (C=N str.), 1578- 1443 (Ar-C=C str. and C-H bending), 1335, 1033, (C-C str.), 1241(-C-O str.), 1168, 1033, 938, 803, and 715 (C-Br str.). UV-Vis λ_{max} (CH_3CN, nm): 252, 273 and 345.

6.3.17. Synthesis of 5,8-dibromo-2,3-bis(3-(hexyloxy)phenyl)quinoxaline (73)

Compound **73** was synthesized following a similar procedure as that used for the preparation compound **74**. Thus, zinc dust (7.1 g, 108.56 mmol), 4,7-dibromobenzo[*c*][1,2,5]thiadiazole (**35**) (2.6 g, 8.84 mmol) and acetic acid (84.5 mL) and 1,2-bis(3-(hexyloxy)phenyl)ethane-1,2-dione (**70**) (1.2 g, 2.92 mmol) were used. Compound **73** (1.2 g, 65.2%) was obtained as a pale pink solid.

Mp = 88.5- 90.5^{o}C. ^{1}H-NMR (400.13 MHz, $CDCl_3$) δ_{ppm}: 7.93 (2H, *s*, H-6, H-7), 7.28-7.25 (4H, *m*, H-5′, H-6′), 7.21 (2H, *d*, *J* = 7.2 Hz, H-2′), 6.96 (2H, *d*, *J* = 7.9 Hz, H-4′), 3.89 (4H, *t*, *J* = 6.4Hz, H-1″), 1.78- 1.73 (4H, *q*, H-2″), 1.48- 1.43 (4H, *m*, H-5″), 1.36 (8H, *br*, 4×CH_2), 0.94 (6H, *t*, *J* = 6.4 Hz, H-6″). ^{13}C-NMR (100.6 MHz, $CDCl_3$) δ_{ppm}: 159.1 (C-3′), 154.0 (C-2, C-3), 139.3 (C-9, C-10), 139.1 (C-1′), 133.1 (C-6, C-7), 129.3 (C-5′), 123.7 (C-5, C-8), 122.6 (C-6′), 116.5 (C-4′), 115.7 (C-2′), 68.1 (C-1″), 31.6 (C-4″), 29.1 (C-2″), 25.7 (C-3″), 22.6 (C-5″), 14.1 (C-6″). FT-IR (KBr, cm^{-1}): 3070 (ArC-H str.), 2931, and 2856 (C-H str.), 1603 (C=N str.), 1584- 1444 (C-H bending or Ar-C=C str.), 1384-

1334 (C-C- str.), 1244 (-C-O str.), 1032, 937, 686 (C-Br str.), 588. UV-Vis λ_{max} (CH_3CN, nm): 254, 272 and 354.

6.3.18. Synthesis of 2, 5-bis (tri-n-butylstannyl)thiophene (78)

In a 250 mL, three-necked round bottomed flask equipped with a reflux condenser, pressure equalizing addition funnel and nitrogen inlet in a sonication bath, magnesium turnings (1.6 g, 66.67 mmol) and dry THF (100 mL) were mixed and sonicated at room temperature. A small amount of iodine solution in dry THF was added to initiate the reaction. To this, a solution of 2,5-dibromothiophene (**76**) (5.0 g, 20.66 mmol) in dry THF (5.0 mL) was added drop wise over a period of 20 minutes and the mixture was sonicated for about 3h at room temperature resulting in a yellow solution. To the mixture Bu_3SnCl (**77**) (16.8 mL, 61.94 mmol) was added through pressure equalized addition funnel over a period of 15 minutes which resulted in the formation of light green solution. Then the reaction mixture was further sonicated at room temperature for about 4h. TLC of the reaction mixture using hexane:diethyl ether (4.9:0.1) showed a single spot which moved with the solvent front that confirmed complete conversion of the starting material. The sonication was stopped and saturated NH_4Cl (350 mL) was added and extracted with ethyl acetate (4×100 mL). The organic layer was separated and was washed with brine solution (200 mL) and dried over anhydrous Na_2SO_4. The solvent was removed under reduced pressure to afford deep green crude product (19.49 g) which was further purified by vacuum distillation to afford compound **78** (11.0 g, 80.1%) as a colorless oily liquid. The product boiled at 174-185^oC (0.12 mmHg).

^{1}H-NMR (400.13 MHz, $CDCl_3$) δ_{ppm}: 7.49 (2H, *s,* H-3, H-4), 1.68 (12H, *q*, H-3′), 1.45 (12H, *sextet,* H-2′), 1.22 (12H, *t,* H-1′), 0.99 (18H, *t,* H-4′). ^{13}C-NMR (100.6 MHz, $CDCl_3$) δ_{ppm}: 141.8 (C-2, C-5), 135.8 (C-3, C-4), 29.1 (C-2′), 27.4 (C-3′), 13.7 (C-4′), 10.9 (C-1′). FT-IR (KBr, cm^{-1}): 3054, 2926, 2957, 2852 (Ar and aliphatic C-H str.), 1463, 1376 (C-H bending and C=C str.), 1073 (C-S), 950, 489. UV-Vis λ_{max} ($CHCl_3$, nm): 250.

6.3.19. Synthesis of tetrakis(triphenylphosphine)palladium(0)

A mixture of palladium dichloride (0.5 g, 2.82 mmol), triphenylphosphine (3.7 g, 33.86 mmol) and DMSO (34 mL) were placed in a 100 mL Schlenk flask which was fitted with a fritted glass funnel attached to a second inverted 100 mL Schlenk flask equipped with a magnetic stirring bar and nitrogen inlet. The yellow mixture was heated under nitrogen atmosphere in an oil bath until complete solution occurred at around 140^{o}C. The heater was then removed and the solution was rapidly stirred for about 15 minutes. Hydrazine hydrate (0.6 g, 11.20 mmol) was then rapidly added with a syringe. The yellow solution was then cooled to room temperature while stirring the reaction mixture, which resulted in the formation of yellow solid. The yellow solid was collected by filtration, washed successively with absolute ethanol (2 x10 mL) and diethyl ether (2x10 mL) and dried under vacuum for 2 hours by passing a slow stream of nitrogen through the funnel to afford $Pd(PPh_3)_4$ (3.0 g, 90.9%) as a yellow crystalline solid.

6.4. Syntheses of polymers

6.4.1. Synthesis of poly[2,3-bis-(3-octyloxyphenyl)quinoxaline-5,8-diyl-*alt*-thiophene-2,5-diyl] (52)

In a 25 mL three-necked round bottomed flask equipped with a reflux condenser, nitrogen inlet and magnetic stirrer, a mixture of compound **51** (277.6 mg, 0.40 mmol), **78** (264.0 mg, 0.40 mmol) and freshly prepared $Pd(PPh_3)_4$ (64.7 mg, 0.06 mmol) were placed. The mixture was dissolved in toluene (10 mL) and the reaction mixture was kept under nitrogen atmosphere. The reaction mixture was then heated at 110^{o}C for 44 h, cooled to room temperature and added into methanol. The solid material was collected by filtration through 0.45-μm Teflon filter, dried, and was redissolved in chloroform. The solution was then stirred with EDTA solution at room temperature overnight. The chloroform layer was separated and was washed with deionized water three times, concentrated to small volume and precipitated from methanol. The crude polymer mixture was collected by filtration and was Soxhlet-extracted with methanol, acetone and finally with chloroform. The chloroform extract was evaporated concentrated to a

small volume under reduced pressure, and the polymer was precipitated from methanol, filtered then dried in a vacuum oven at 50^{o}C for 12 h to afford **52** (214.6 mg, 86.4%) as deep blue solid.

^{1}H NMR (400.13 MHz, $CDCl_3$) δ_{ppm}: 8.08 (2H, *br*, Ar-H), 7.49-7.12 (8H, *br*, Ar-H), 6.84 (2H, *br*, Ar-H), 3.72 (4H, *br*, -OCH_2), 1.60 (4H, *br*, -CH_2), 1.16 (20H, *br*, -CH_2), 0.80 (6H, *br*, CH_3).

6.4.2. Synthesis of poly[2,3-bis-(3-decyloxyphenyl)quinoxaline-5,8-diyl-*alt*-thiophene-2,5-diyl] (82)

Polymer **82** was synthesized following the method described above for the synthesis of **52.** Thus, compound **74** (192.2 mg, 0.26 mmol), compound **78** (169 mg, 0.26 mmol), freshly prepared $Pd(PPh_3)_4$ (43.3 mg, 0.04 mmol) and toluene (8.0 mL) were used to afford polymer **82** (84.5 mg, 48.9%) as deep blue solid.

^{1}H NMR (400.13 MHz, $CDCl_3$, δ_{ppm}): 8.28-8.01 (2H, *br*, Ar-H), 7.66-7.12 (8H, *br*, Ar-H), 6.84 (2H, *br*, Ar-H), 3.74 (4H, *br*, -OCH_2), 1.60 (4H, *br*, -CH_2), 1.18 (28H, *br*, -CH_2), 0.80 (6H, *br*, CH_3).

6.4.3. Synthesis of poly[2,3-bis-(3-dodecyloxyphenyl)quinoxaline-5,8-diyl-*alt*-thiophene-2,5-diyl] (83)

The synthesis of polymer **83** followed the same method used for the synthesis of polymer **52.** Thus, where, compound **75** (404.5 mg, 0.50 mmol), compound **78** (331.0 mg, 0.50 mmol), freshly prepared $Pd(PPh_3)_4$ (80.9 mg, 0.07 mmol) and toluene (10 mL) were employed to afford polymer **83** (206.8 mg, 56.4%) as dark blue solid.

^{1}H NMR (400.13 MHz, $CDCl_3$) δ_{ppm}: 8.28- 8.01 (2H, *br*, Ar-H), 7.61- 7.12 (8H, *br*, Ar-H), 6.84 (2H, *br*, Ar-H), 3.82 (4H, *br*, -OCH_2), 1.60 (4H, *br*, -CH_2), 1.19 (36H, *br*, -CH_2), 0.86 (6H, *br*, CH_3).

6.4.4. Synthesis of poly[2,3-bis-(3-hexyloxyphenyl)quinoxaline-5,8-diyl-*alt*-thiophene-2,5-diyl] (81)

The synthesis of polymer **81** followed the same method used for the synthesis of polymer **52.** Thus, compound **73** (320.0 mg, 0.50 mmol), compound **78** (331.0 mg, 0.50 mmol), freshly prepared $Pd(PPh_3)_4$ (64.7 mg, 0.06 mmol) and toluene (10 mL) were used to afford polymer **81** (240.5 mg, 85.1%) as a dark blue solid.

^{1}H NMR (400.13 MHz, $CDCl_3$) δ_{ppm}: 8.23- 8.05 (2H, *br*, Ar-H), 7.49- 7.09 (8H, *br*, Ar-H), 6.84 (2H, *br*, Ar-H), 3.74 (4H, *br*, -OCH_2), 1.63 (4H, *br*, -CH_2), 1.16 (8H, *br*, -CH_2), 0.84 (6H, *br*, CH_3).

7. REFERENCES

1. Carraher Jr., C. E.; Seymour, R. B. In *Polymer Chemistry*; CRC Press, 2012; p. 1.
2. Ravve, A. *Principles of Polymer Chemistry*; 3rd ed.; Springer New York: New York, NY, 2012.
3. Ayalew Hussen MSc. Project, Department of Chemistry, Addis Ababa University, Ethiopia, 2009.
4. Zarina, O. Exploring quinoxaline-based conjugated polymers towards organic solar cells. PhD Dissertation, University of Hasselt, Belgium, 2008.
5. McNeil, R.; R.S.; Wardlaw, J. H.; Weiss, D. E.; *Australian J. Chem.* **1963**, *16*, 1056.
6. Shirakawa, H.; Louis, E. J.; MacDiarmid, A. G.; Chiang, C. K.; Heeger, A. J.; *J. Chem. Soc. Chem. Commun.* **1977**, 578.
7. Unlu, N. A.; Deniz, T. K.; Sendur, M.; Cirpan, A.; *Macromol. Chem. Phys.* **2012**, *213*, 1885.
8. Zhang, G.; Fu, Y.; Zhang, Q.; Xie, Z.; *Polymer* **2010**, *51*, 2313.
9. Tsami, A.; Bu¨nnagel, T. W.; Farrell, T.; Scharber, M.; Choulis, S. A.; Brabecd, C. J.; Scherf, U.; *J. Mater. Chem.* **2007**, *17*, 1353.
10. Manuel, J.; *Environ. Health Perspect.* **2005**, *113*, A301.
11. Zhou, E.; Cong, J.; Yamakawa, S.; Wei, Q.; Nakamura, M.; Tajima, K.; Yang, C.; Hashimoto, K.; *Macromolecules* **2010**, *43*, 2873.
12. Dennler, G.; Scharber, M. C.; Brabec, C. J.; *Adv. Mater.* **2009**, *21*, 1323.
13. Bundgaard, E.; Krebs, F. C.; *Sol. Energy Mater. Sol. Cells* **2007**, *91*, 954.
14. Windera, C.; Sariciftcia, N. S.; *J. Mater. Chem.* **2004**, *14*, 1077.
15. Carsten, B.; He, F.; Son, H. J.; Xu, T.; Yu, L.; *Chem. Rev.* **2011**, *111*, 1492.
16. Wan, Z.; Jones, C. D.; Mitchell, D.; Y. Pu, J.; Zhang, T. Y.; *J. Org. Chem.* **2006**, *71*, 826.
17. Jansen, H. P.; Sharpless, K. B.; *J. Org. Chem.* **1974**, *39*, 2314.
18. Schmidt, B.; Krehl, S.; Hauke, S.; *J. Org. Chem.* **2013**, *78*, 5472.
19. Chen, S.; Liu, Z.; Shi, E.; Chen, L.; Wei, W.; Li, H.; Cheng, Y.; Wan, X.; *Org. Lett.* **2011**, *13*, 2274.
20. Gadisa, A.; Mammo, W.; Admassie, S.; Zhang, F.; Andersson, M. R.; Inganäs, O.; *Adv. Funct. Mater.* **2007**, *17*, 3836.
21. Hellström, S.; Lindgren, L. J.; Zhou, Y.; Zhang, F.; Inganäsb, O.; Andersson, M. R.; *Polym. Chem.* **2010**, *1*, 1272.
22. Wu, H.; Qu, B.; Cong, Z.; Liu, H.; Tian, D.; Gao, B.; An, Z.; Gao, C.; Xiao, L.; Chen, Z.; Liu, H.; Gong, Q.; Wei, W.; *J. React. Funct. Polym.* **2012**, *72*, 897.
23. Baek, J.-B.; Harris, F. W.; *Macromolecules* **2005**, *38*, 297.
24. Hahnvajanawong, V.; Waengdongbung, W.; Piekkaew, S.; Phungpis, B.; Theramongkol, P.; *Science Asia* **2013**, *39*, 50.
25. Enders, D.; Han, J.; *Tetrahedron: Asymmetry* **2008**, *19*, 1367.
26. Aupoix, A.; Pe´got, B.; Vo Thanh, G.; *Tetrahedron Lett.* **2010**, *66*, 1352.
27. Safari, J.; Zarnegar, Z.; Ahmadi, M.; Seyyedi, S.; J. *Saudi Chem. Soc.* **2012**, http://dx.doi.org/10.1016/j.jscs.2012.05.005.
28. Mavis, M. .; Yolacan, C.; Aydogan, F.; *Tetrahedron Lett.* **2010**, *51*, 4509.
29. Mousavi, M.; Seyfi, H.; *Org. Chem. J.* **2012**, *3*, 28.

30. Joo, C.; Kang, S.; Kim, S. M.; Han, H.; Yang, J. W.; *Tetrahedron Lett.* **2010**, *51*, 6006.
31. Lindgren, L. J.; Zhang, F.; Andersson, M.; Barrau, S.; Hellstrom, S.; Mammo, W.; Perzon, E.; Inganäs, O.; Andersson, M. R.; *Chem. Mater.* **2009**, *21*, 3491.
32. Simion, C.; Simion, A. M.; *U.P.B. Sci. Bull., Series B,* **2007**, *69*, 50.
33. Skobridis, K.; Theodorou, V.; Weber, E.; *ARKIVOC* **2006**, 102.
34. Kim, J. H.; Song, C. E.; Kim, H. U.; Kang, I. N.; Shin, W. S.; Park, M. J.; Hwang, D. H.; *J. Polym. Sci. A Polym. Chem.* **2013**, *51*, 4136.
35. Lai, M. H.; Chueh, C. C.; Chen, W. C.; Wu, J. L.; Chen, F. C.; *J. Polym. Sci. A Polym. Chem.* **2009**, *47*, 973.
36. Matsumoto, M.; Matsumura, Y.; Iio, A.; Yonezawa, T.; *Bull. Chem. Soc. Jpn.* **1970**, *43*, 1496.
37. Keshav, M. Synthesis and Reactions of Quinoxalines, Cochin University of Science and Technology, 1990.
38. Ramachandran C. V., S. Synthesis and Characterisation of Hetrocycles derived from quinoxalines and mucobromic acid, Cochin University of Science and Technology: Kochi, 1998.
39. Brown, D. J. *Quinoxalines, Supplement II, in the Chemistry of Heterocyclic Compounds*; Taylor, E. C.; Wipf, P., Eds.; John Wiley & Sons: New Jersey, 2004.
40. Ji, J.; Lee, K. I.; *J. Korean Chem. Soc.* **2005**, *49*, 150.
41. Wang, E.; Hou, L.; Wang, Z.; Hellström, S.; Zhang, F.; Inganäs, O.; Andersson, M. R.; *Adv. Mater.* **2010**, *22*, 5240.
42. Kim, Y.; Yeom, H. R.; Kim, J. Y.; Yang, C.; *Energy Environ. Sci.* **2013**, *6*, 1909.
43. Lee, S. K.; Lee, S. K.; Lee, W. H.; Cho, J. M.; Park, S. J.; Park, J. U.; Shin, W. S.; Lee, J. C.; Kang, I. N.; Moon, S. J.; *Macromolecules* **2011**, *44*, 5994.
44. Peng, Q.; Xu, J.; Zheng, W.; *J. Polym. Sci. A Polym. Chem.* **2009**, *47*, 3399.
45. Bérubé, N.; Gaudreau, J.; Côté, M.; *Macromolecules* **2013**, *46*, 6873.
46. Patil, A. V.; Lee, W. H.; Lee, E.; Kim, K.; Kang, I. N.; Lee, S. H.; *Macromolecules* **2011**, *44*, 1238.
47. Choi, Y. S.; Lee, W. hyung; Kim, J. R.; Lee, S. K.; Shin, W. S.; Moon, S. J.; Park, J. W.; Kang, I. N.; *Bull. Korean Chem. Soc.* **2011**, *32*, 417.
48. Kleinhenz, N.; Yang, L.; Zhou, H.; Price, S. C.; You, W.-C.; *Macromolecules* **2011**, *44*, 872.
49. Brédas, J. L.; *J. Chem. Phys.* **1985**, *82*, 3808.
50. Chen, C. H.; Hsieh, C. H.; Dubosc, M.; Cheng, Y. J.; Hsu, C. S.; *Macromolecules* **2010**, *43*, 697.
51. Yamamoto, T.; Sugiyama, K.; Kushida, T.; Inoue, T.; Kanbara, T.; *J. Am. Chem. Soc.* **1996**, *118*, 3930.
52. Lee, B. L.; Yamamoto, T.; *Macromolecules* **1999**, *32*, 1375.
53. Jonforsen, M.; Johansson, T.; Spjuth, L.; Inganas, O.; Andersson, M. R.; *Synth. Met.* **2002**, *131*, 53.
54. Jonforsen, M.; Johansson, T.; Inganäs, O.; Andersson, M. R.; *Macromolecules* **2002**, *35*, 1638.
55. Duan, R.; Ye, L.; Guo, X.; Huang, Y.; Wang, P.; Zhang, S.; Zhang, J.; Huo, L.; Hou, J.; *Macromolecules* **2012**, *45*, 3032.

56. Yamamoto, T.; Lee, B. L.; Kokubo, H.; Kishida, H.; Hirota, K.; Takeru, W.; Hiroshi, O.; *Macromol. Rapid Commun.* **2003**, *24*, 440.
57. Dutta, P.; Kim, T.; Choi, H.; Lee, J.; Kim, D. S.; Kim, J. Y.; Yang, C.; *Polym. Chem.* **2014**, *5*, 2540.
58. Lu, Y.; Xiao, Z.; Yuan, Y.; Wu, H.; An, Z.; Hou, Y.; Gao, C.; Huang, J.; *J. Mater. Chem. C,* **2012**, *1*, 630.
59. Yang, R.; Tian, R.; Yan, J.; Zhang, Y.; Yang, J.; Hou, Q.; Yang, W.; Zhang, C.; Cao, Y.; *Macromolecules* **2005**, *38*, 244.
60. White, M. J.; Leeper, F. J.; *J. Org. Chem.* **2001**, *66*, 5124.
61. Marion, N.; Díez-González, S.; Nolan, S. P.; *Angew. Chem. Int. Ed Engl.* **2007**, *46*, 2988.
62. Gerbino, D. C.; Fidelibus, P. M.; Mandolesi, S. D.; Ocampo, R. A.; Scoccia, J.; Podestá, J. C.; *J. Organomet. Chem.* **2013**, *741*, 24.
63. Zalesskiy, S. S.; Ananikov, V. P.; *Organometallics* **2012**, *31*, 2302.
64. Coulson, D. R. In *Inorganic Synthesis*; McGraw-Hill, 1972; Vol. XIII, p. 121.
65. Jespersen, K. G.; Beenken, W. J. D.; Zaushitsyn, Y.; Yartsev, A.; Andersson, M.; Pullerits, T.; Sundström, V.; *J. Chem. Phys.* **2004**, *121*, 12613.
66. Wang, X. Y.; Zhuang, F. D.; Zhou, X.; Yang, D. C.; Wang, J. Y.; Pei, J.; *J. Mater. Chem. C* **2014**, *2*, 8152.
67. Huang, Y.; Zhang, M.; Ye, L.; Guo, X.; Han, C. C.; Li, Y.; Hou, J.; *J. Mater. Chem.* **2012**, *22*, 5700.
68. Kim, D. H.; Lee, B.-L.; Moon, H.; Kang, H. M.; Jeong, E. J.; Park, J.-I.; Han, K. M.; Lee, S.; Yoo, B. W.; Koo, B. W.; Kim, J. Y.; Lee, W. H.; Cho, K.; Becerril, H. A.; Bao, Z.; *J. Am. Chem. Soc.* **2009**, *131*, 6124.
69. Zhang, G.; Guo, J.; Zhang, J.; Li, P.; Ma, J.; Wang, X.; Lu, H.; Qiu, L.; *Polym. Chem.* **2015**, Advance Article DOI: 10.1039/C4PY00916A.
70. Admassie, S.; Inganas, O.; Mammo, W.; Perzon, E.; Andersson, M. R.; *Synth. Met.* **2006**, *156*, 614.
71. Keshtov, M. L.; Marochkin, D. V.; Kochurov, V. S.; Khokhlov, A. R.; Koukarascd, E. N.; Sharma, G. D.; *Polym. Chem.* **2013**, *4*, 4033.
72. Bredas, J. L.; Silbey, R.; Boudreaux, D. S.; Chance, R. R.; *J. Am. Chem. Soc.* **1983**, *105*, 6555.
73. Wang, K.; Zhang, Z.-G.; Fu, Q.; Li, Y.; *Macromol. Chem. Phys.* **2014**, *215*, 597.
74. Zhuang, W.; Lundin, A.; Andersson, M. R.; *J. Mater. Chem. A* **2014**, *2*, 2202.
75. Yang, G.-Z.; Wang, W.-Z.; Wang, M.; Liu, T.; *J. Phys. Chem. B* **2007**, *111*, 7747.
76. Gadisa, A.; Oosterbaan, W. D.; Vandewal, K.; Bolsée, J.-C.; Bertho, S.; D'Haen, J.; Lutsen, L.; Vanderzande, D.; Manca, J. V.; *Adv. Funct. Mater.* **2009**, *19*, 3300.
77. Li, Y.; Zou, J.; Yip, H.-L.; Li, C.-Z.; Zhang, Y.; Chueh, C.-C.; Intemann, J.; Xu, Y.; Liang, P.-W.; Chen, Y.; Jen, A. K.-Y.; *Macromolecules* **2013**, *46*, 5497.

8. APPENDICES

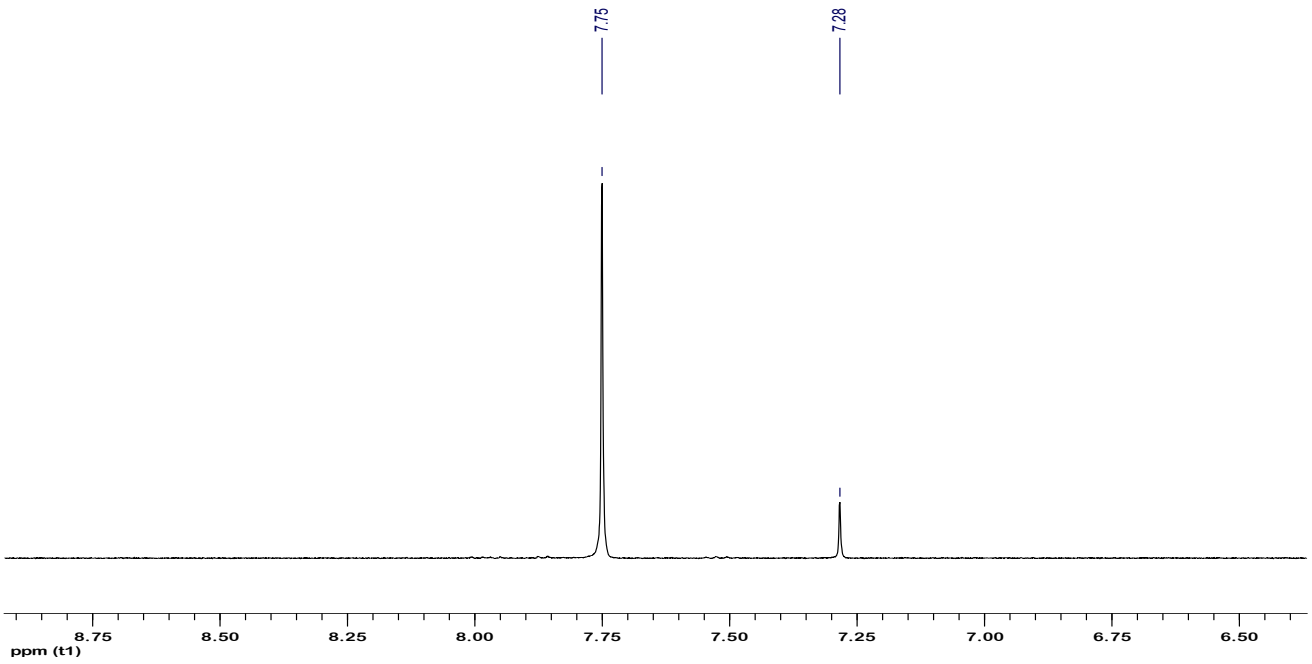

Appendix 1: ^{1}H-NMR spectrum of 4,7-dibromobenzo[*c*][1,2,5]thiadiazole (**35**).

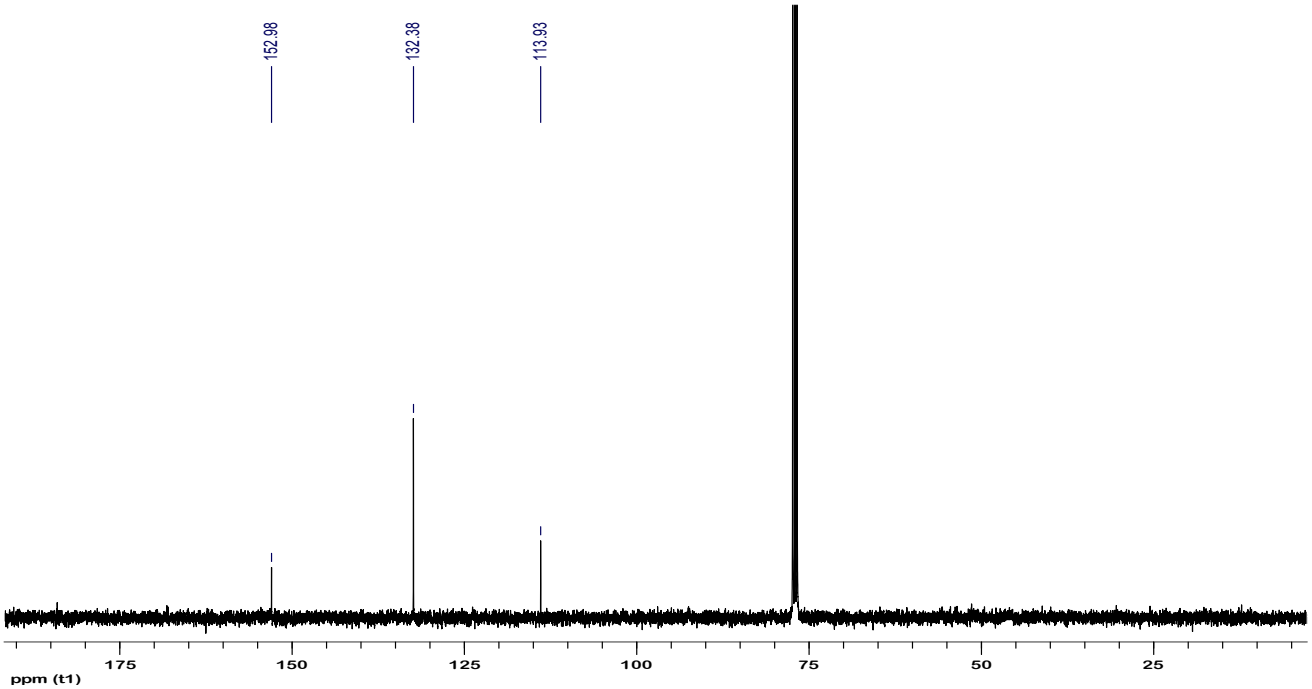

Appendix 2: ^{13}C-NMR spectrum of 4,7-dibromobenzo[*c*][1,2,5]thiadiazole (**35**).

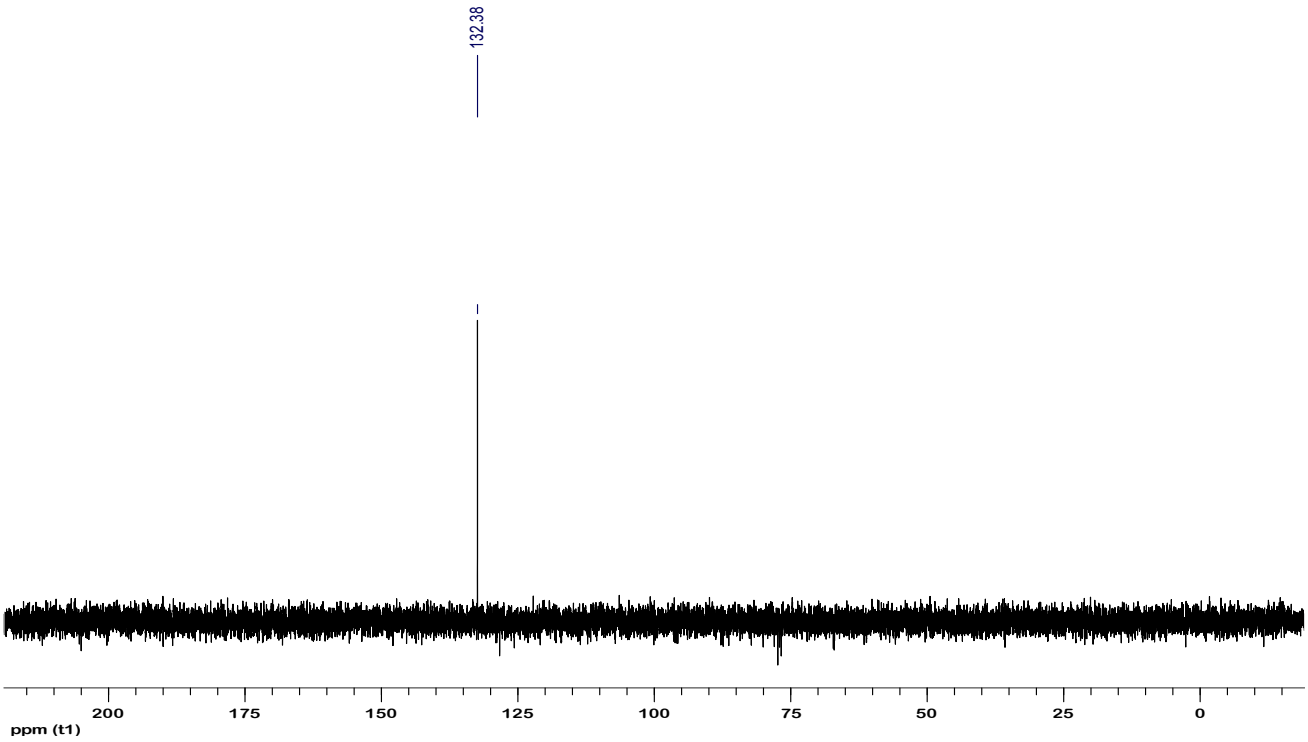

Appendix 3: DEPT-135 spectrum of 4,7-dibromobenzo[*c*][1,2,5]thiadiazole (**35**).

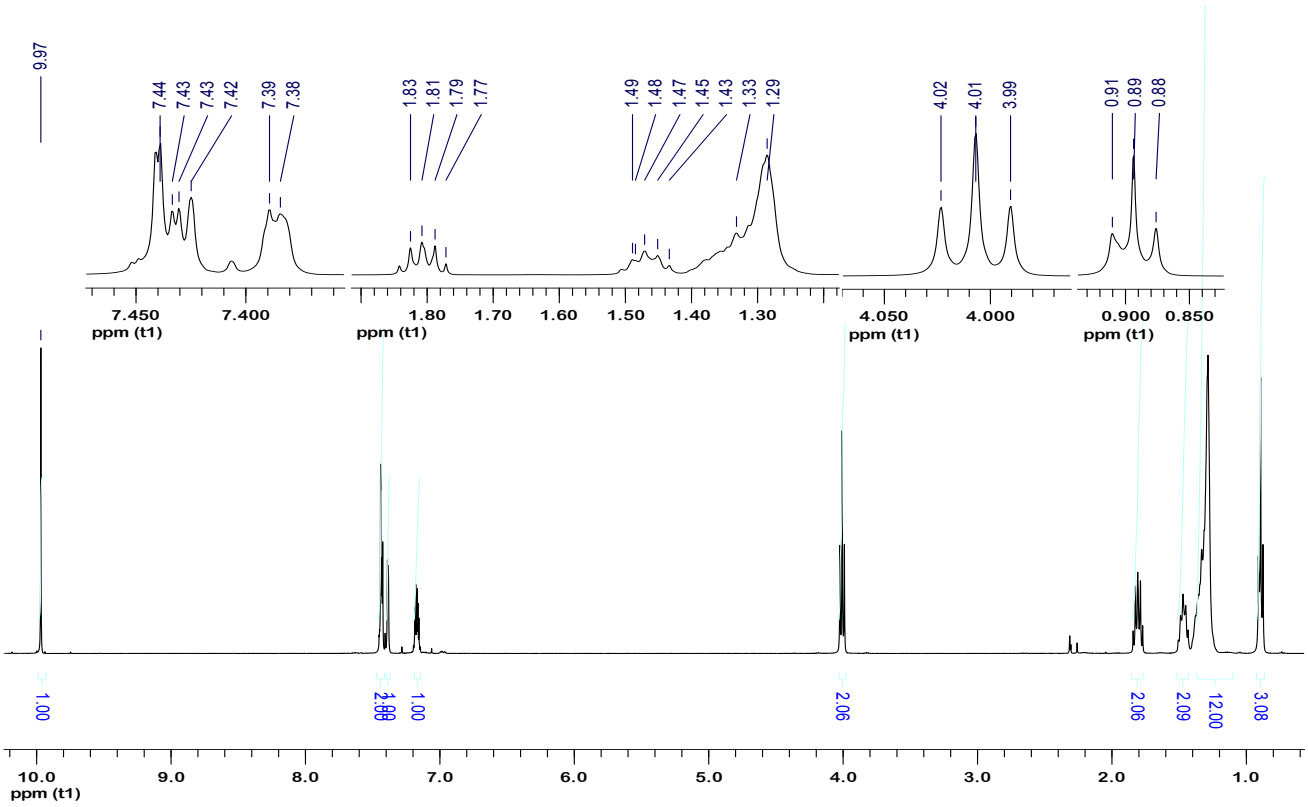

Appendix 4: ^{1}H-NMR spectrum of 3-(decyloxy)benzaldehyde (**64**).

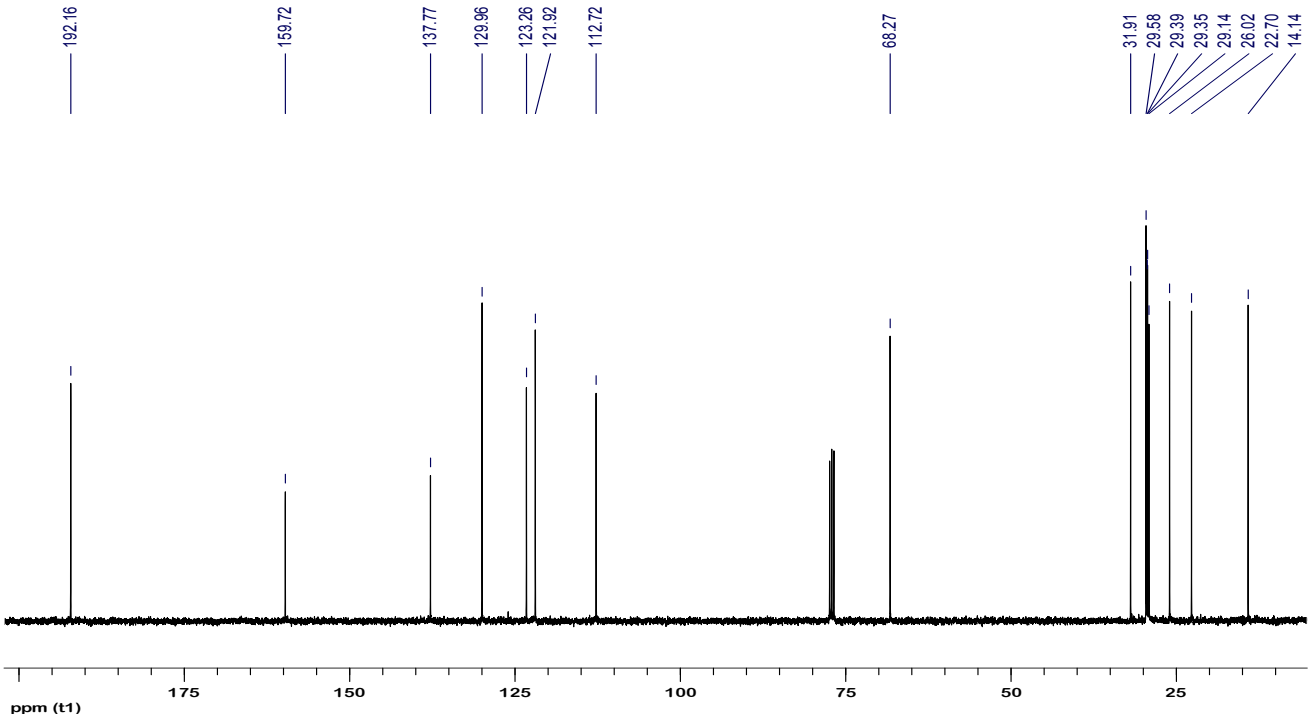

Appendix 5: ^{13}C-NMR spectrum of 3-(decyloxy)benzaldehyde (**64**).

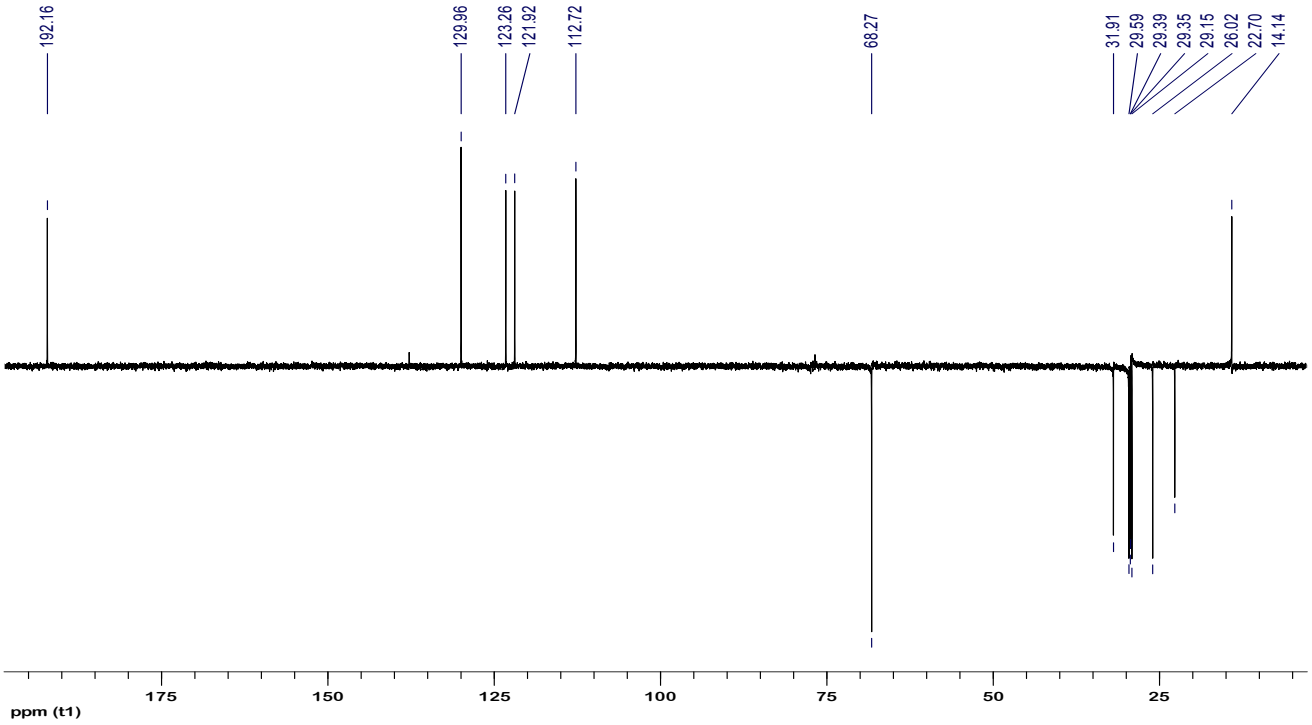

Appendix 6: DEPT-135 spectrum of 3-(decyloxy)benzaldehyde (**64**).

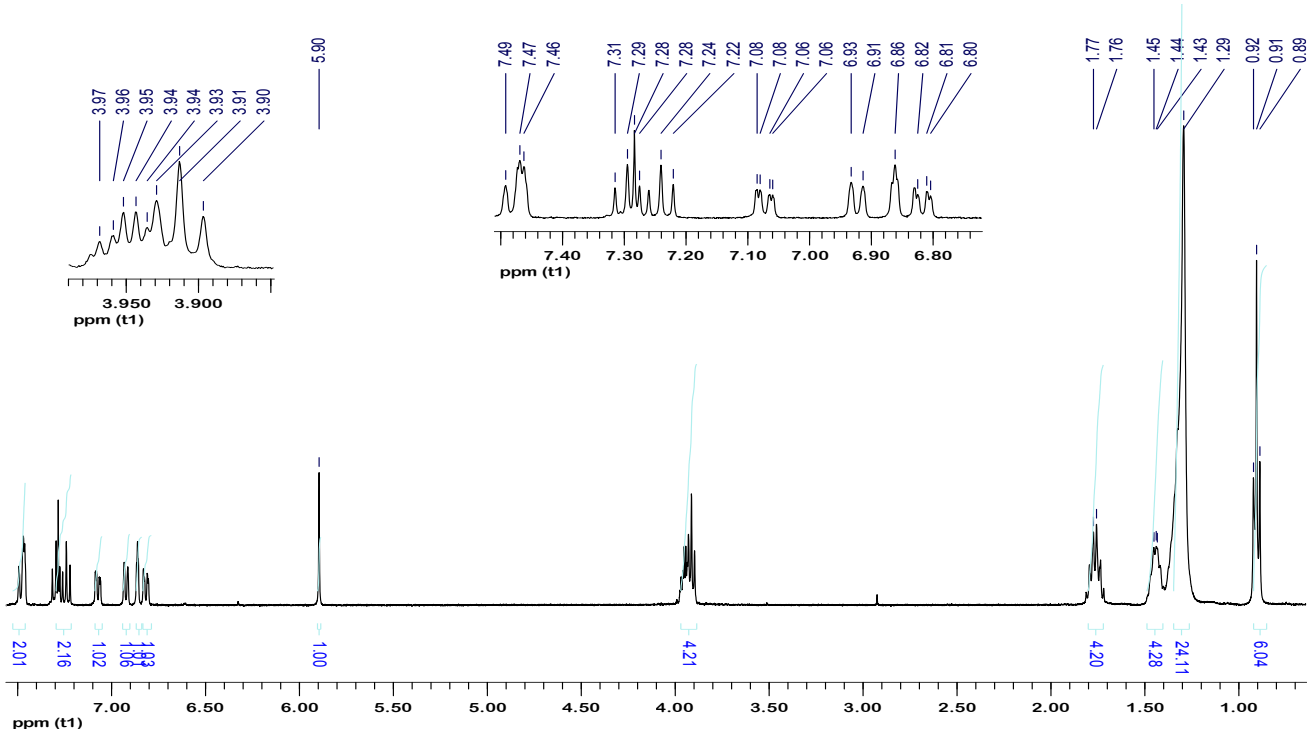

Appendix 7: ^{1}H-NMR spectrum of 2-hydroxy-1,2-bis(3-decyloxyphenyl)ethanone (**68**).

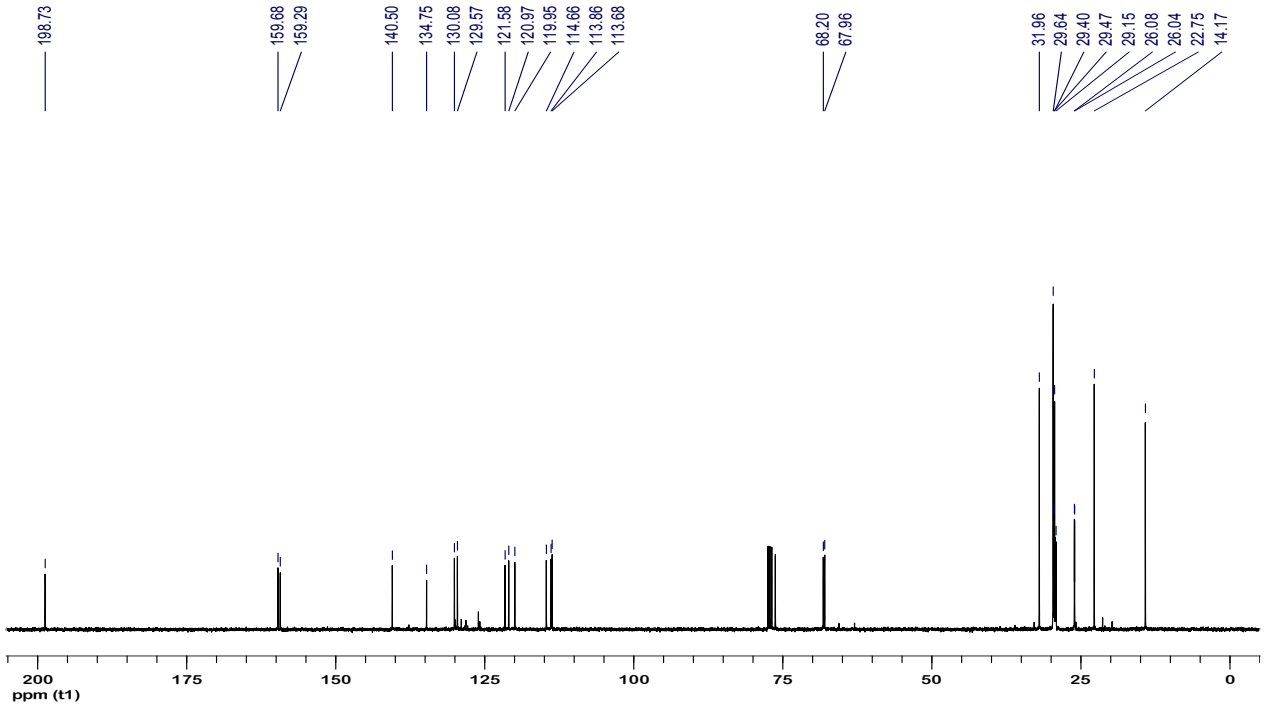

Appendix 8: ^{13}C-NMR spectrum of 2-hydroxy-1,2-bis(3-decyloxyphenyl)ethanone (**68**).

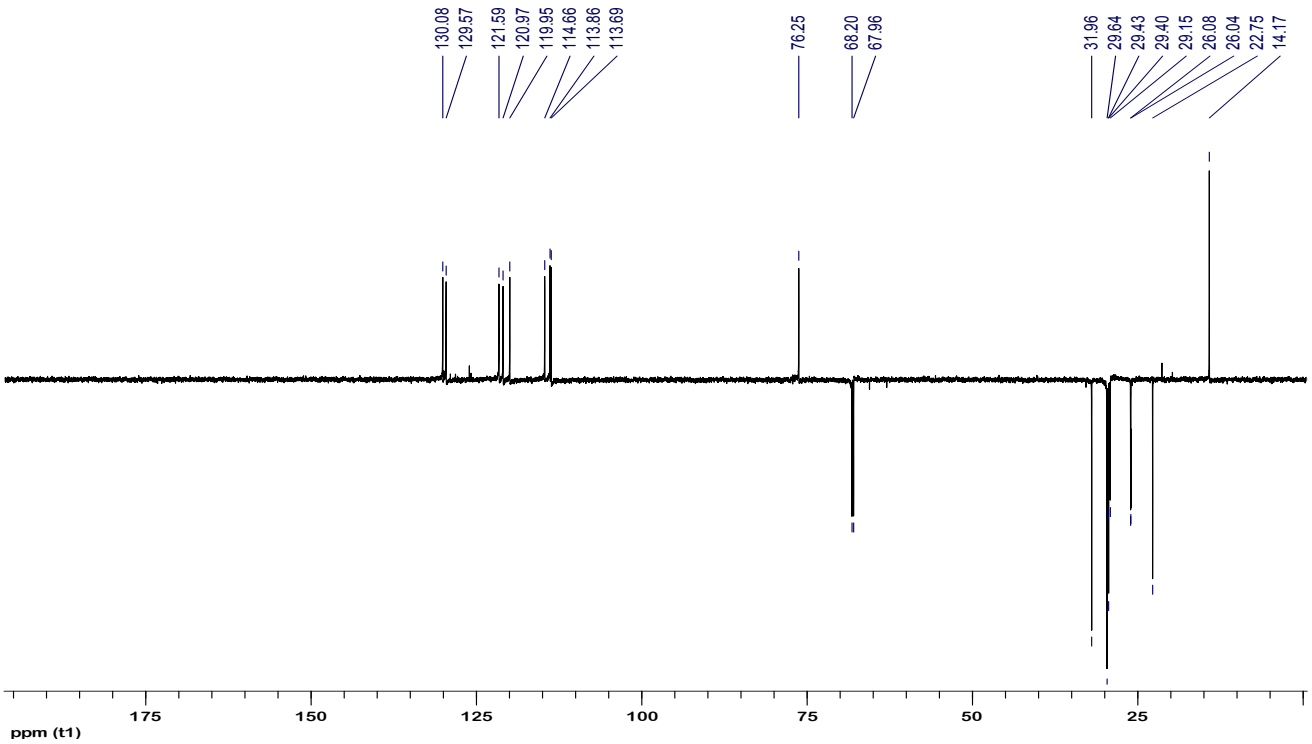

Appendix 9: DEPT-135 spectrum of 2-hydroxy-1,2-bis(3-decyloxyphenyl)ethanone (**68**).

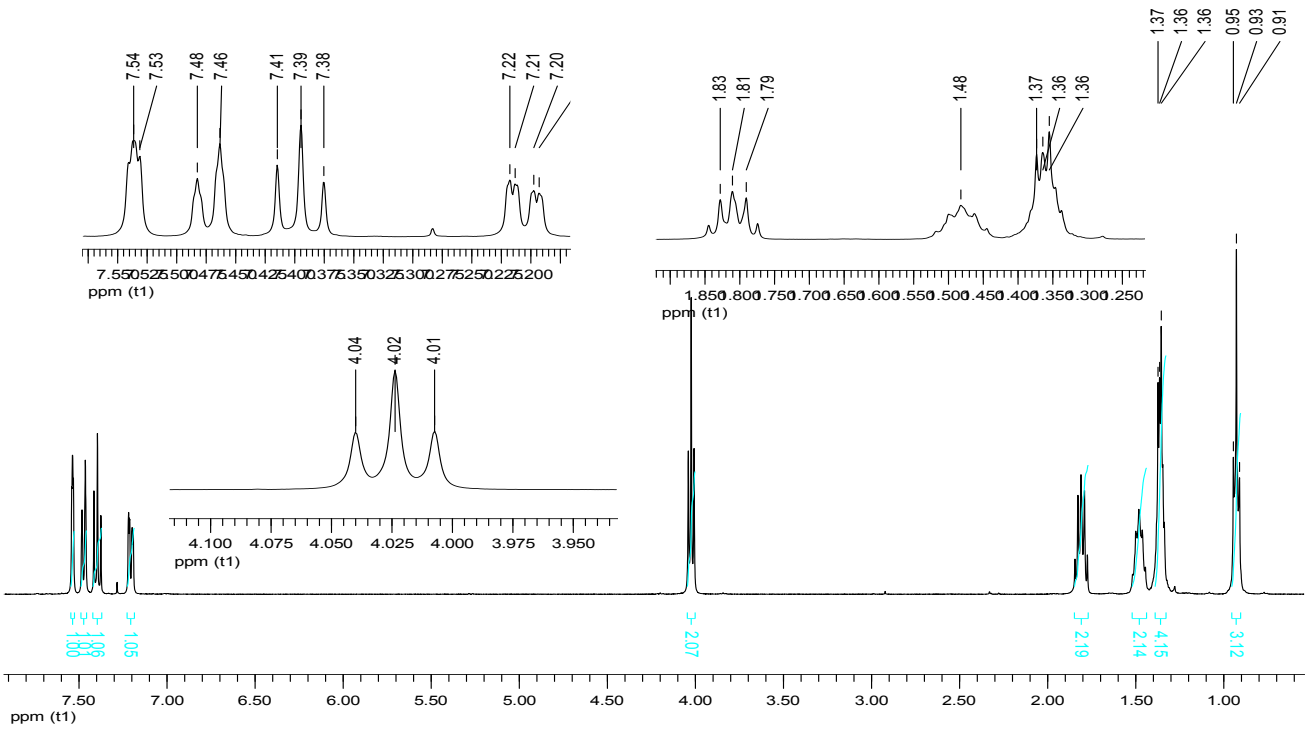

Appendix 10: ^{1}H-NMR spectrum of 1,2-bis(3-(hexyloxy)phenyl)ethane-1,2-dione (**70**).

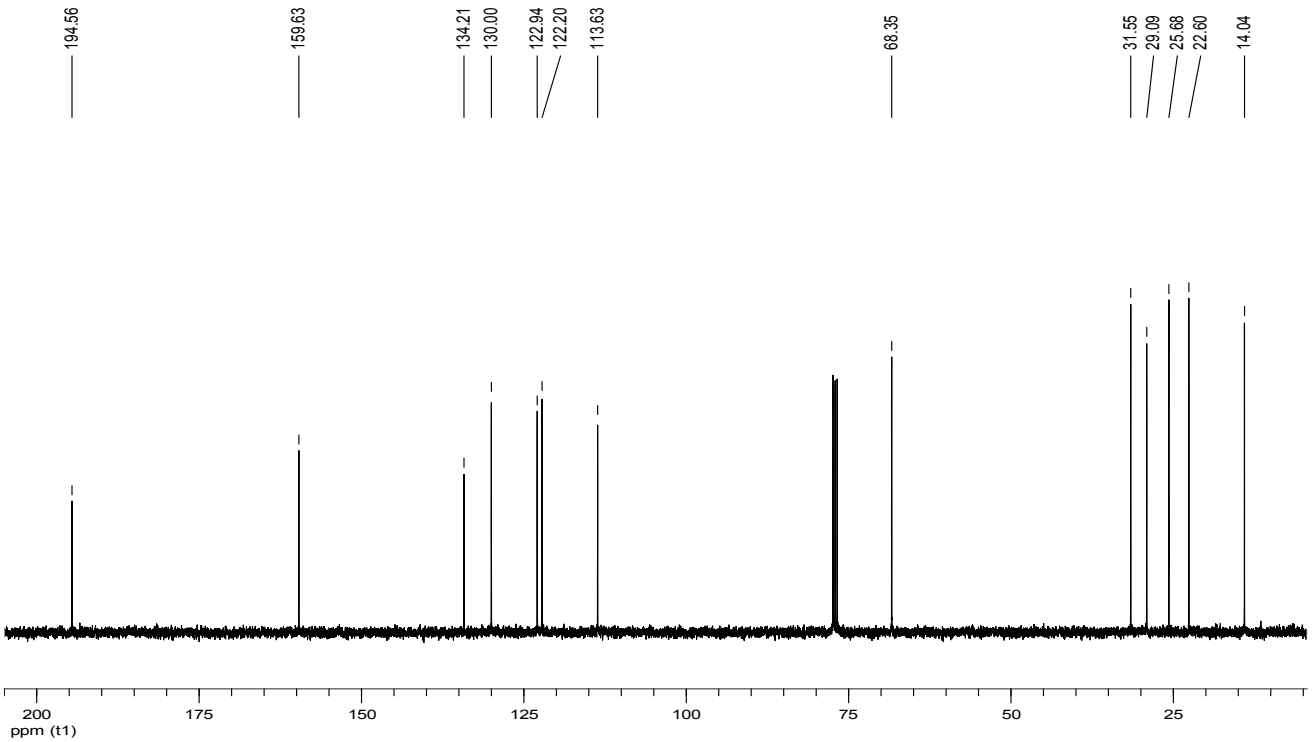

Appendix 11: ^{13}C-NMR spectrum of 1,2-bis(3-(hexyloxy)phenyl)ethane-1,2-dione (**70**).

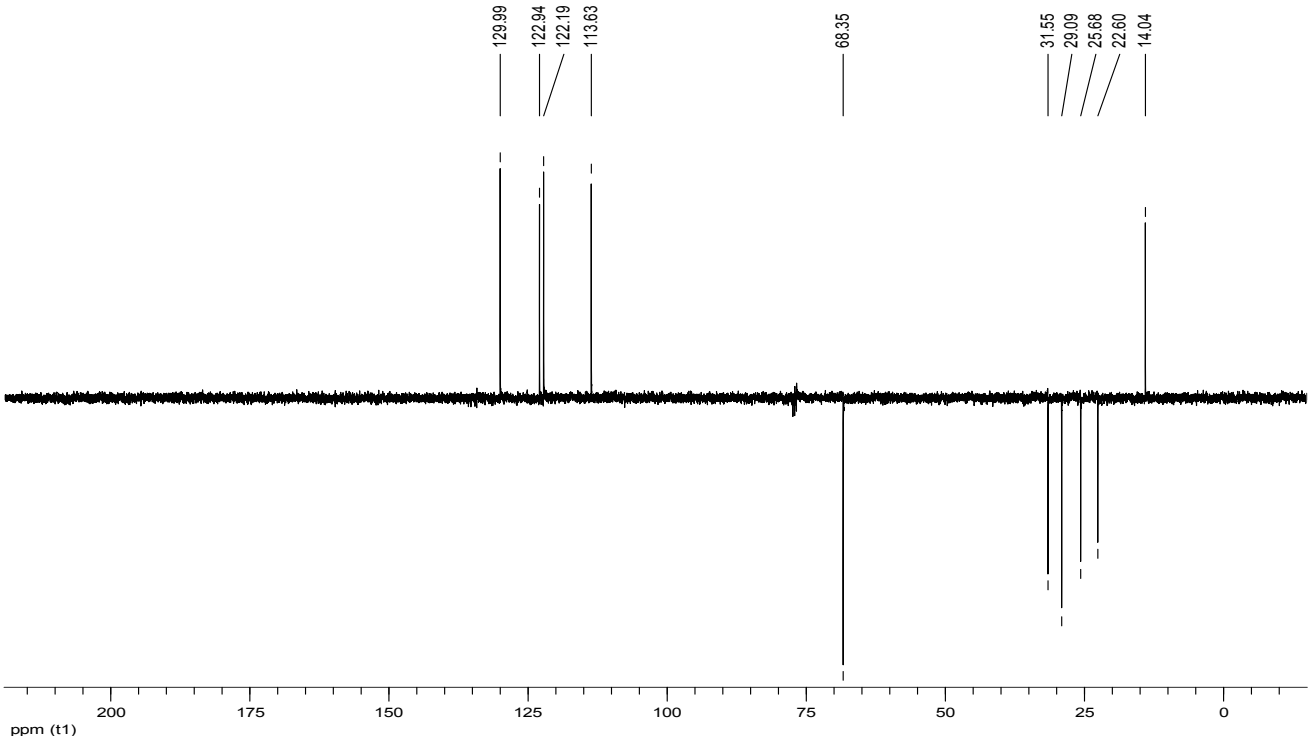

Appendix 12: DEPT-135 spectrum of 1,2-bis(3-(hexyloxy)phenyl)ethane-1,2-dione (**70**).

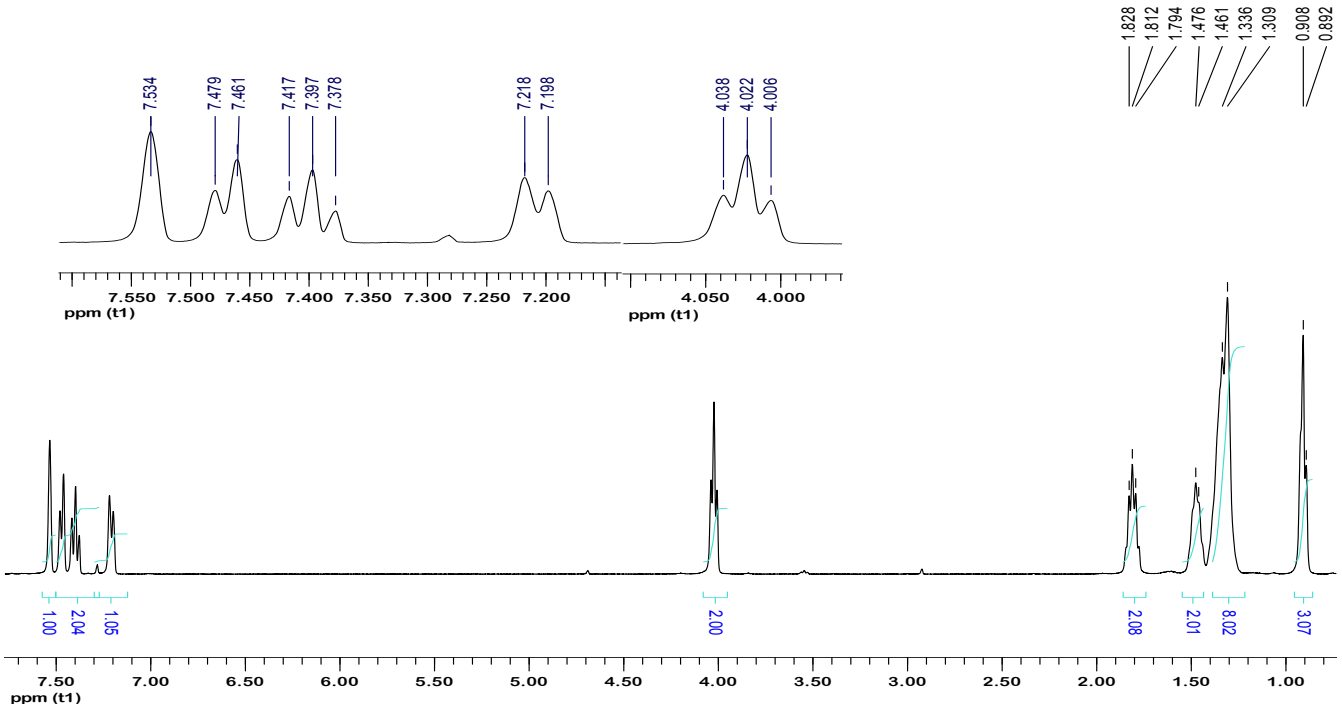

Appendix 13: ^{1}H-NMR spectrum of 1,2-bis(3-(octyloxy)phenyl)ethane-1,2-dione (**25**).

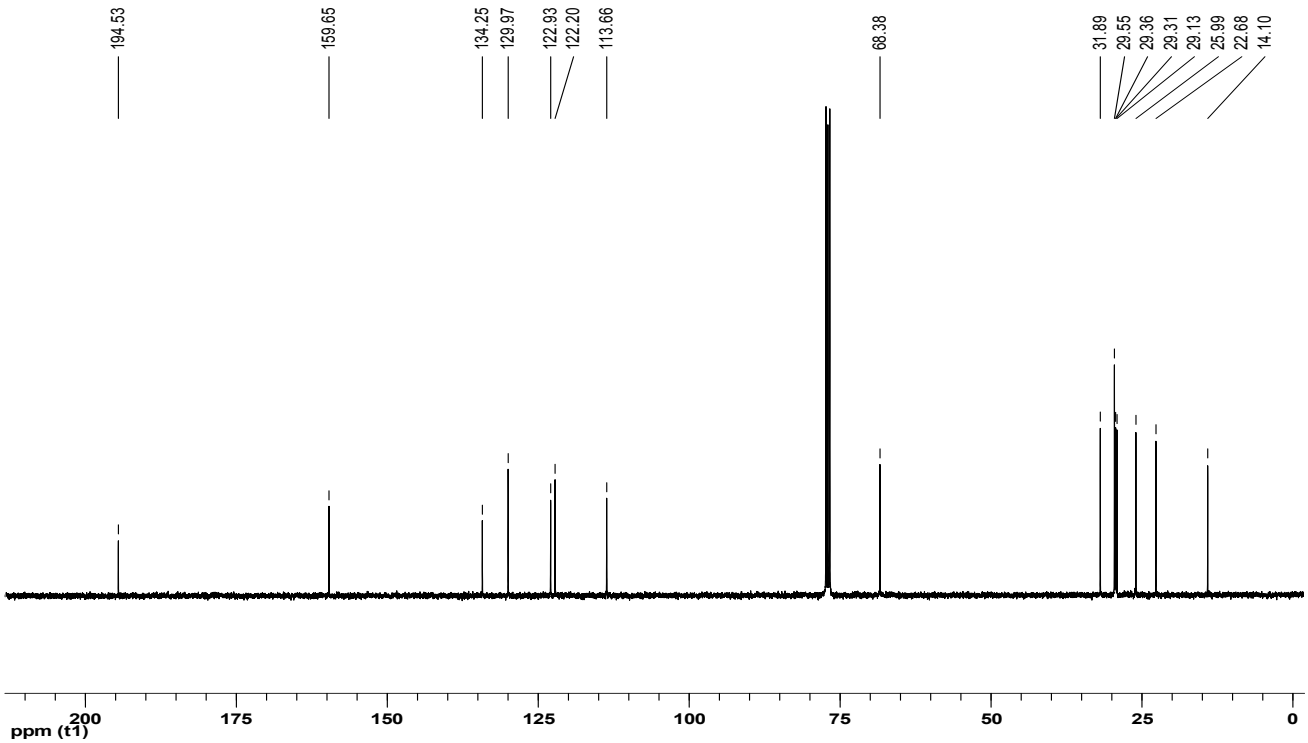

Appendix 14: ^{13}C-NMR spectrum of 1,2-bis(3-(octyloxy)phenyl)ethane-1,2-dione (**25**).

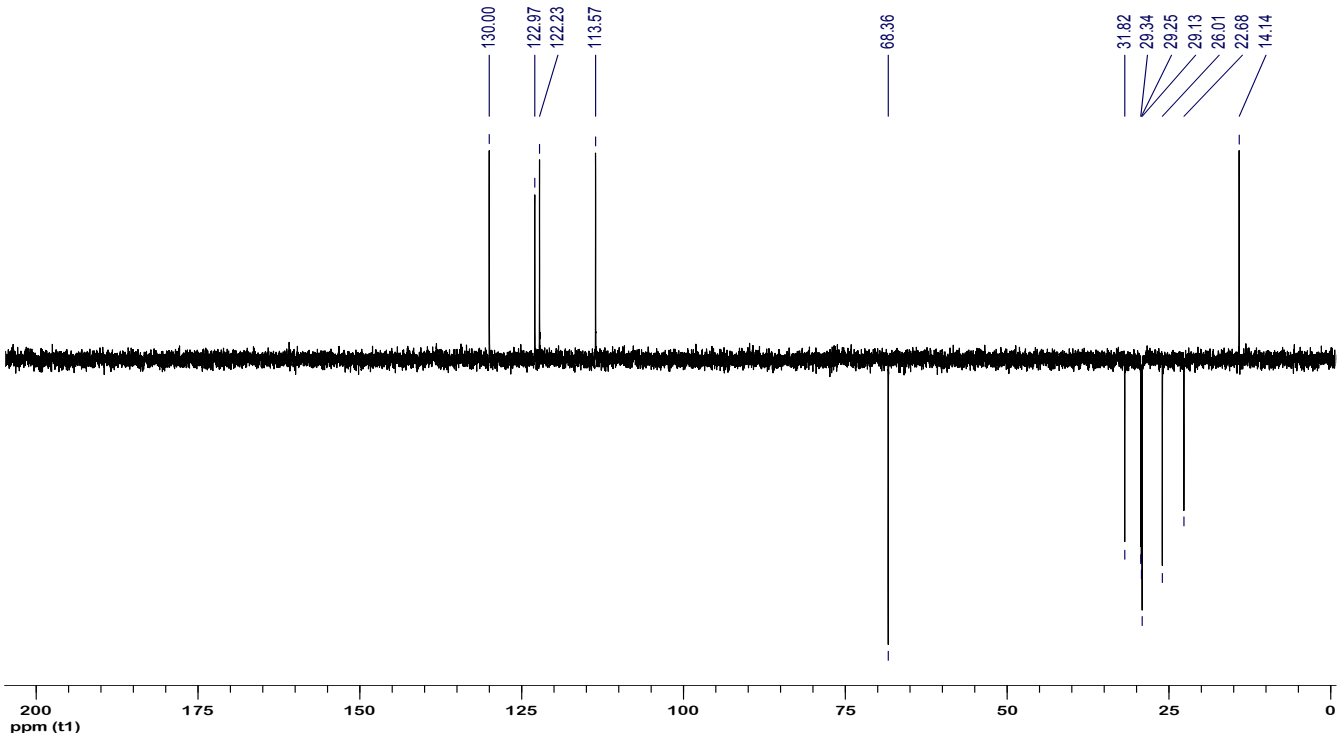

Appendix 15: DEPT-135 spectrum of 1,2-bis(3-(octyloxy)phenyl)ethane-1,2-dione (**25**).

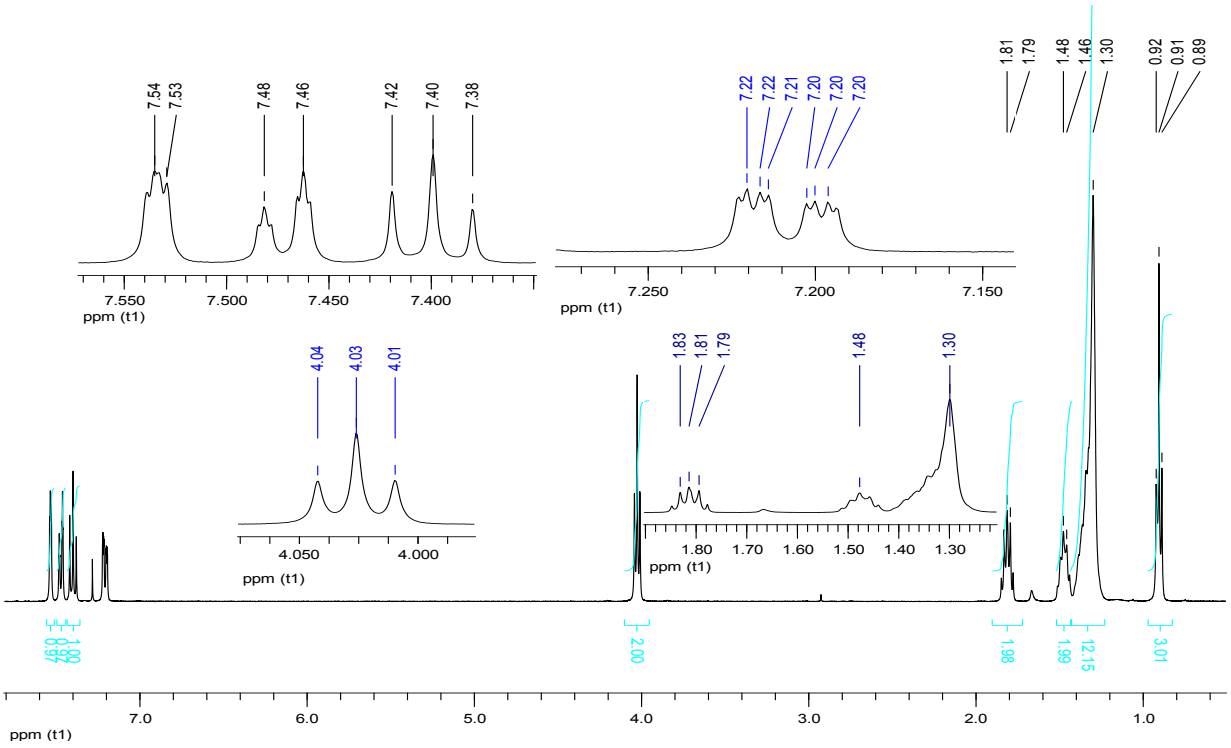

Appendix 16: ^{1}H-NMR spectrum of 1,2-bis(3-(decyloxy)phenyl)ethane-1,2-dione (**71**).

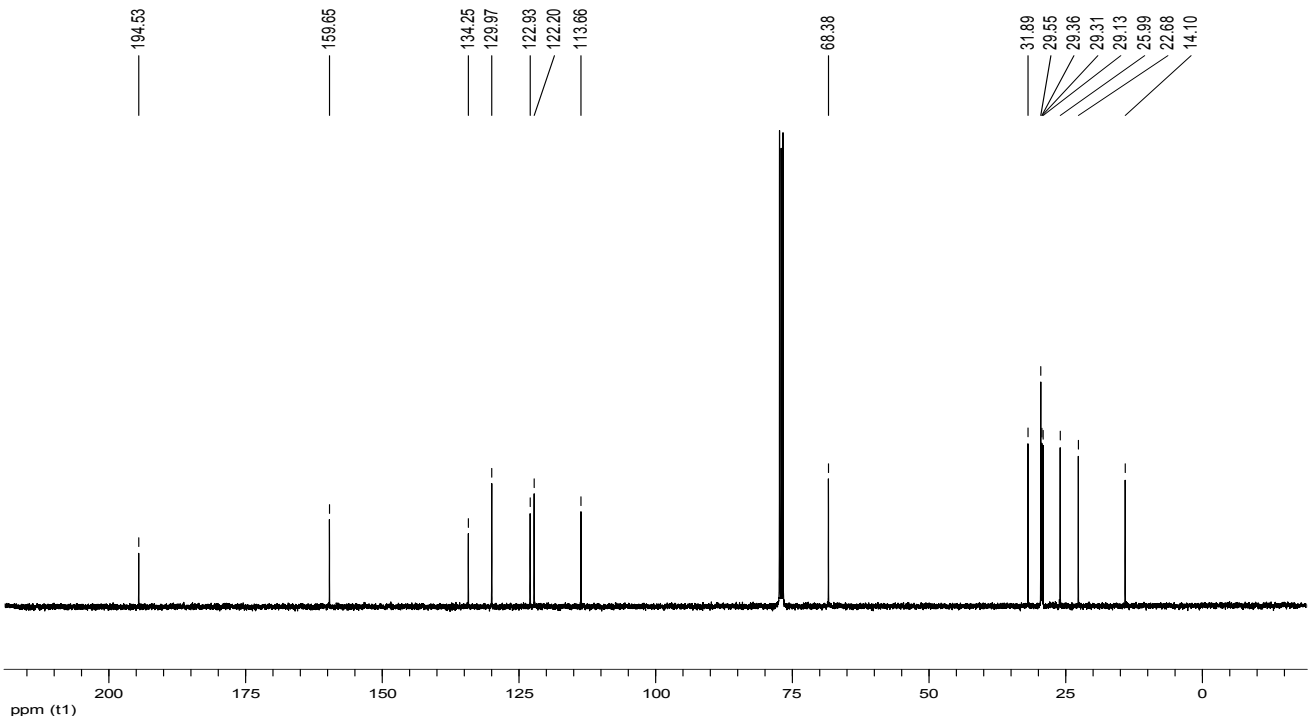

Appendix 17: ^{13}C-NMR spectrum of 1,2-bis(3-(decyloxy)phenyl)ethane-1,2-dione (**71**).

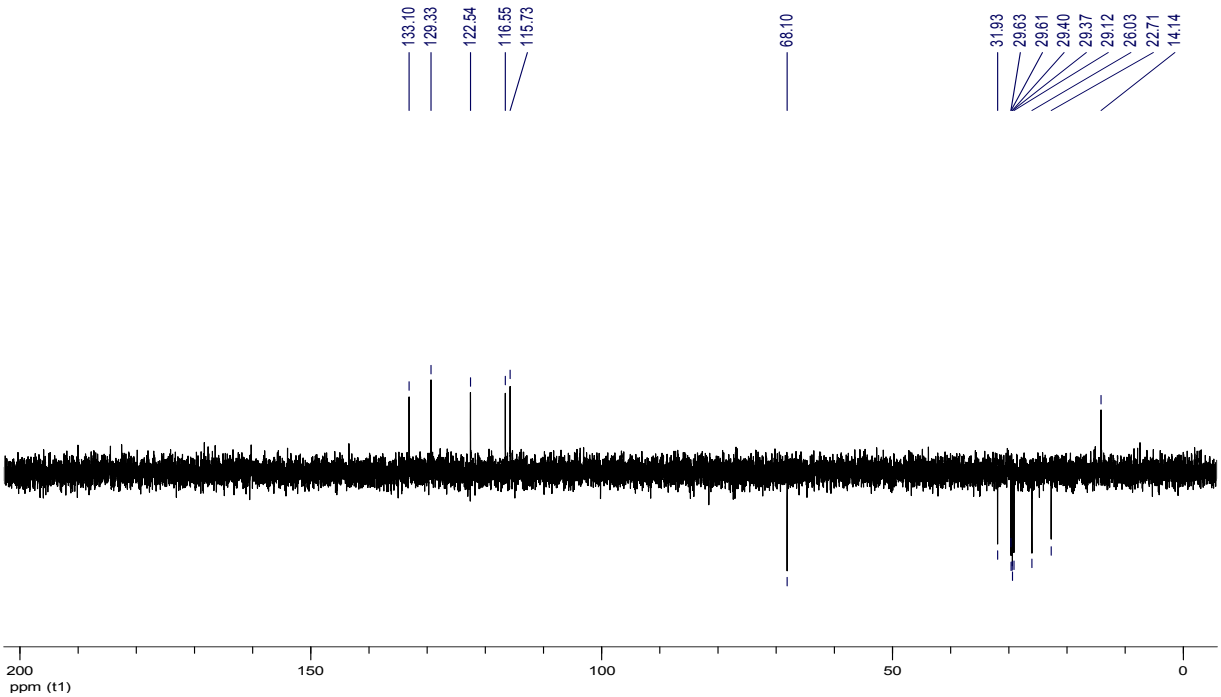

Appendix 18: DEPT-135 spectrum of 1,2-bis(3-(decyloxy)phenyl)ethane-1,2-dione (**71**).

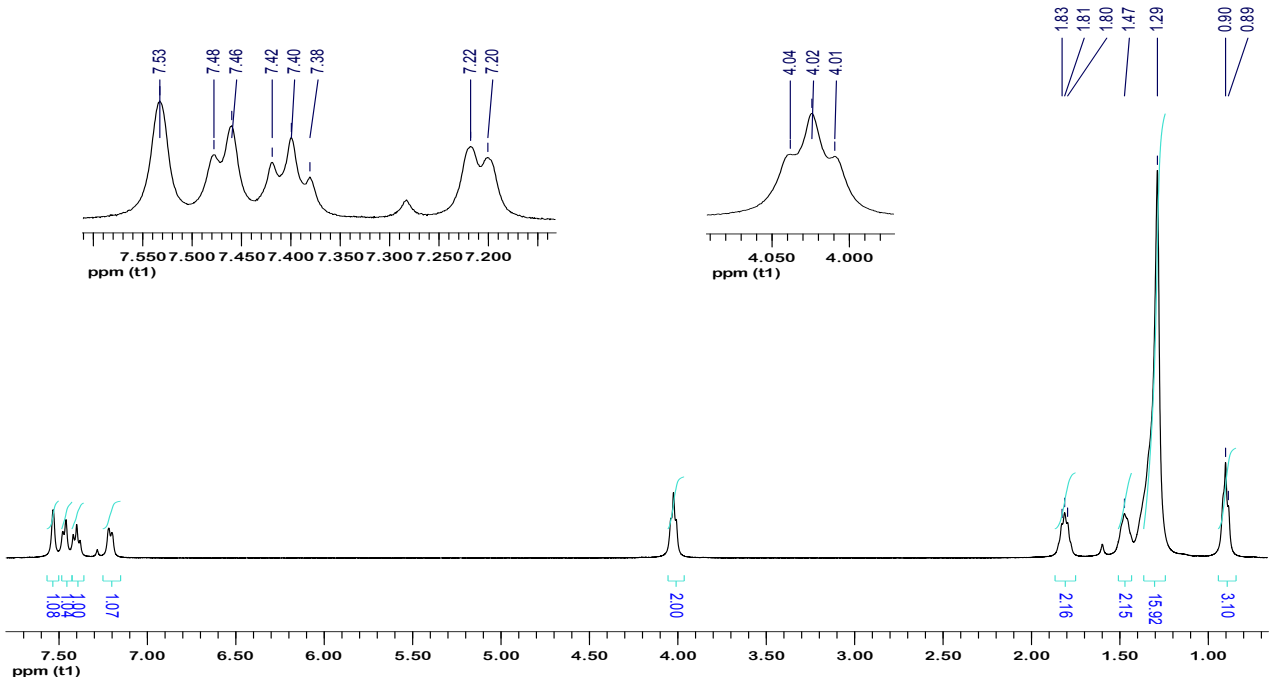

Appendix 19: ^{1}H-NMR spectrum of 1,2-bis(3-(dodecyloxy)phenyl)ethane-1,2-dione (**72**).

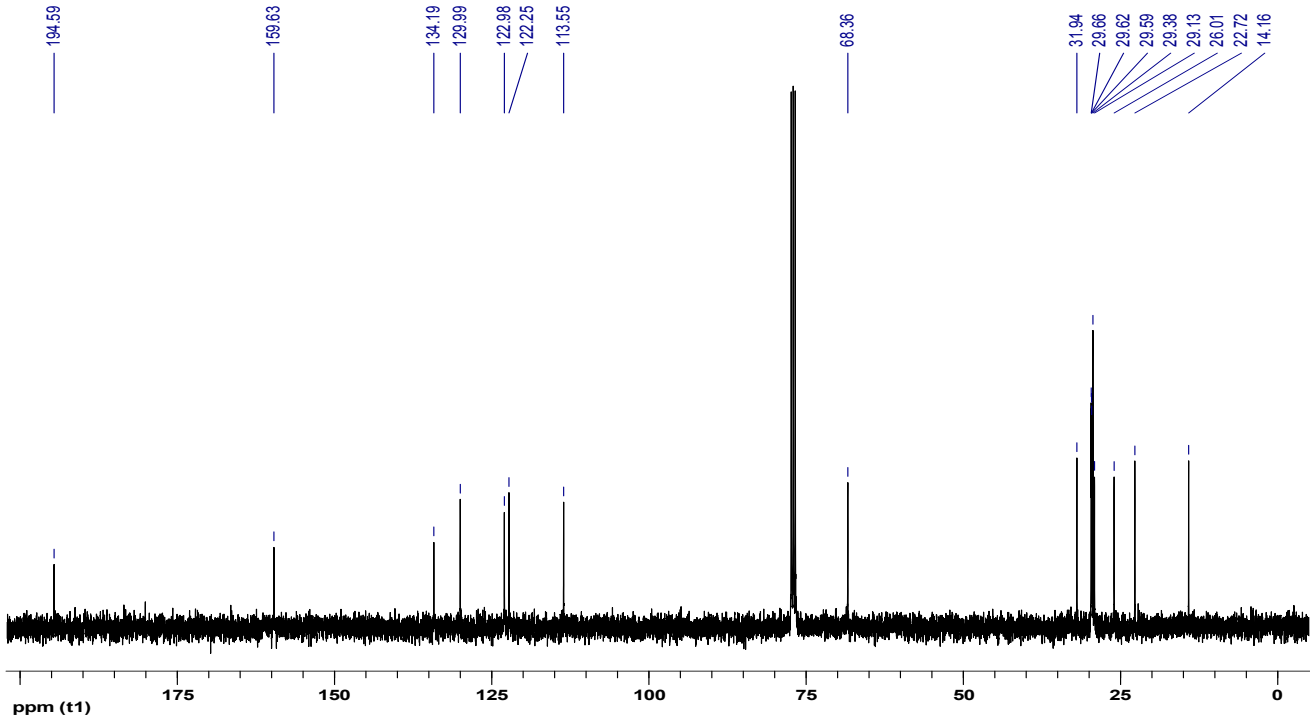

Appendix 20: ^{13}C-NMR spectrum of 1,2-bis(3-(dodecyloxy)phenyl)ethane-1,2-dione (**72**).

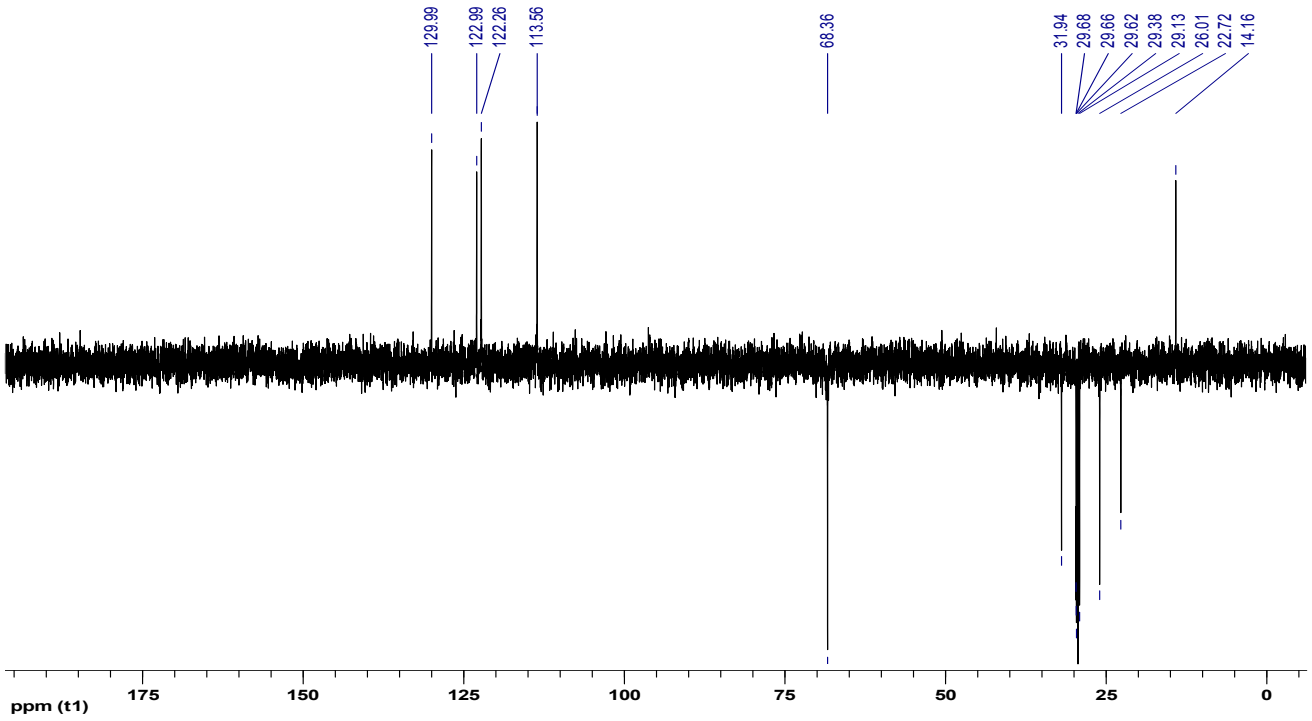

Appendix 21: DEPT-135 spectrum of 1,2-bis(3-(dodecyloxy)phenyl)ethane-1,2-dione (**72**).

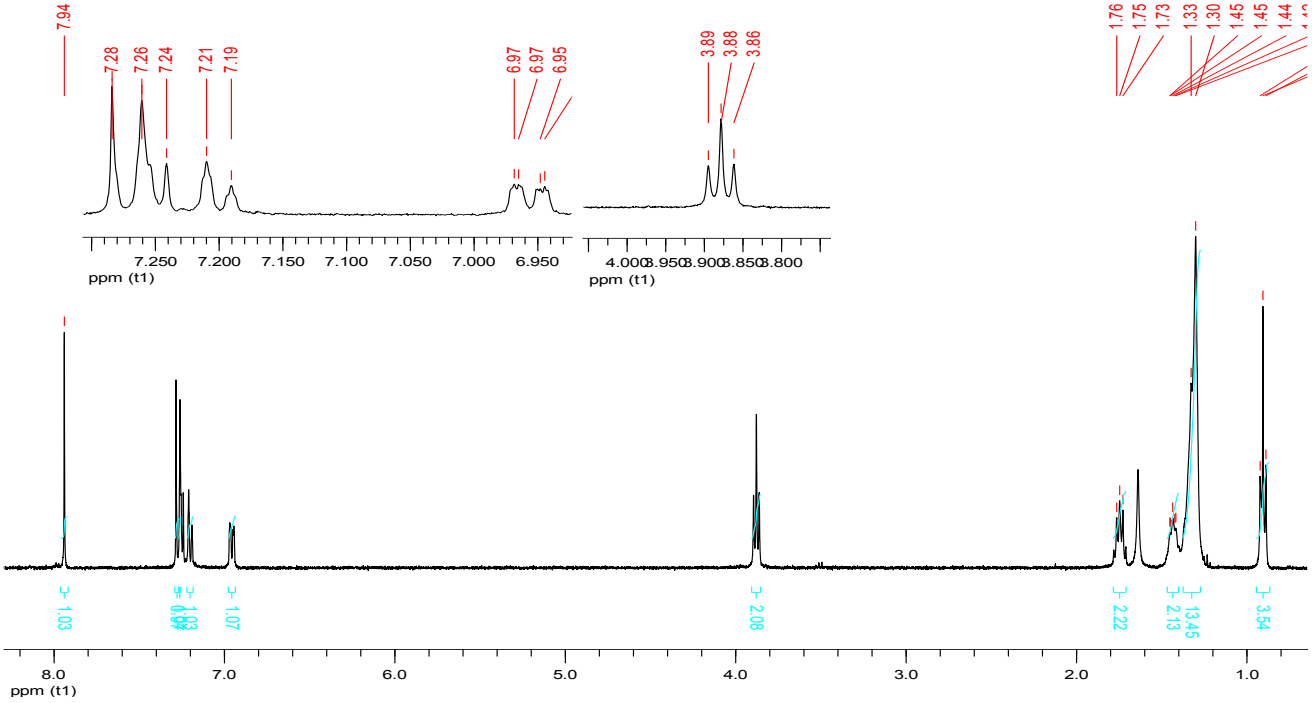

Appendix 22: ^{1}H-NMR spectrum of 5,8-dibromo-2,3-bis(3-decyloxyphenyl)-quinoxaline (**74**).

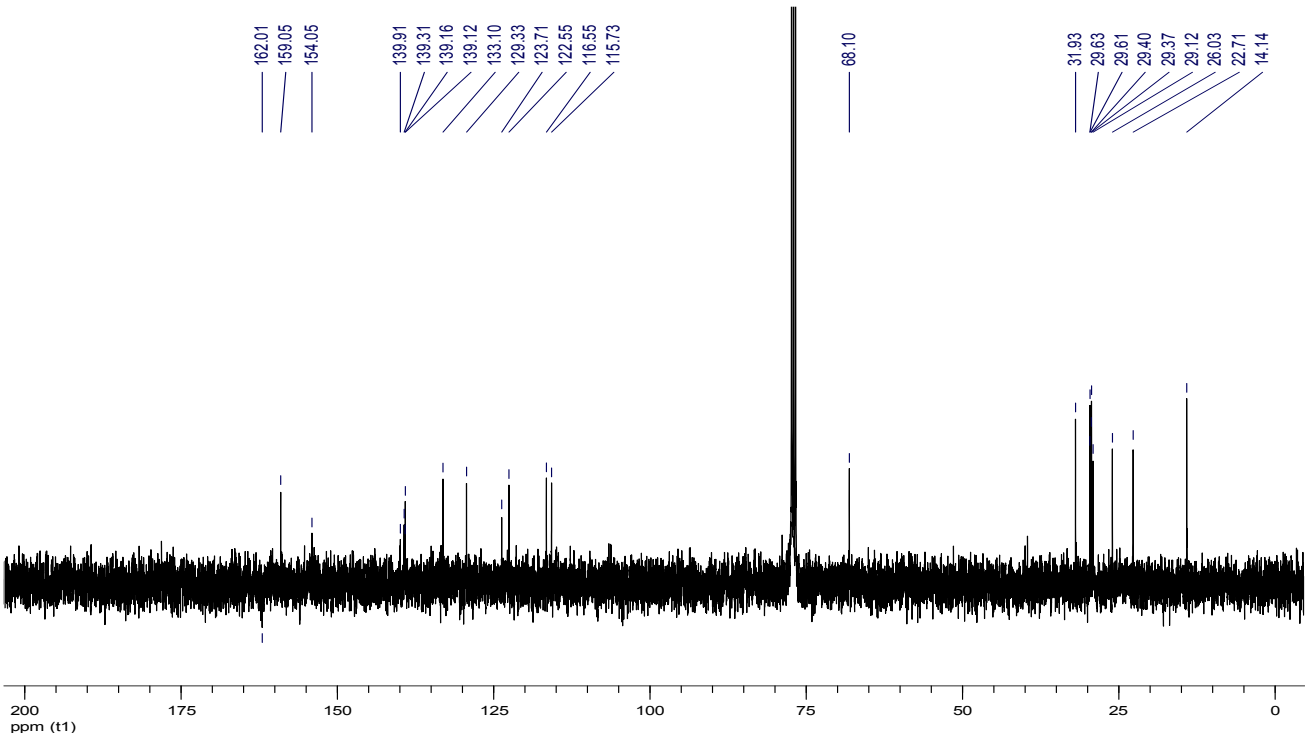

Appendix 23: ^{13}C-NMR spectrum of 5,8-dibromo-2,3-bis(3-decyloxyphenyl) quinoxaline (**74**).

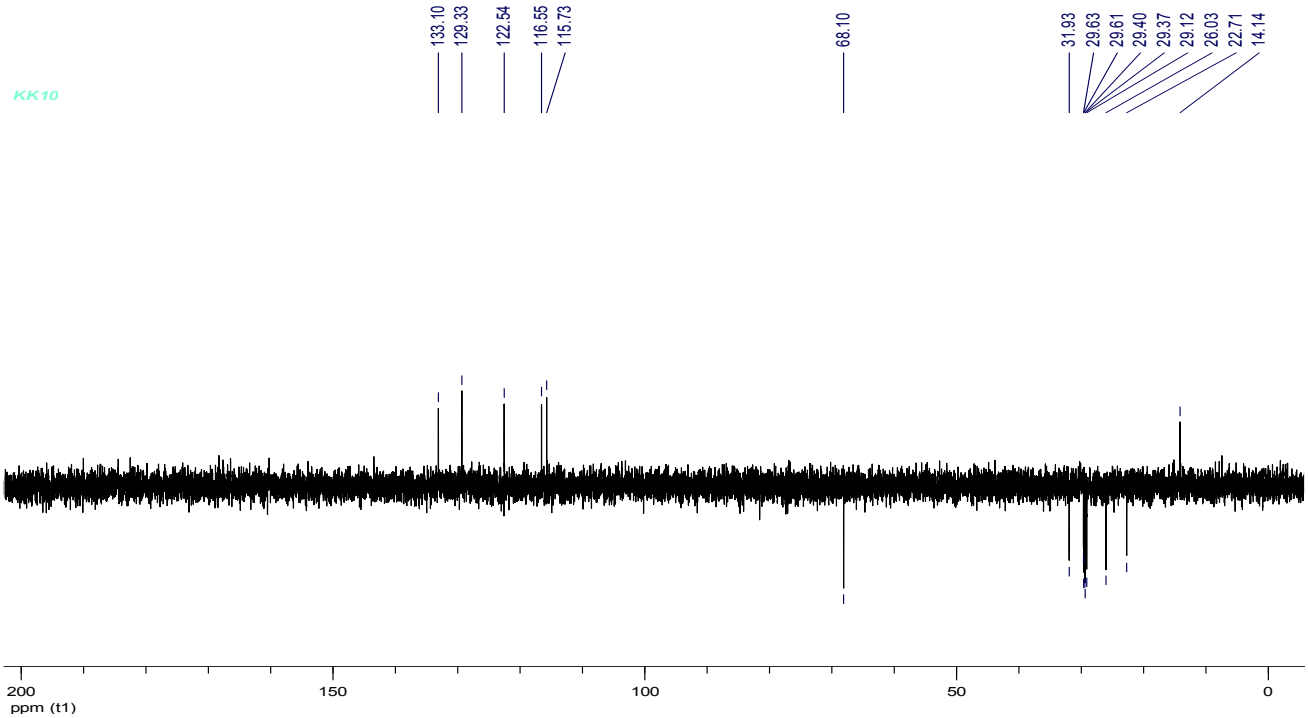

Appendix 24: DEPT-135 spectrum of 5,8-dibromo-2,3-bis(3-decyloxyphenyl) quinoxaline (**74**).

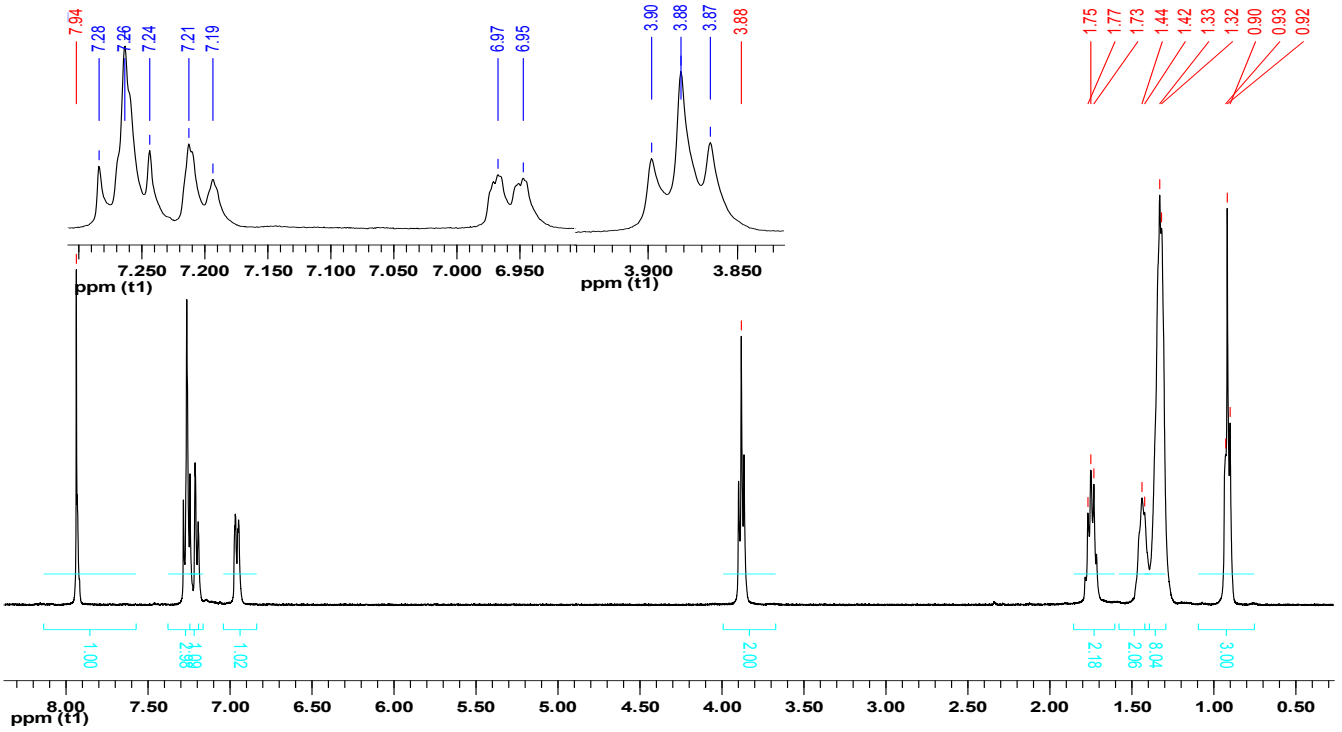

Appendix 25: ^{1}H-NMR spectrum of 5,8-dibromo-2,3-bis(3-octyloxyphenyl)quinoxaline (**51**).

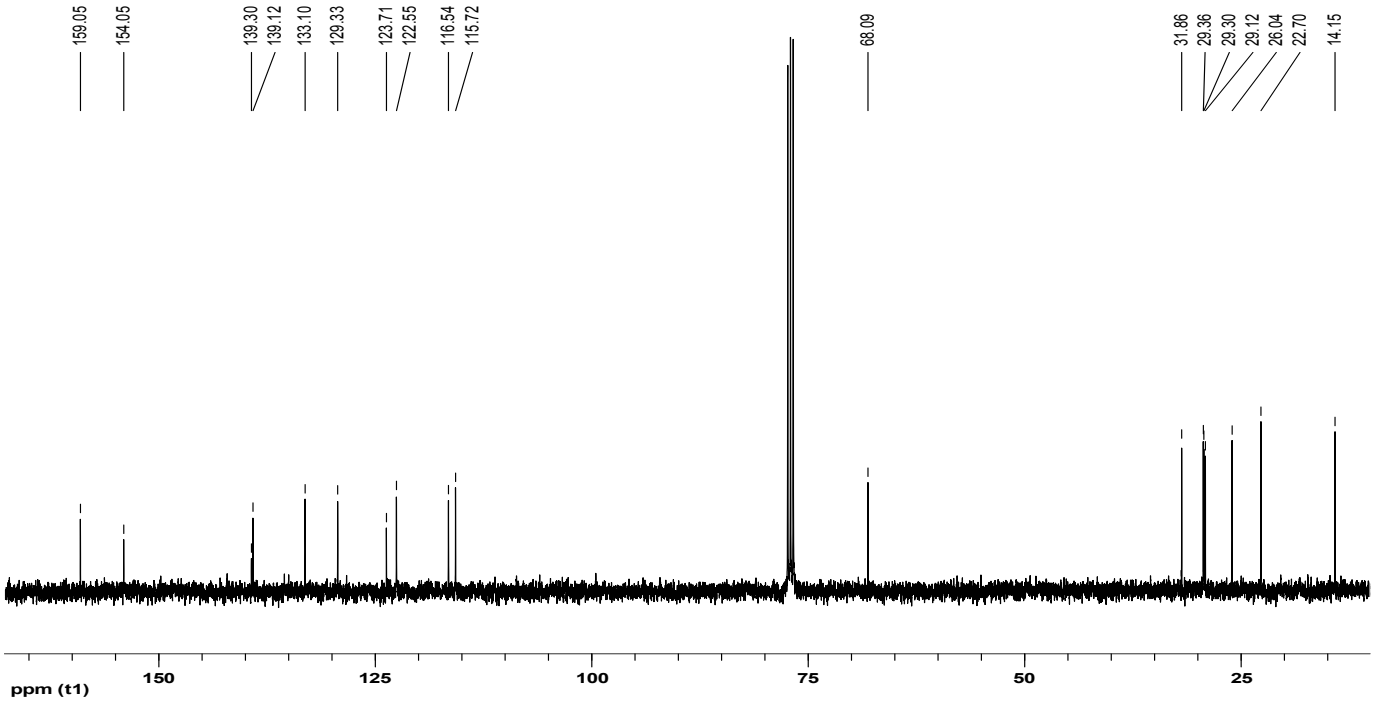

Appendix 26: ^{13}C-NMR spectrum of 5,8-dibromo-2,3-bis(3-octyloxyphenyl)-quinoxaline (**51**).

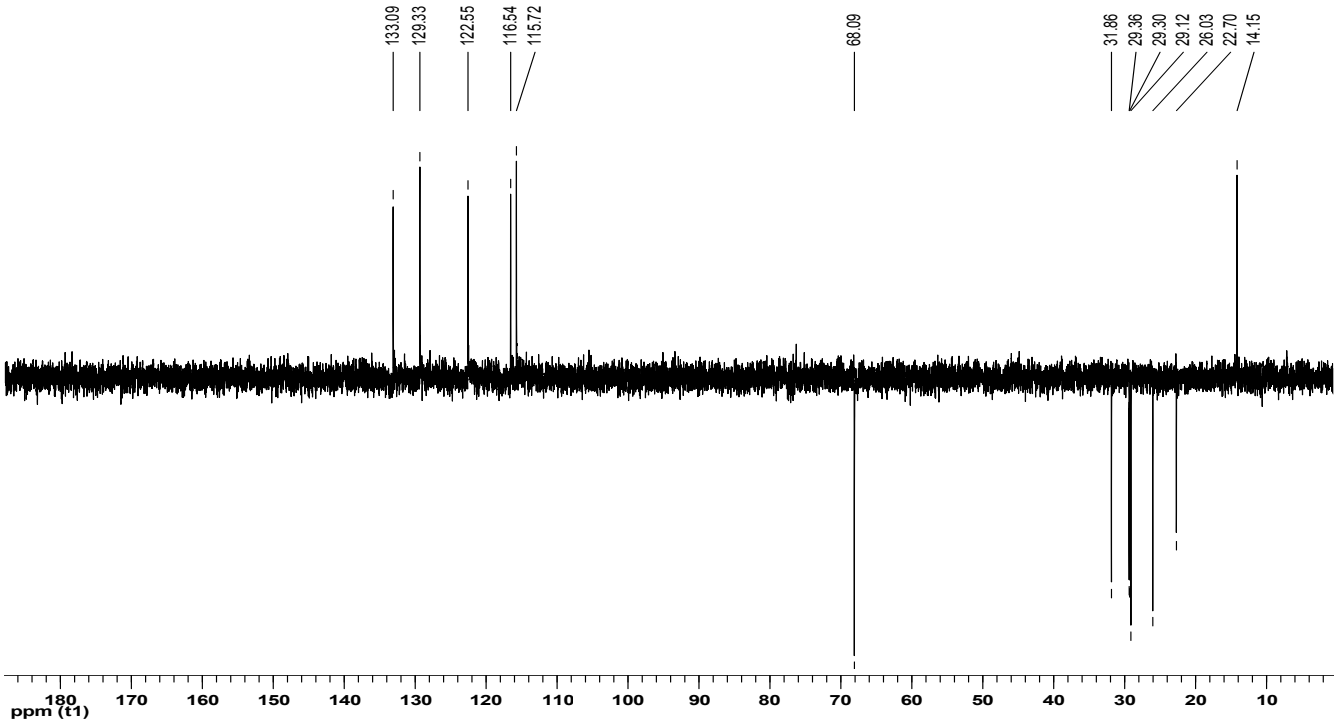

Appendix 27: DEPT-135 spectrum of 5,8-dibromo-2,3-bis(3-octyloxyphenyl)-quinoxaline (**51**).

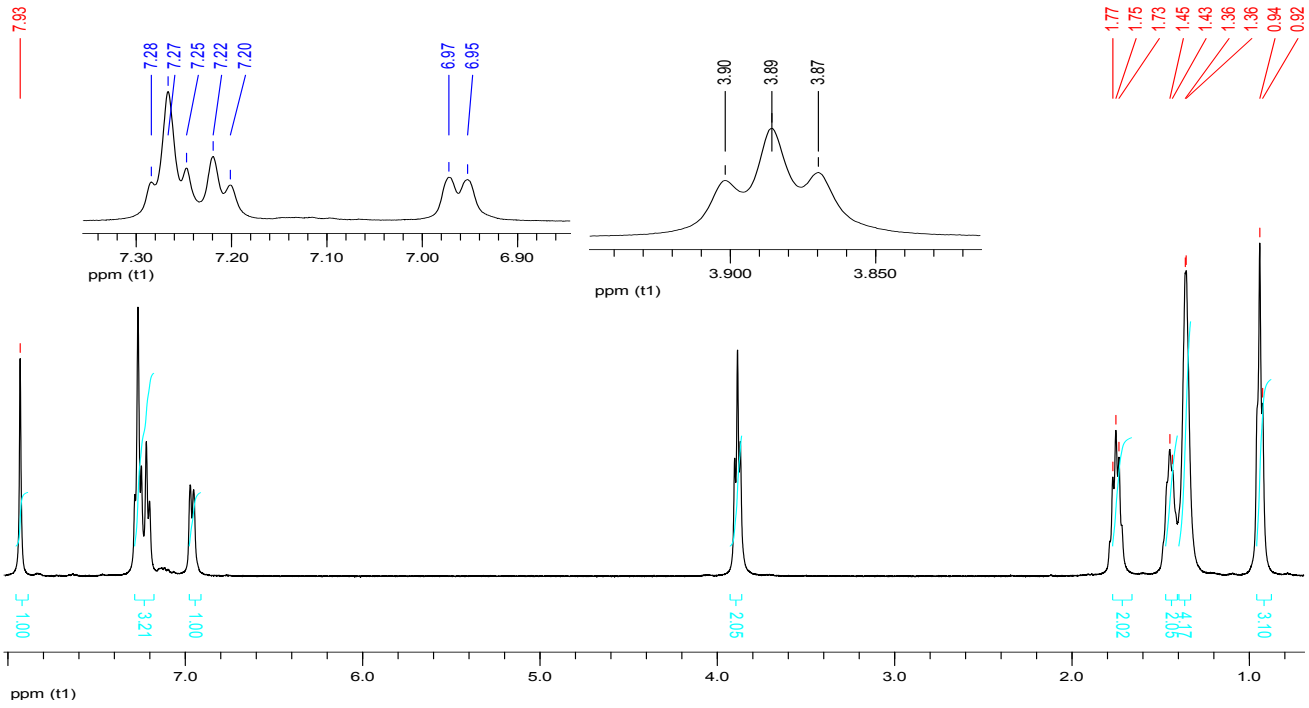

Appendix 28: ^{1}H-NMR spectrum of 5,8-dibromo-2,3-bis(3-hexyloxyphenyl)-quinoxaline (**73**).

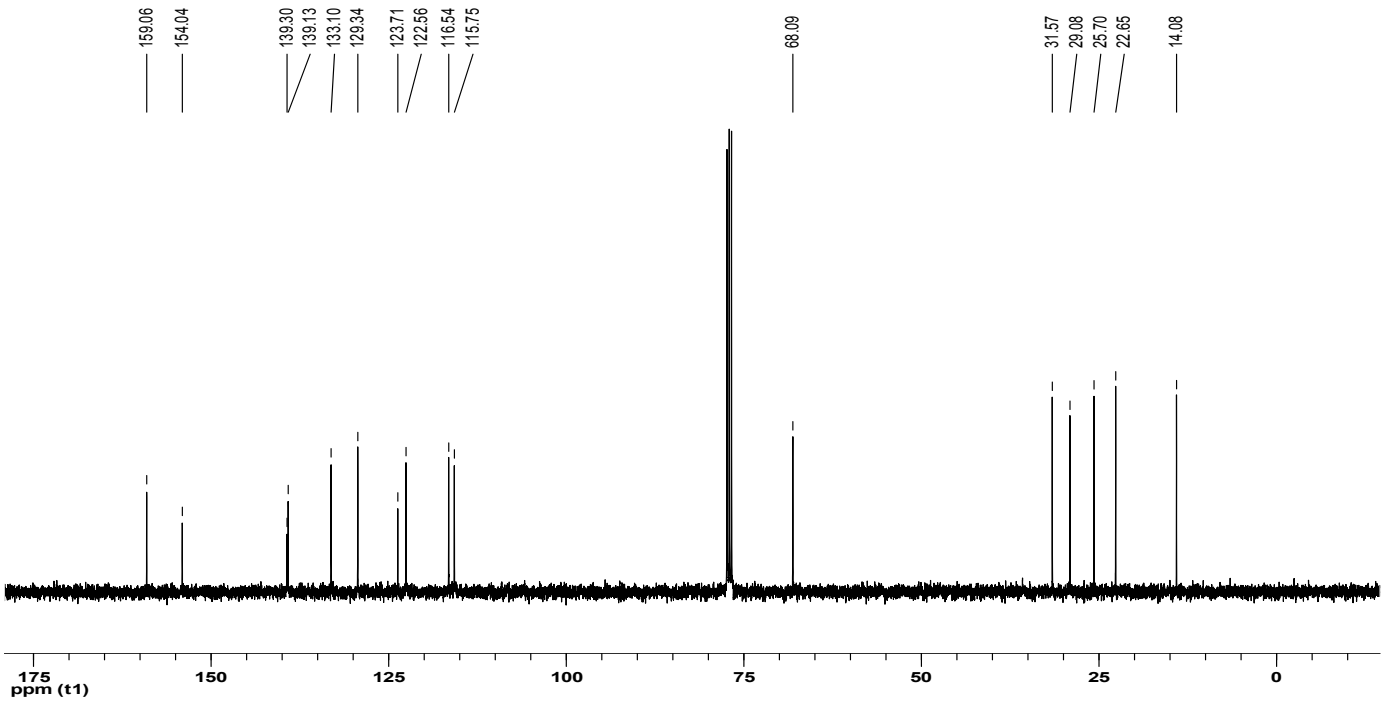

Appendix 29: ^{13}C-NMR spectrum of 5,8-dibromo-2,3-bis(3-hexyloxyphenyl)-quinoxaline (**73**).

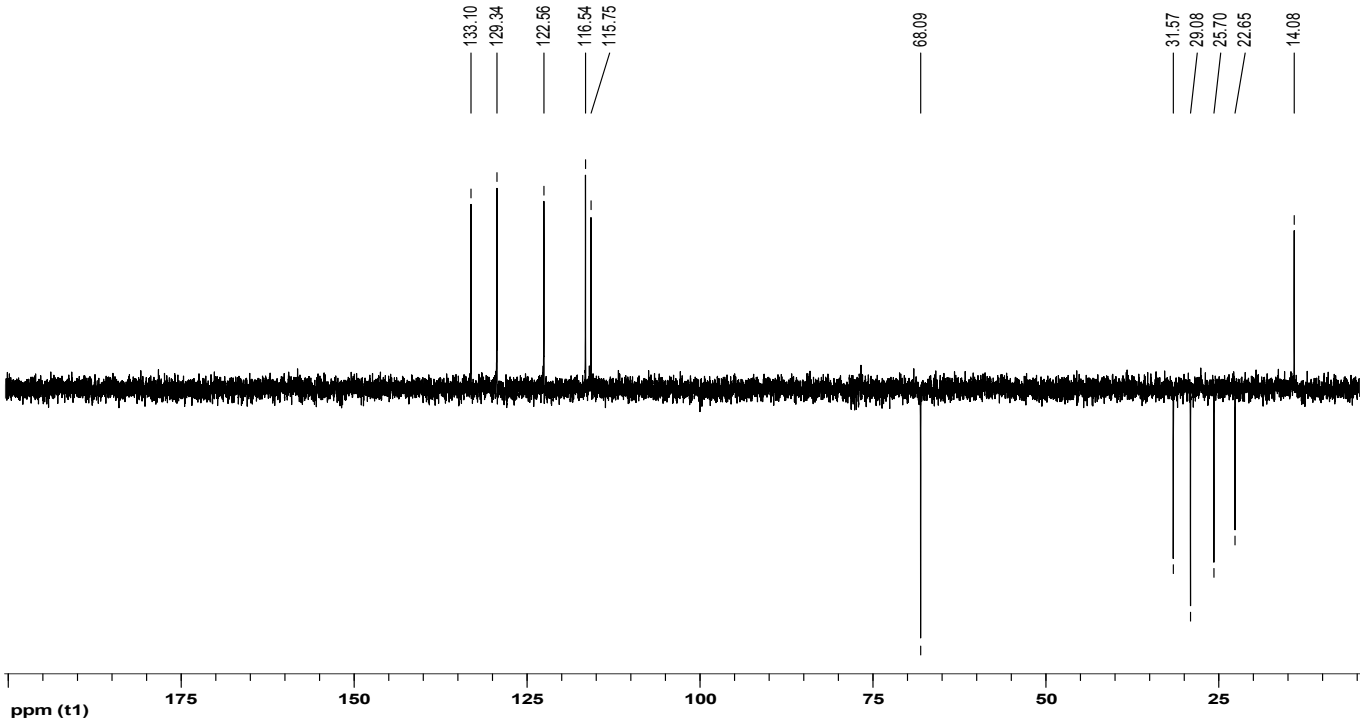

Appendix 30: DEPT-135 spectrum of 5,8-dibromo-2,3-bis(3-hexyloxyphenyl)-quinoxaline (**73**).

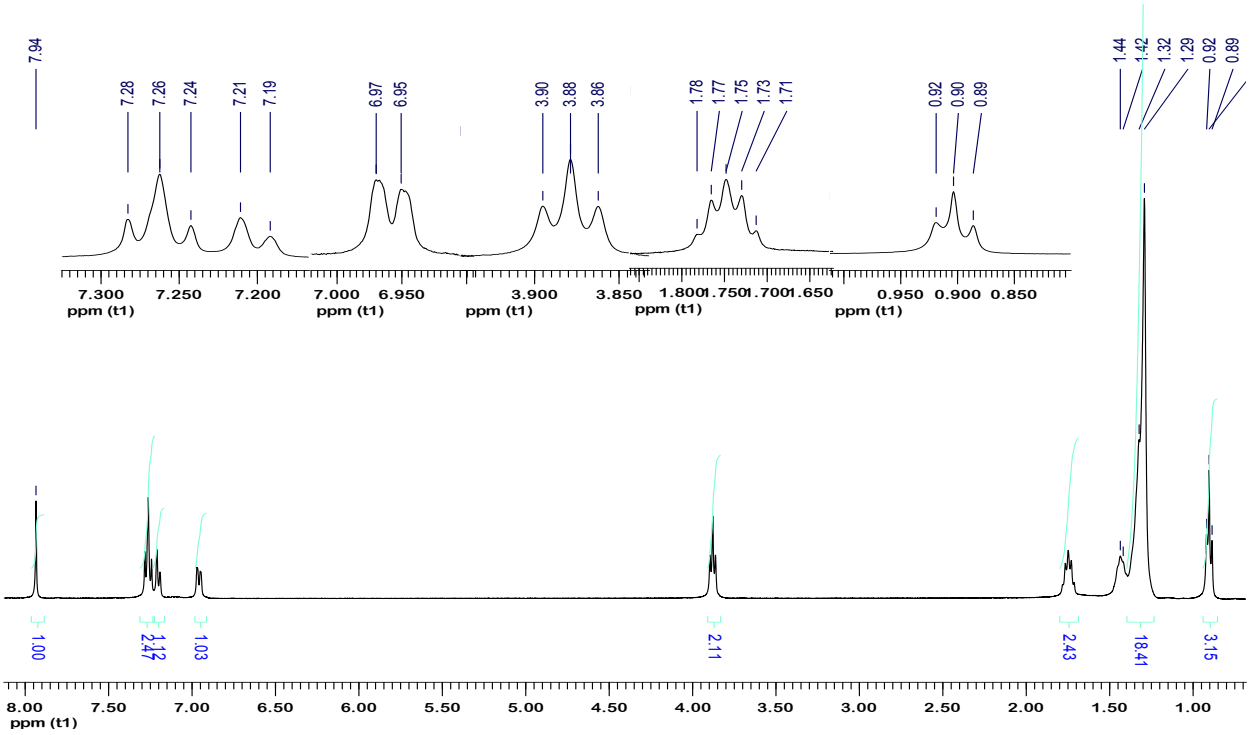

Appendix 31: ^{1}H-NMR spectrum of 5,8-dibromo-2,3-bis(3-dodecyloxyphenyl)-quinoxaline (**75**).

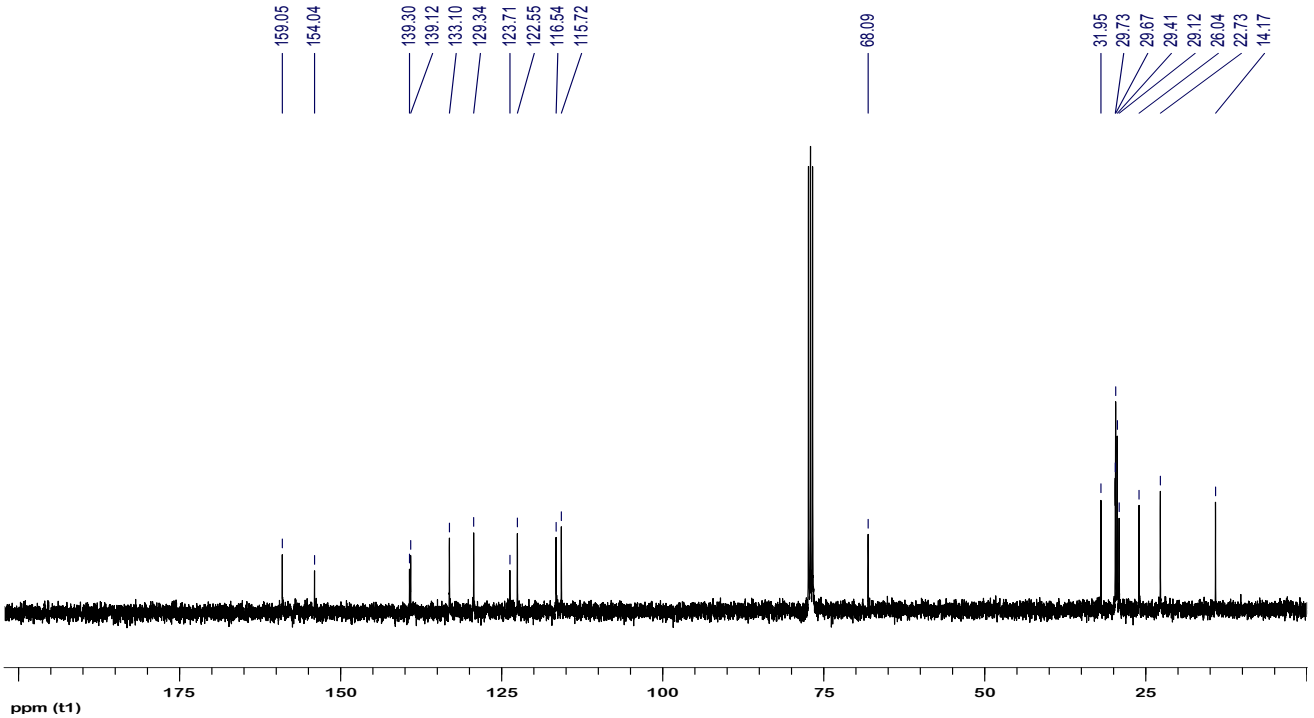

Appendix 32: ^{13}C-NMR spectrum of 5,8-dibromo-2,3-bis(3-dodecyloxyphenyl)-quinoxaline (**75**).

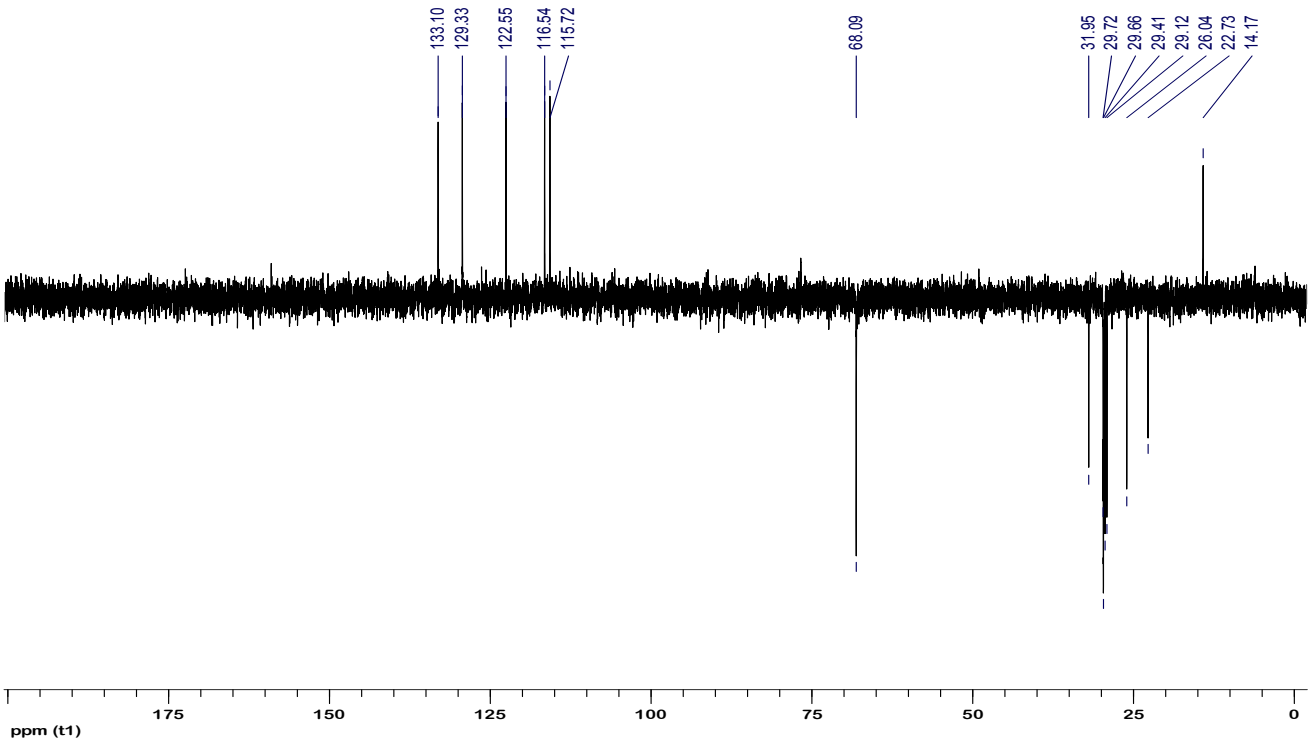

Appendix 33: DEPT-135 spectrum of 5,8-dibromo-2,3-bis(3-dodecyloxyphenyl)-quinoxaline (**75**).

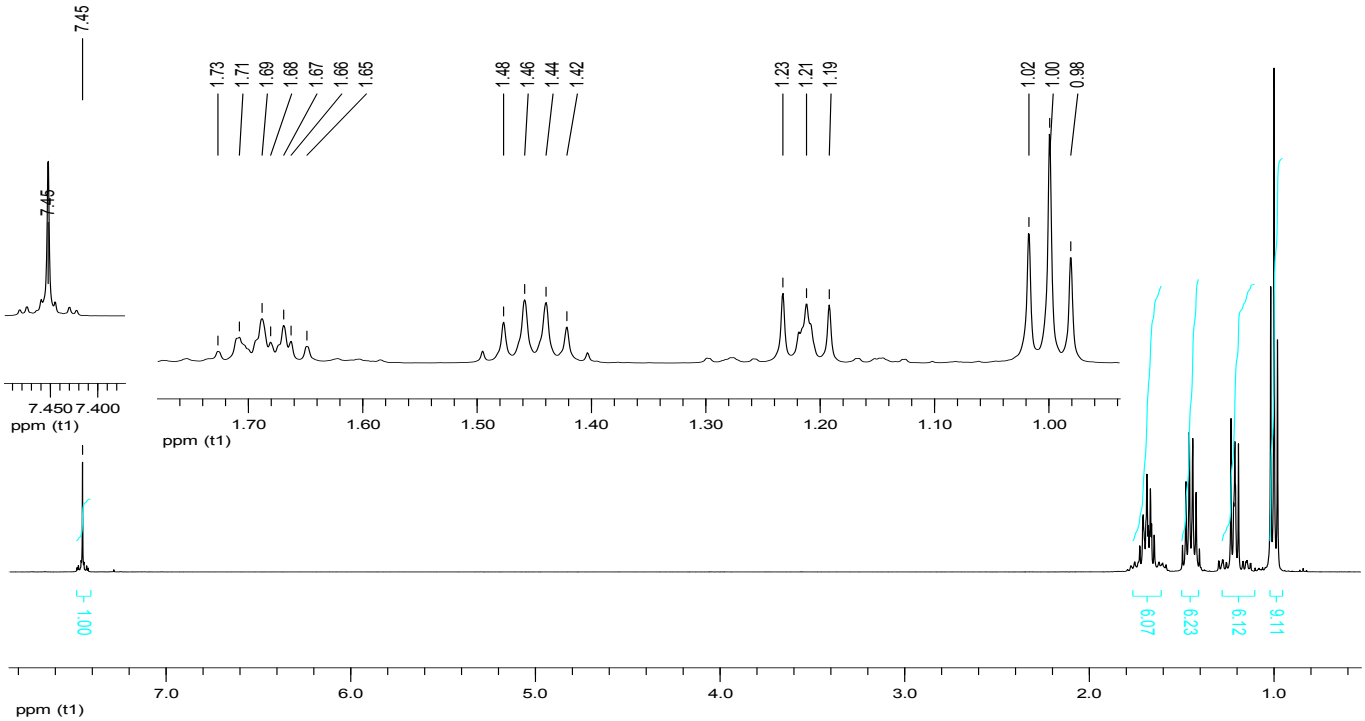

Appendix 34: ^{1}H-NMR spectrum of 2,5-bis(tri-*n*-butylstannyl)thiophene (**78**).

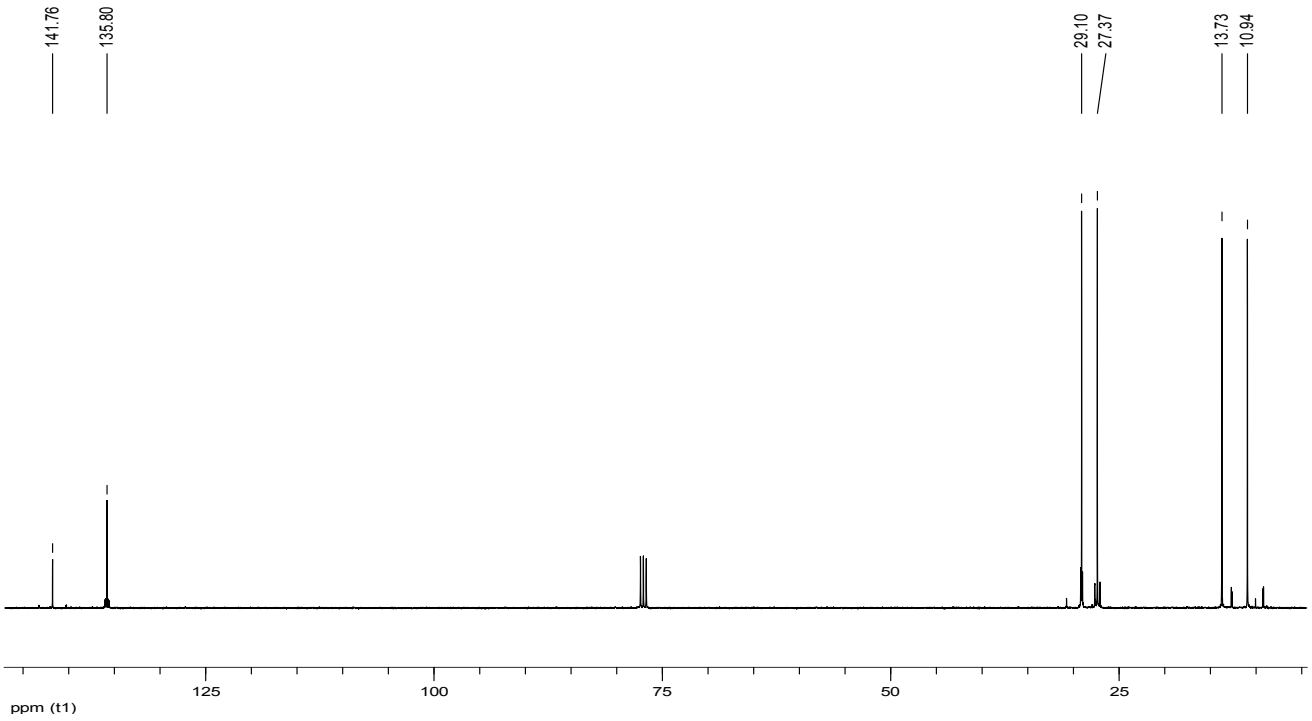

Appendix 35: ^{13}C-NMR spectrum of 2,5-bis(tri-*n*-butylstannyl)thiophene (**78**).

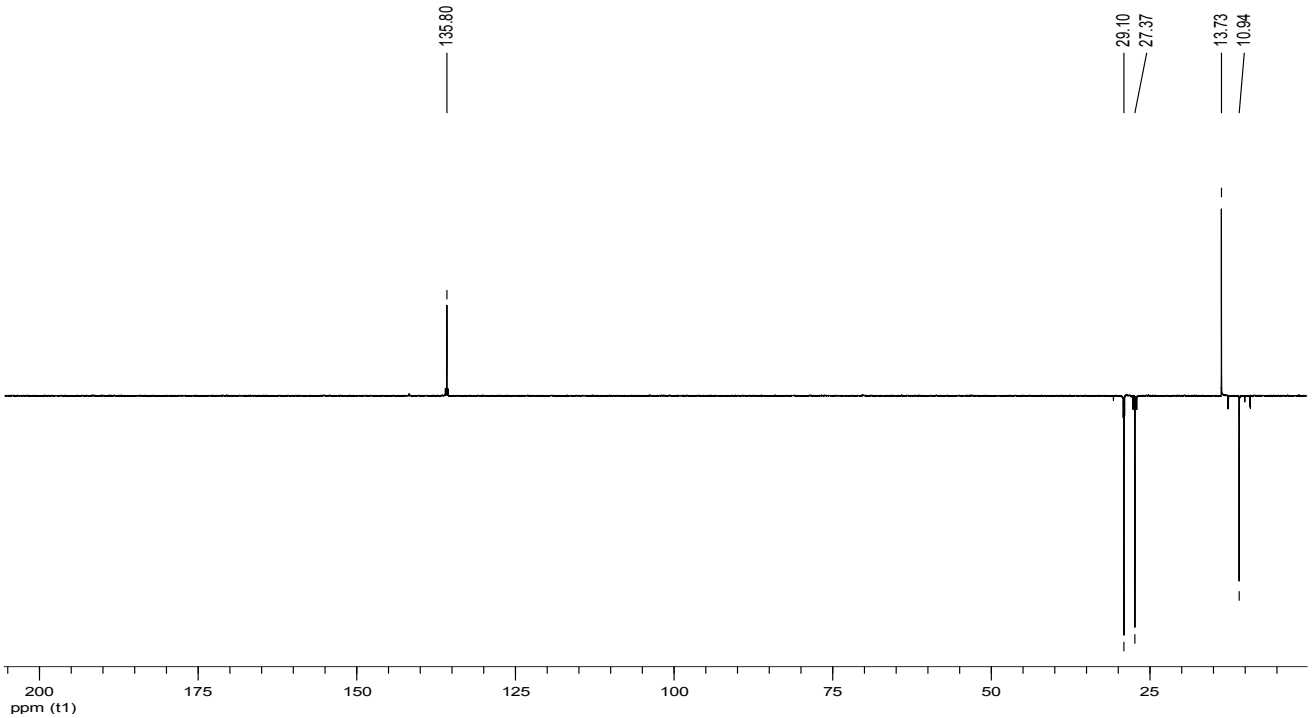

Appendix 36: DEPT-135 spectrum of 2,5-bis(tri-*n*-butylstannyl)thiophene (**78**).

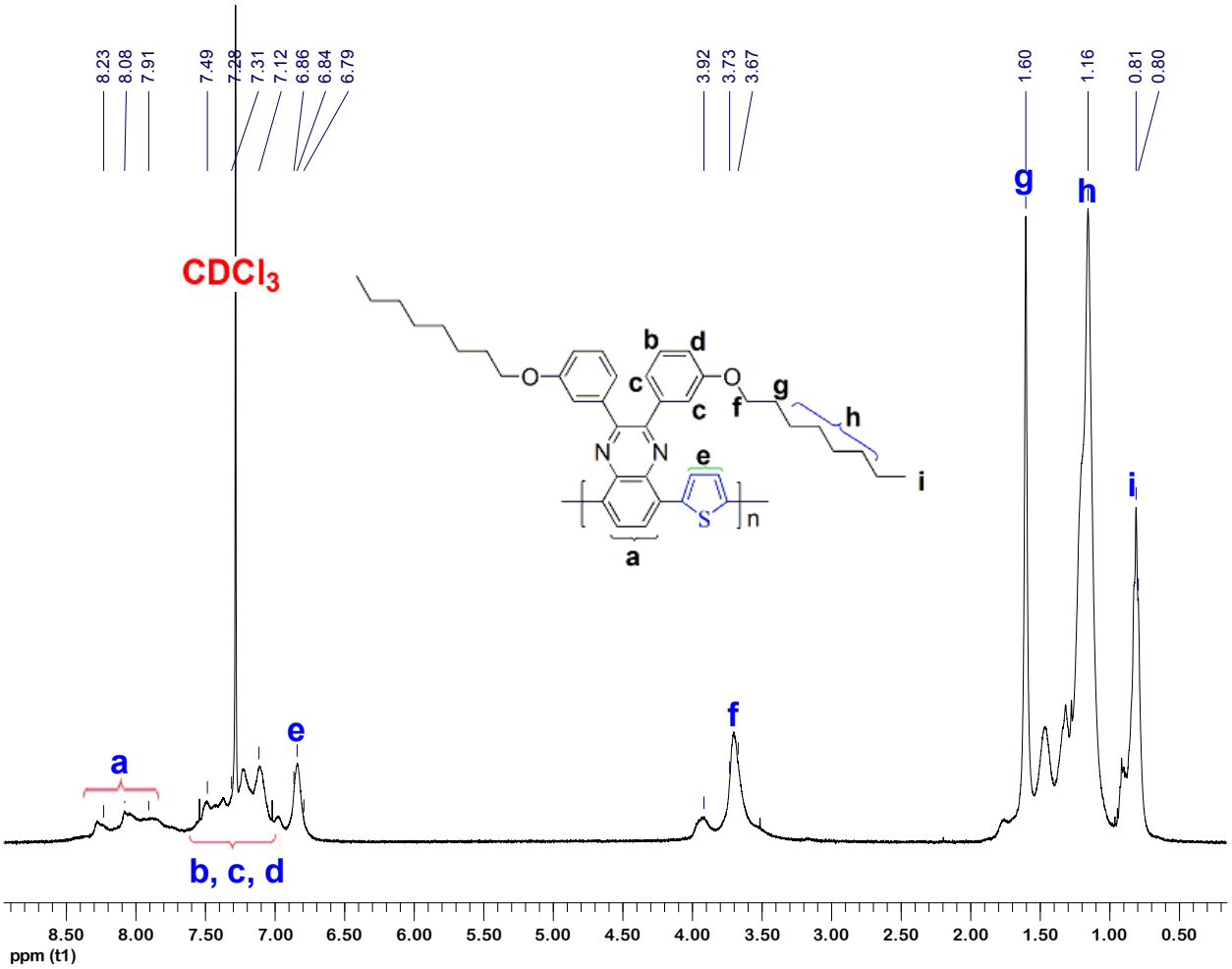

Appendix 37: ^{1}H-NMR spectrum of poly[2,3-bis(3-octyloxyphenyl)quinoxaline-5,8-diyl-*alt*-thiophene-2,5-diyl] (**52**).

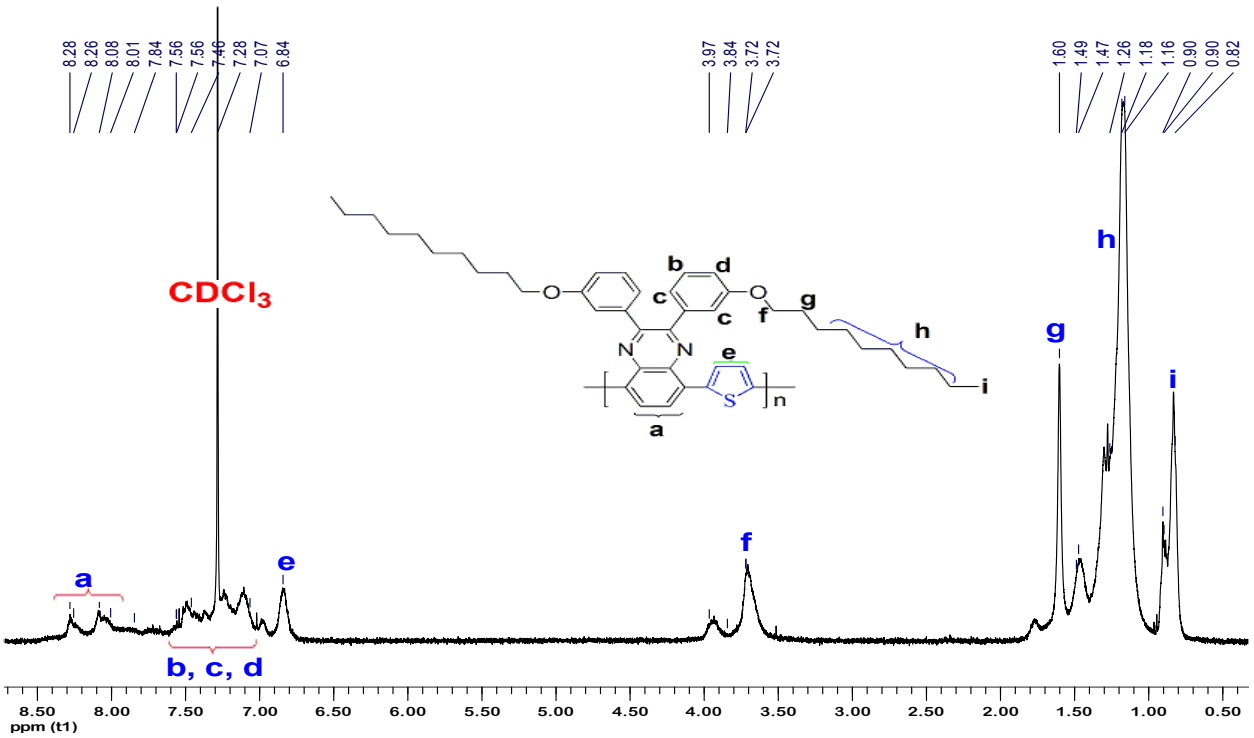

Appendix 38: ^{1}H-NMR spectrum of poly[2,3-bis(3-decyloxyphenyl)quinoxaline-5,8-diyl-*alt*-thiophene-2,5-diyl] (**82**).

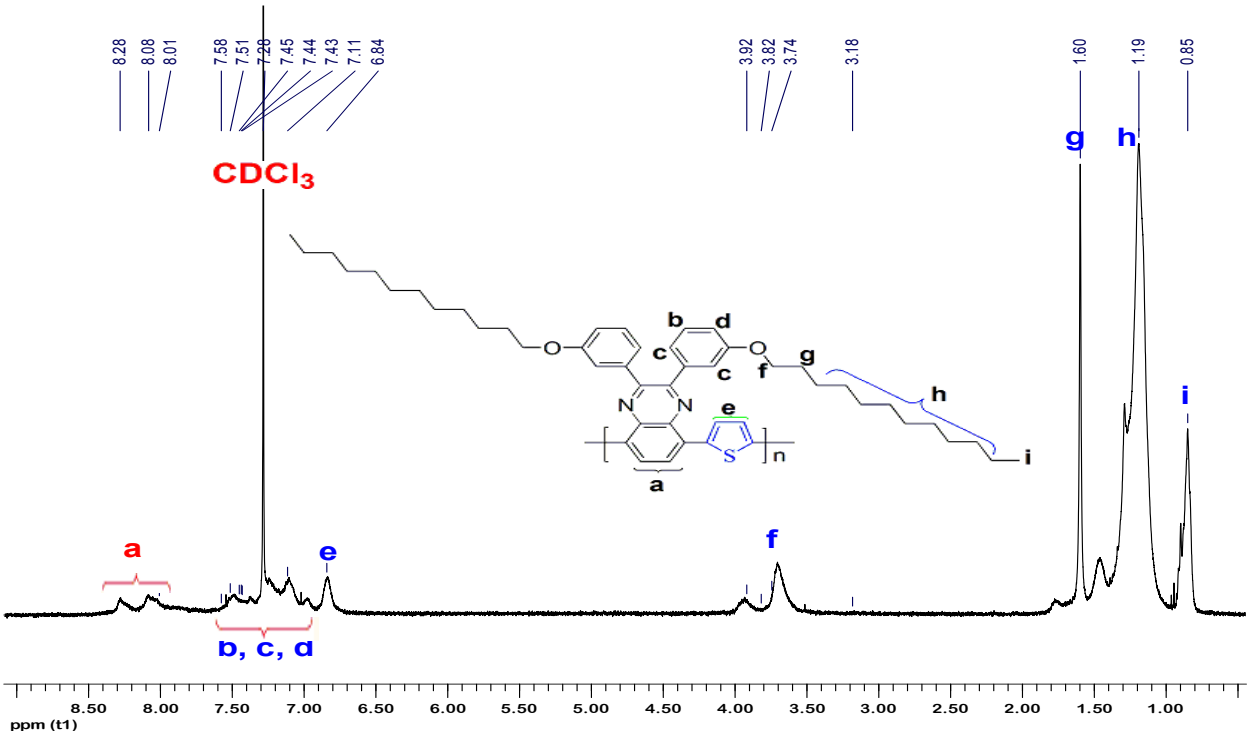

Appendix 39: ^{1}H-NMR spectrum of poly [2,3-bis(3-dodecyloxyphenyl)quinoxaline-5,8-diyl-*alt*-thiophene-2,5-diyl] (**83**).

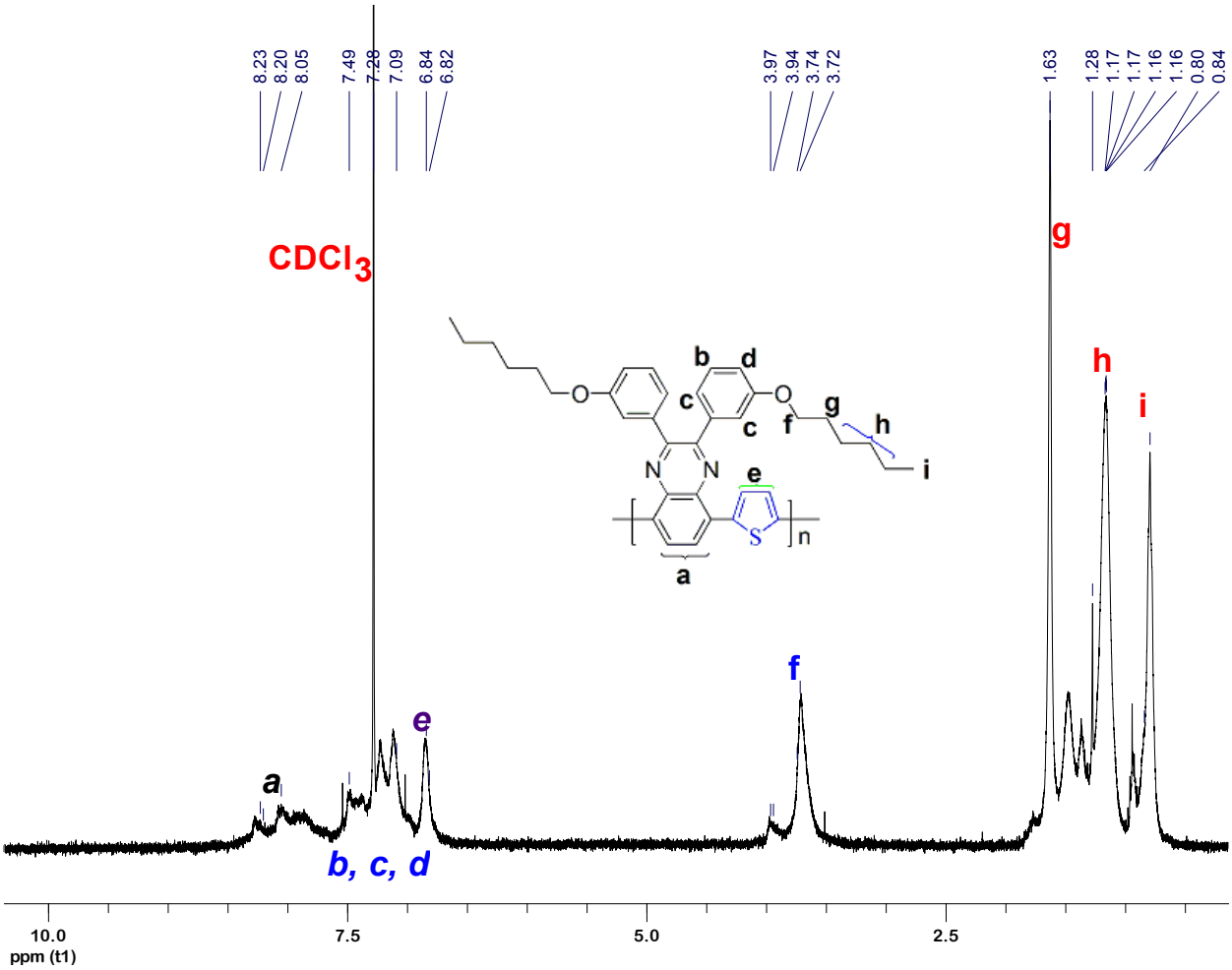

Appendix 40: ^{1}H-NMR spectrum of poly[2,3-bis-(3-hexyloxyphenyl)quinoxaline-5,8-diyl-*alt*-thiophene-2,5-diyl] (**81**).

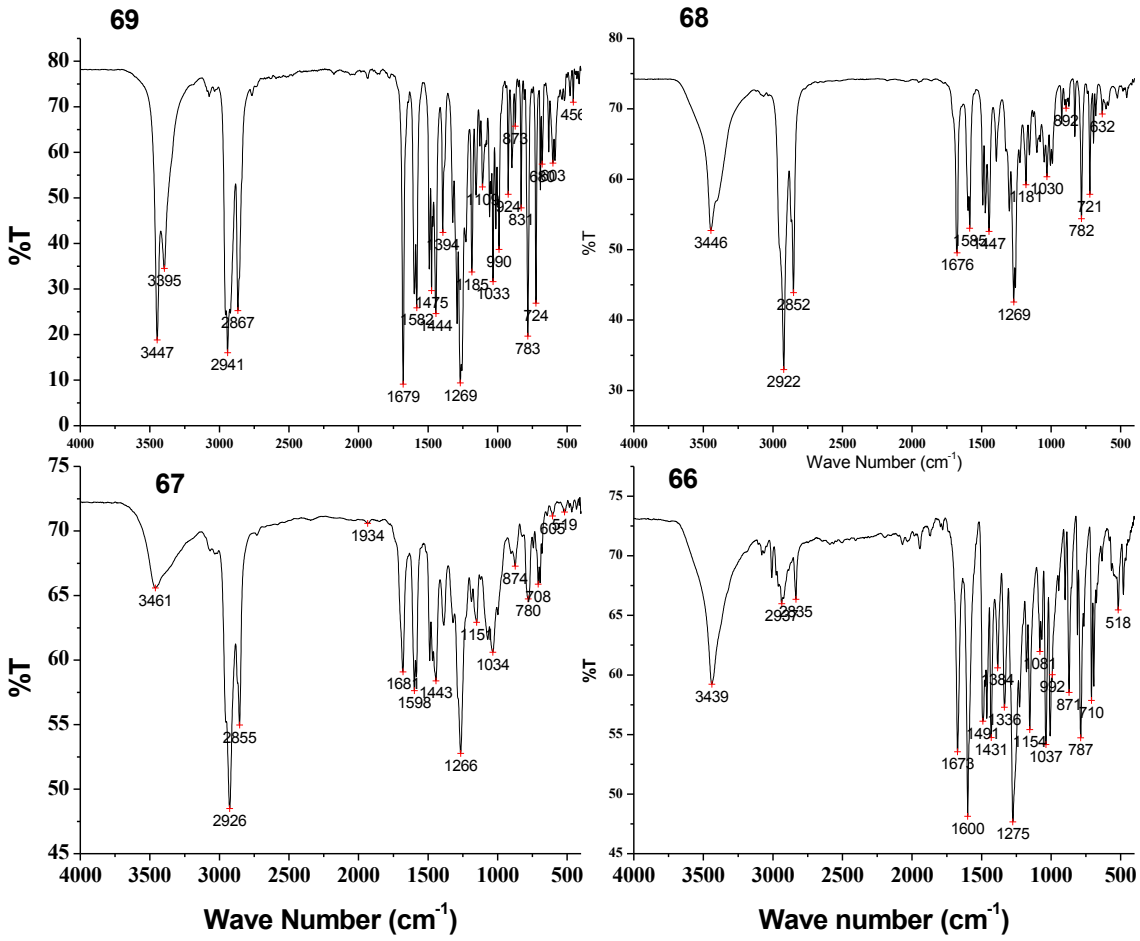

Appendix 41: IR spectra of **66**, **67**, **68** and **69**.